VERTICAL DISTRIBUTION OF ELECTRONS IN THE IONOSPHERE OVER AHMEDABAD

presented

by

S.S.DEGAONKAR

for

the degree of

DOCTOR OF PHILOSOPHY

of

THE GUJARAT UNIVERSITY

October 1961

PHYSICAL RESEARCH LABORATORY
AHMEDABAD-9
INDIA.

PREFACE

A vertical ionospheric sounding recorder of the British D.S.I.R. type was installed at the Physical Research Laboratory, Ahmedabad in 1952 and regular observations started in 1953. The writer has been associated with the day to day maintenance of the equipment, scaling of the records and analysis of recorded data since the beginning of the IGY. The favourable situation of Ahmedabad has enabled much valuable data relating to the ionosphere of low latitudes to be gathered during low, high and waning periods of sunspot activity.

The present thesis begins with a general survey of the behaviour of the F region over Ahmedabad during the years 1953-60. The results are interesting as regards its variations with solar activity and in particular with geomagnetic storms. After briefly reviewing the methods of finding the true heights of reflection of radio waves in the ionosphere, the method adopted at Ahmedabad is described in detail in Chapter II. The results of true height calculations and the effects of magnetic storms on the electron density distribution are presented in Chapter III and IV. Finally, an attempt is made to calculate the ionospheric attenuation of cosmic radio noise at 85 Mc/s observed at Ahmedabad. A significant result that has emerged is that most of the attenuation of this cosmic radio noise takes place in

the ionosphere below 1000 Km and in particular in the F region. It is believed that the thesis contains much new information adding to our knowledge of the ionosphere of low latitudes.

References and acknowledgements are made in appropriate places in the body of the thesis.

S.S. Degaonkar

Countersigned.

ACKNOWLEDGEMENTS

I wish to express my deep gratitude to Professor K.R.Ramanathan, Director, Physical Research Laboratory, Ahmedabad for guidance, keen interest and encouragement at all stages of the work and for providing all the necessary facilities. I have pleasure in acknowledging with many thanks the kind cooperation I received from Dr.K.M.Kothdia, for his advice and discussions, and Mr.J.S.Shirke, for his help in the maintenance of the recorder. My thanks are also due to Dr.R.V.Bhonsle for providing me the cosmic radio noise data and for helpful discussions, and to other colleagues in the department, Mr.A.K.Sul in particular. Finally, I express my grateful thanks to the Council of Scientific & Industrial Research, India, for financial support.

D.S.DEGAONKAR.

C O N T E N T S

CHAPTER III

RESULTS OF CALCULATION OF VARIATION OF ELECTRON DENSITY WITH TIME DURING

Page

CHAPTER IV

EFFECT OF SOLAR MAGNETIC STORM ON THE ELECTRON DENSITY DISTRIBUTION

CHAPTER V

CALCULATION OF IONOSPHERIC ATTENUATION AT 25 MC/S COSMIC RADIO NOISE AT AHMEDABAD ON THE BASIS OF $\int N\nu\,ds$

Page

CHAPTER IV

EFFECT OF SOLAR MAGNETIC STORM ON THE ELECTRON DENSITY DISTRIBUTION

CHAPTER V

CALCULATION OF IONOSPHERIC ABSORPTION AT 25 MC/S COSMIC RADIO NOISE AT AHMEDABAD ON THE BASIS OF $\int N \nu \, dh$

List of figures

Symbols and Abbreviations

f_o, f_o	:	Ordinary wave critical frequency
f_x	:	Extra-ordinary wave critical frequency
h_p	:	Height of maximum electron density on the assumption of parabolic distribution of electrons with height
h'	:	Minimum virtual height
N_m	:	Maximum electron density
h_m	:	True height of maximum electron density
H	:	Horizontal component of the earth's magnetic field
R_z	:	Zurich relative sunspot number
IMT	:	Ideal mean time corresponding to 75° for Ahmedabad
UT	:	Universal time
RWD	:	Regular World Day
SWI	:	Special World Interval
IGY	:	International Geophysical Year
IGC	:	International Geophysical Cooperation
URSI	:	International Scientific Radio Union
CRPL	:	Central Radio Propagation Laboratory
CSIR	:	Council of Scientific & Industrial Research, India

CHAPTER I

NORMAL SURVEY OF THE BEHAVIOUR OF THE F REGION OF THE IONOSPHERE OVER AHMEDABAD

1 INTRODUCTION

The standard method of exploring the ionosphere is by sending up in a vertical direction pulses of radio waves of gradually increasing frequency and recording the time delays between the emission and the reception of pulses reflected from the ionosphere. This method is originally due to Breit and Tuve. The time delay between the emitted and the received pulses is usually expressed as the virtual height h' of the reflecting layer, in calculating which it is assumed that the pulse travels with the phase velocity of light c, so that $h' = \frac{1}{2} c \tau$.

2. EXPERIMENTAL SET UP AND DATA AT AHMEDABAD

A multifrequency sweep recorder MkII type of British design was installed at the Physical Research Laboratory, Ahmedabad (23°N, 72.6°E) in 1953 and regular soundings were started in February 1953. The sweep frequency range is 0.6 to 25 Mc/s and is divided into five bands. The peak pulse power varies from 1700 watts in the low frequency range to about

250 watts in the high frequency range. The normal soundings are made at a pulse width of 100-150 μ secs. The aerial system consists of two pairs of vertical rhombics at right angles, two for transmitting and two for receiving the higher and lower frequencies. As a normal routine, the vertical soundings of the ionosphere are made automatically at every integral hour corresponding to 75° EMT. But during the IGY and IGC, this schedule was changed to more frequent soundings. Thus on Regular World Days half hourly records were taken and on SWI's once every fifteen minutes. The records normally scaled are for foE, foEs, foF1, foF1.5, foF2, h'E, h'Es, h'F1, hpF2 and h'F2. Since the beginning of 1955, the hourly ionospheric data of Ahmedabad are published along with other Indian ionospheric stations in a monthly bulletin of the Radio Research Committee of the CSIR. Some of the parameters which are scaled at Ahmedabad but not published include f-min, fminF, foE1, foE2, h'E1, h'E2 and h'F1.5. The accuracy of scaling is 0.1 Mc/s in the critical frequencies and 10 km in heights.

A detailed study of the behaviour of the E, E2 and F1 layers over Ahmedabad during the years 1953-56 has been made by Rastogi (1956) and of the F region during the years 1953-57 by Kotadia (1958) in their doctoral dissertations. We propose to give here an account of the behaviour of the F region over Ahmedabad over a period of eight years from 1953-60 with particular emphasis on the period 1957-60. The peak period of solar activity was 1953-53. The years 1953-54

represented an epoch of minimum sunspots, while the next sunspot minimum is expected in 1963-64. The mean Zurich sunspot number was highest in October 1957 (about 284); in December 1960 it had fallen to 87 i.e. nearly 1/3 of that in October 1957. The sunspot activity at the end of 1960 was similar to that at the end of 1955.

3. VARIATION OF foF2 AT AHMEDABAD DURING 1953-60

We have plotted in Fig.1.1, 1.2 and 1.3 the monthly median values of foF2 in the years 1953-60 to study its annual variation. For clarity, we have shifted each month's curve both laterally and vertically with a view to produce a three-dimensional effect.

We shall divide the epoch into two groups, one representing low sunspot period and the other high sunspot period.

3.1 Variation of foF2 in the years 1953-55.

The critical frequency of the F2 layer in low sunspot years 1953-55 showed a diurnal variation having a maximum between 14-15 hrs IST on the average and a minimum about 40 minutes before ground sunrise. The noon foF2 showed a seasonal variation with maxima in equinoxes and minimum in summer and winter. We shall summarise the salient points as revealed by the study of the figure as a whole.

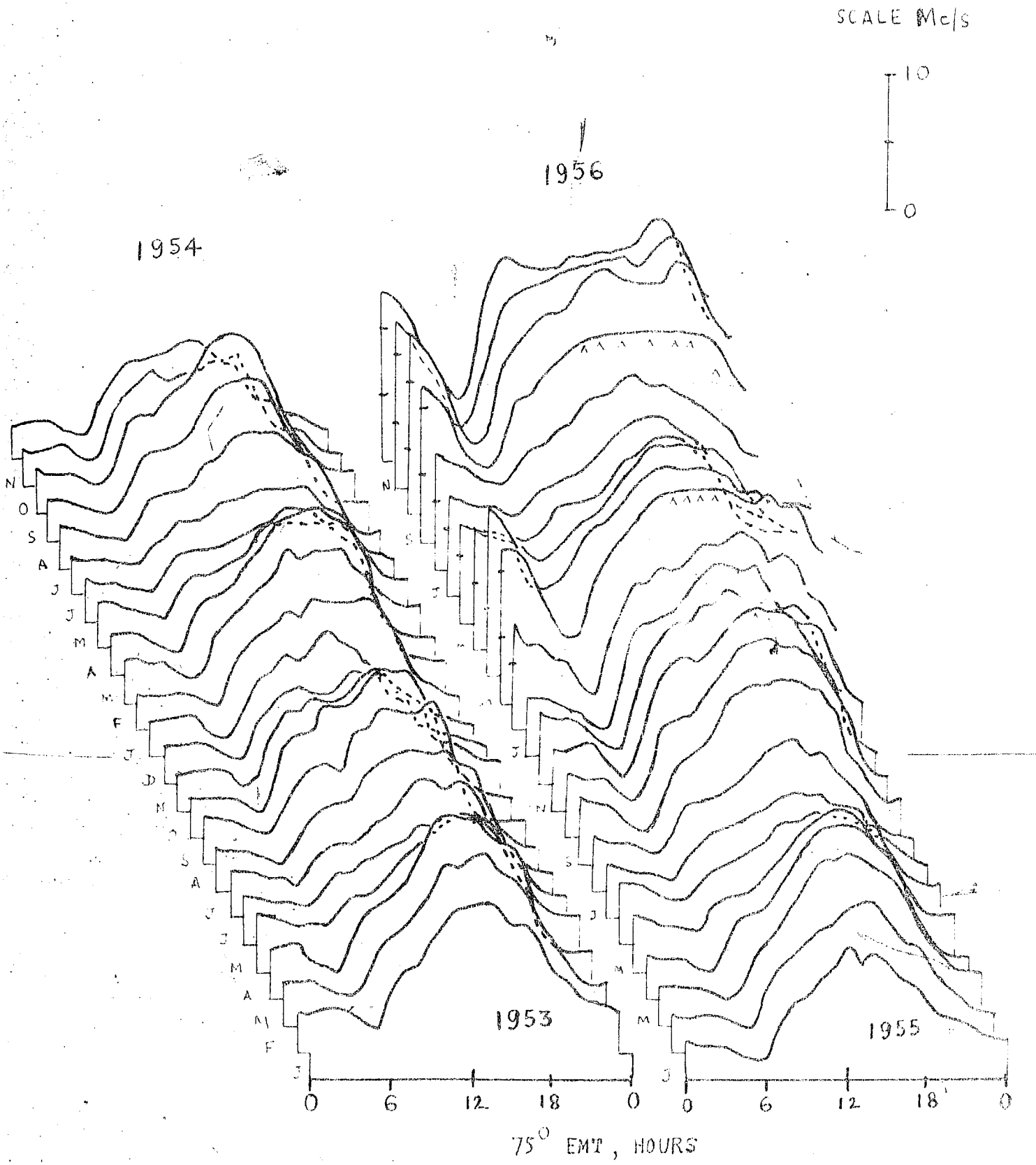

FIG. 1.1 ANNUAL VARIATION OF MONTHLY MEDIAN foF2 AT AHMEDABAD

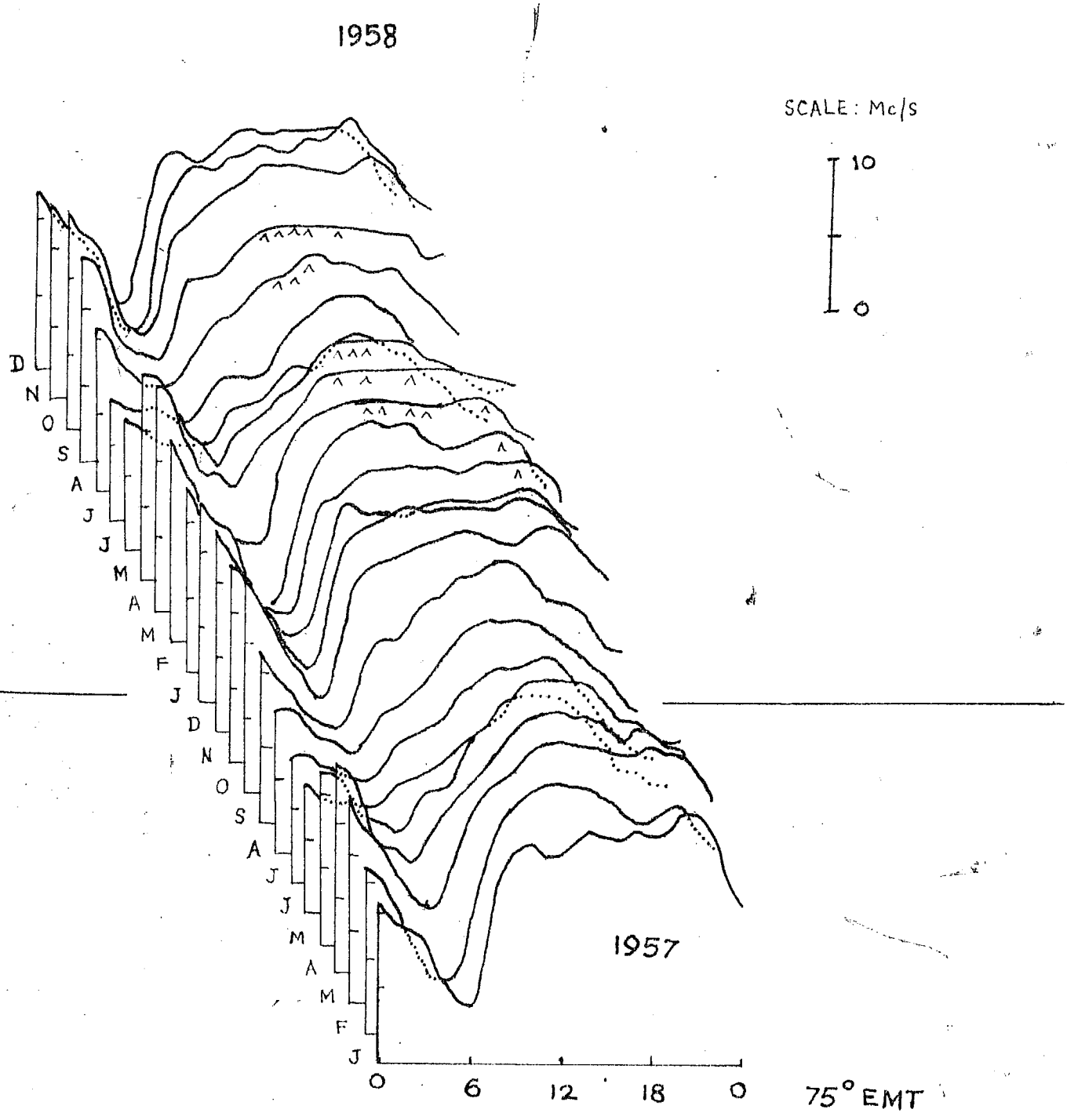

FIG. 1·2 ANNUAL VARIATION OF MONTHLY MEDIAN f_0F_2 AT AHMEDABAD DURING 1957-58

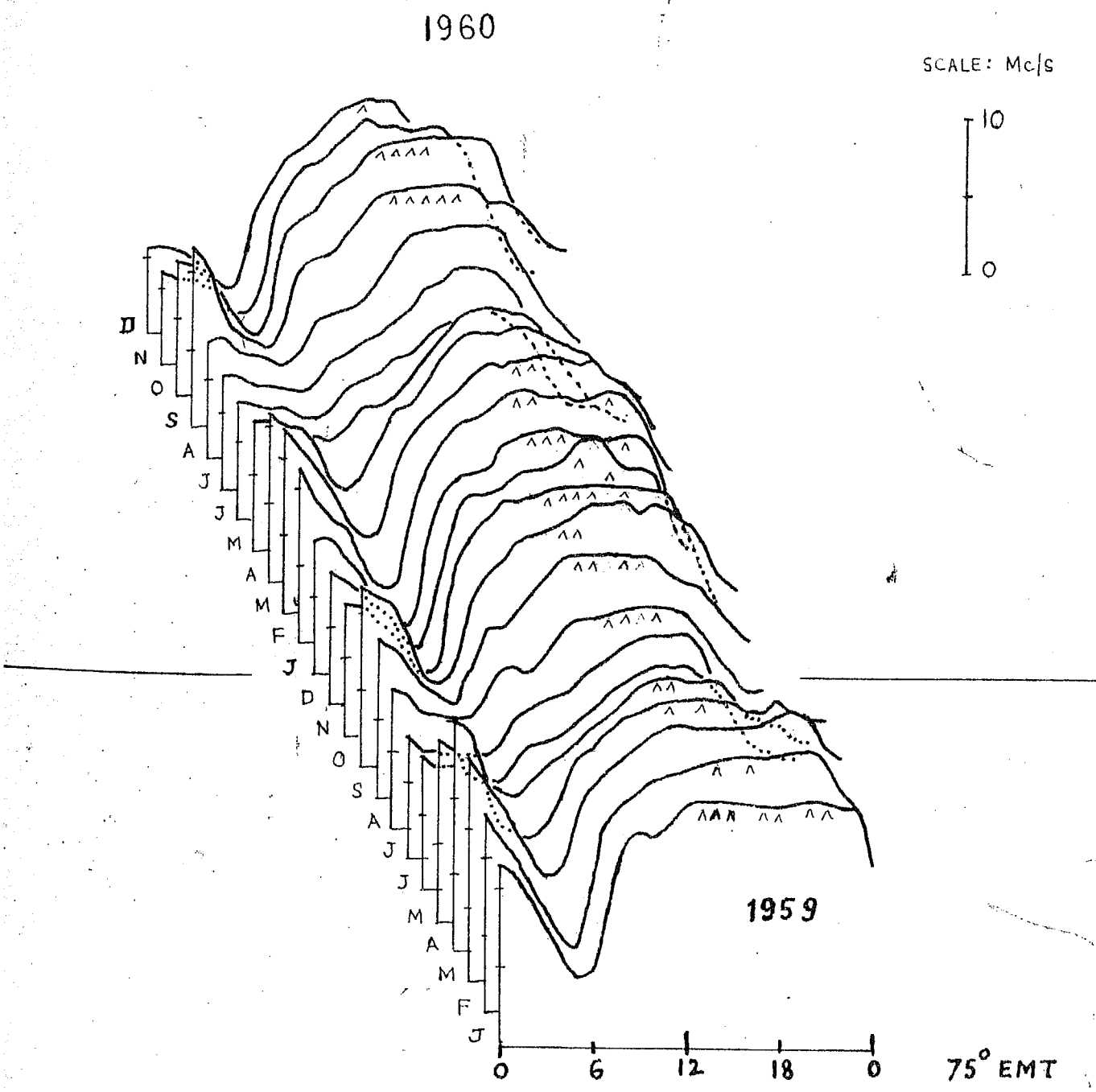

FIG. 1.3 ANNUAL VARIATION OF MONTHLY MEDIAN f_0F_2 AT AHMEDABAD DURING 1959-60

3.1.1 Summer

(1) The range of daily variation in foF2 was about 3.4 Mc/s with maximum at about 13 hrs and minimum at about 05 hrs local time.

(2) The maximum foF2 was least in June (about 8 Mc/s) with an annual variation of 9 to 10 Mc/s; the minimum foF2 had an annual variation of 2 to 3 Mc/s.

(3) The foF2 after it reached its peak value in the afternoon decreased rapidly to nearly half its value upto 20-22 hrs; then the rate of decay slowed down till it reached its minimum at 05 hrs. The rate of increase of foF2 between 06-09 hrs was also gradual.

3.1.2 Winter and equinoxes

(1) The range of daily variation was 8-9 Mc/s in winter and 11 to 12 Mc/s in equinoxes. The peak foF2 occurred a little earlier at about 14 hrs; the minimum occurred at about 05 hrs in both equinoxes and winter.

(2) The peak foF2 did not differ much from its summer value in winter, but it was a little higher, about 13 Mc/s, in equinoxes. The minimum value was between 2 to 2.5 Mc/s.

(3) The foF2 decreased rapidly in winter after reaching its peak in the afternoon and in contrast to the behaviour in summer, it either remained steady after 21 hrs or increased slowly till 03 hrs. The rate of increase of foF2 between 00-03 hrs was faster than in summer. The afternoon peak of foF2 was rather sharp as compared to the broad peak in summer.

(4) The midnight foF2 was between 1.5-2.5 Mc/s except in the second half of 1955 when the value increased to about 5 Mc/s.

3.2 Variation of foF2 during 1954-60

The foF2 variation in high sunspot years was quite different from that in low sunspot period. The sharp daytime peak in foF2 found in winter and equinoxes in low sunspot period was replaced by a daytime plateau which remained high through the day and till about midnight. We shall note here the characteristic features in its seasonal variation.

3.2.1 Summer

(1) The diurnal range of foF2 variation was nearly the same as that in low sunspot years, the difference being only in the maximum and minimum values. The maximum occurred between 15-16 hrs in the afternoon with an annual variation of 13 to

16 Mc/s; the minimum was about 7 Mc/s and it occurred at about 05 hrs. This means that the proportionate rise in the minimum value of foF2 from low sunspots to high sunspots was more than twice, while it was not so in the case of peak foF2.

(2) The midnight foF2 was between 7-9 Mc/s with a little largish value at times. Here too the rate of decay of foF2 after midnight was slow; and similarly the rate of increase between 04-08 hrs remained gradual.

(3) The foF2 after its peak value in the afternoon decreased throughout the night.

3.2.2 Winter and equinoxes

(1) The daily range of foF2 variation was between 8-9 Mc/s. There was no sharp maximum in the afternoon as in the summer months but a broad plateau exceeding 15 Mc/s from 09 hrs till midnight. The early morning minimum was of the order of 6-7 Mc/s and at times even lower.

(2) The midnight foF2 was very high, about 14-15 Mc/s and on some individual days it exceeded 17 Mc/s. The rate of decay of foF2 after midnight was very sharp and so also the rate of increase between

f-PLOT OF IONOSPHERIC DATA, AHMEDABAD

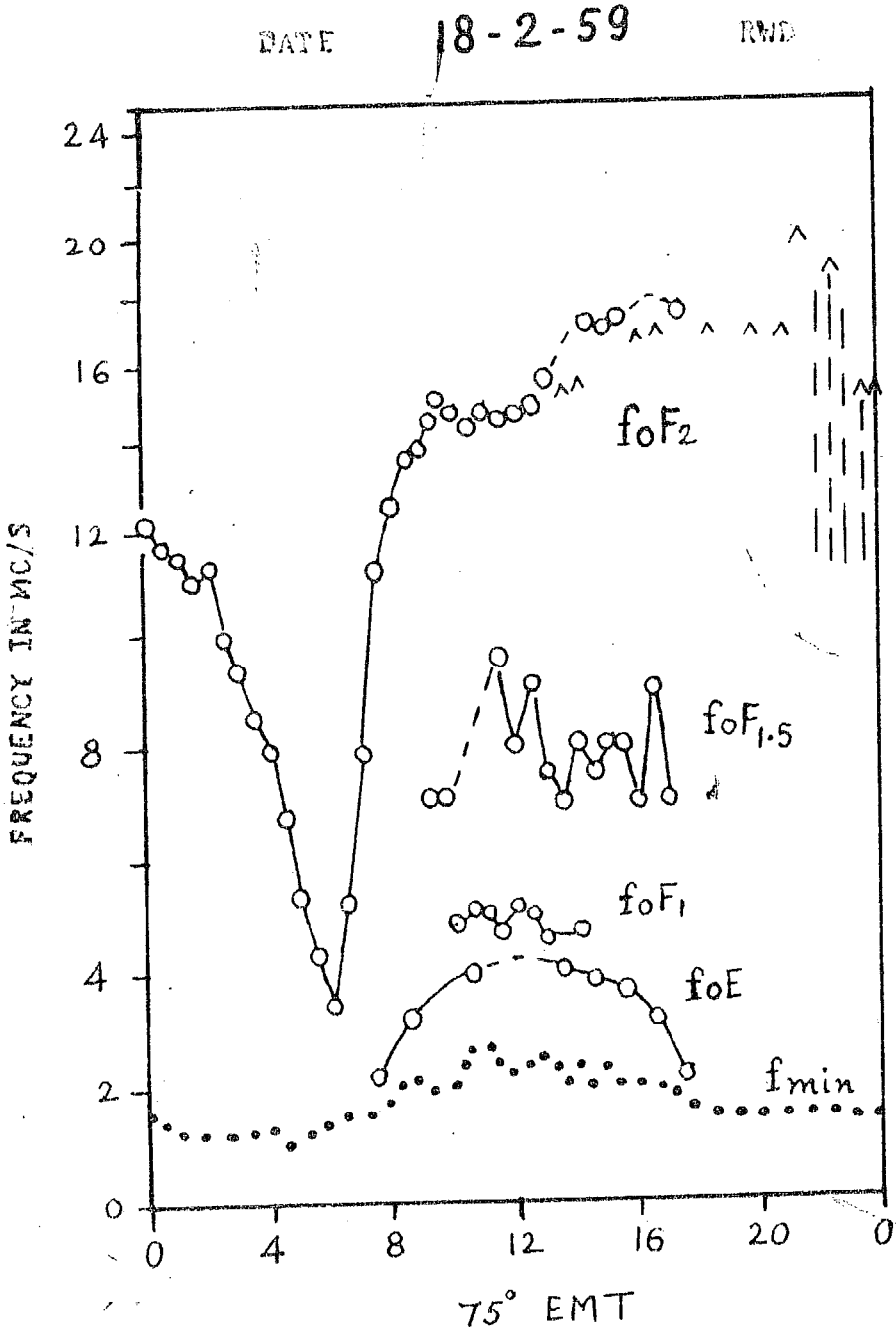

FIG 1·4

06-03 hrs after sunrise. We show in Fig.1.4 an f-plot on 18-2-1959 showing a steep fall between midnight and 03 hrs and a sharp rise afterwards.

(3) Quite often a pre-midnight rise in foF2 was observed in the equinoctial period between 20-21 hrs accompanied by F scatter.

4. AN INTERMEDIATE $F_{1.5}$ LAYER

An interesting feature of the high sunspot period was that another intermediate stratification called $F_{1.5}$ between the normal F1 and F2 layers appeared more or less regularly at Ahmedabad during daytime between 09-17 hrs. This did not obey $(\cos \chi)^n$ law and therefore was similar in characteristics to the F2 layer. This can be seen in Fig.1.4 which shows $F_{1.5}$ layer and also F1 layer. From its study at Ahmedabad, Kotadia (1967) concluded that the $F_{1.5}$ layer was apparently formed by the pushing up of electrons mechanically, by electromagnetic drift forces. The occurrence of $F_{1.5}$ was not regular in low sunspot years except during some rare magnetic disturbances in 1954-55.

5. foF2 and hrF2 AT FIXED HOURS OF THE DAY

In order to study the annual variation at fixed hours of the day, we have plotted in Fig.1.5, the monthly median

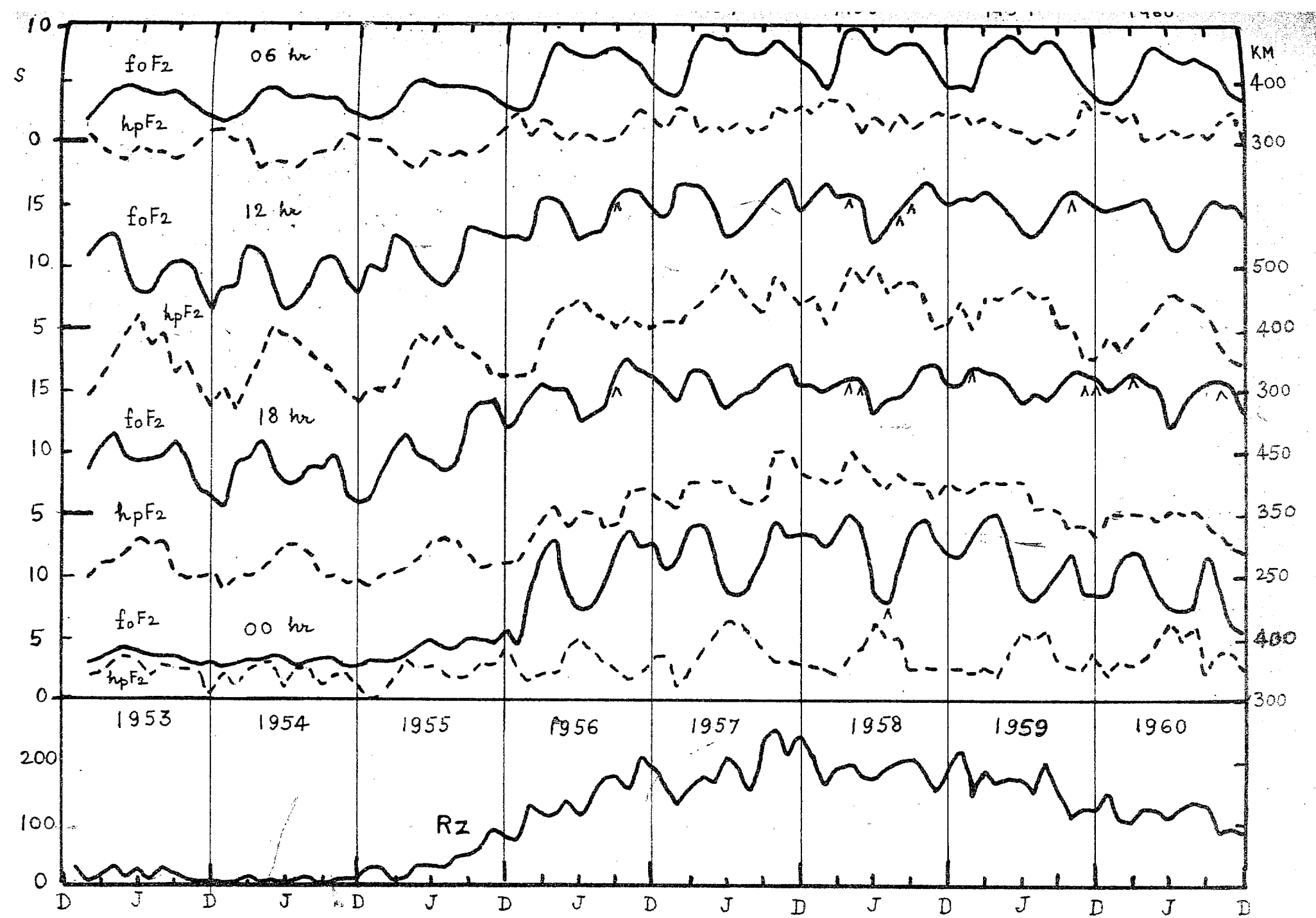

FIG. 15 MONTHLY MEDIAN foF2 AND hpF2 AT 06, 12, 18, AND 00 HRS AT AHMEDABAD, 1953-60 AND MEAN MONTHLY RELATIVE SUNSPOT NUMBER (ZÜRICH)

values of foF2 and hpF2 at 00, 12, 18 and 00 hrs. The monthly mean relative Zurich sunspot number is also shown at the bottom of the figure. Here are some main points :-

(1) With the advent of increasing sunspot number, the mean level of the parameters of the F2 region started rising, became maximum in 1957-58 and began to decline in 1960.

(2) The foF2 variation was fairly simple at these hours with minimum occurring in June-July and maximum in equinoxes and some winters.

(3) At 06 and 18 hrs, the dip in foF2 was more pronounced in January-February than in June-July, while at 12 and 00 hrs, the dip was sharp in summer and shallow in winter.

(4) There was hardly any seasonal variation in the midnight foF2 in low sunspot years 1953-55; but from 1956, strong seasonal variation was evident with foF2 4 to 5 times higher in winter and equinoxes and about 2 to 3 times higher in summer than those in the low sunspot period.

(5) The variation in hpF2 was not so clear though it showed a prominent peak in summer in low sunspots which corresponded well to the summer minimum of foF2.

(6) There was apparently no good correlation between the F2 parameters and the Zurich sunspot number.

6. VARIATION OF NOON foE AND THE SUB-SOLAR FREQUENCY K F1 FOR YEARS 1958-60

It would be worthwhile to compare the variation in the monthly median noon critical frequency of the E layer at Ahmedabad during 1958-60. It is well known that the E and F1 layers show a variation with cos χ though there are slight deviations from Chapman's law.

We have shown in Fig.1.6 the monthly median foE at noon, the sub-solar frequency K and the monthly mean solar flux at 3000 Mc/s in units of 10^{-22} watts $(m^2 cs)^{-1}$ measured at Ottawa and reported in the CRPL Bulletins, Part B series.

For studying the solar effect on the E layer, we have used the sub-solar frequency K. This was obtained by plotting on a double log scale the median foE observed at Ahmedabad against cos χ (or sec χ). The graph is usually a straight line showing that

$$foE = K (\cos \chi)^n$$

where χ is the sun's zenith angle. Its intercept on the frequency axis where $\chi = 0$ gives the value K and the slope of the line gives the exponent n. According to the Chapman theory, the value n would be equal to 0.25, while experimentally it has been found to be always higher. It varied between 0.27 and 0.33 at Ahmedabad. It is meaningful to study the variation of K since the cos χ element is normalised in this case. The following points are noteworthy from Fig.1.6.

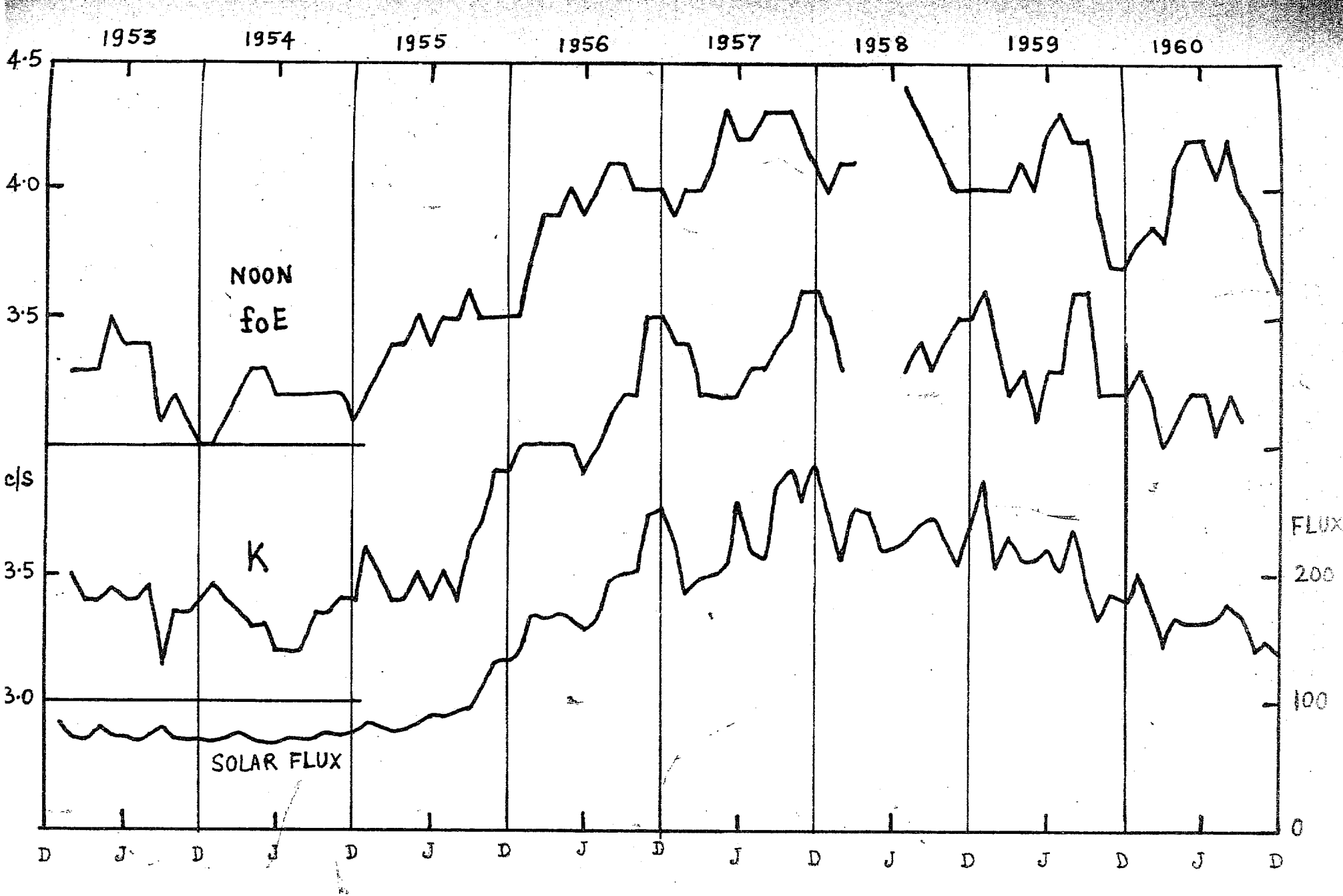

FIG.1·6 NOON MEDIAN foE , SUB-SOLAR FREQUENCY K AT AHMEDABAD AND 2800 Mc/s SOLAR RADIATION FLUX DURING 1953-60

(1) The noon foF2 exhibited an annual variation with maximum in summer and minimum in winter through the sunspot cycle. It was about 1.4 times larger on the average in high sunspot years than in low.

(2) K showed a peak value in winter around December. This means that if the sun were fixed overhead at the latitude of Ahmedabad, the critical frequency of the E layer would show maximum value in December. The reason can perhaps be attributed to the varying distance between the earth and the sun during a course of a year owing to the ellipticity of the earth's orbit. The sun-earth distance at perihelion on January 4 is about 3 per cent less than that at aphelion on July 6. This would mean a change of about 6 % in the solar ionising radiation assuming an inverse square law. This is, however, only about half of that found in K from summer to winter.

(3) There appears to be a good correlation between K and the 2800 Mc/s solar radiation flux when the flux exceeded about 100.

7. SPREAD F ACTIVITY OVER AHMEDABAD

Vertical radio pulses sent up in the ionosphere are sometimes reflected back not as sharp echoes but as diffuse patches. This occurs most during night and only in some seasons.

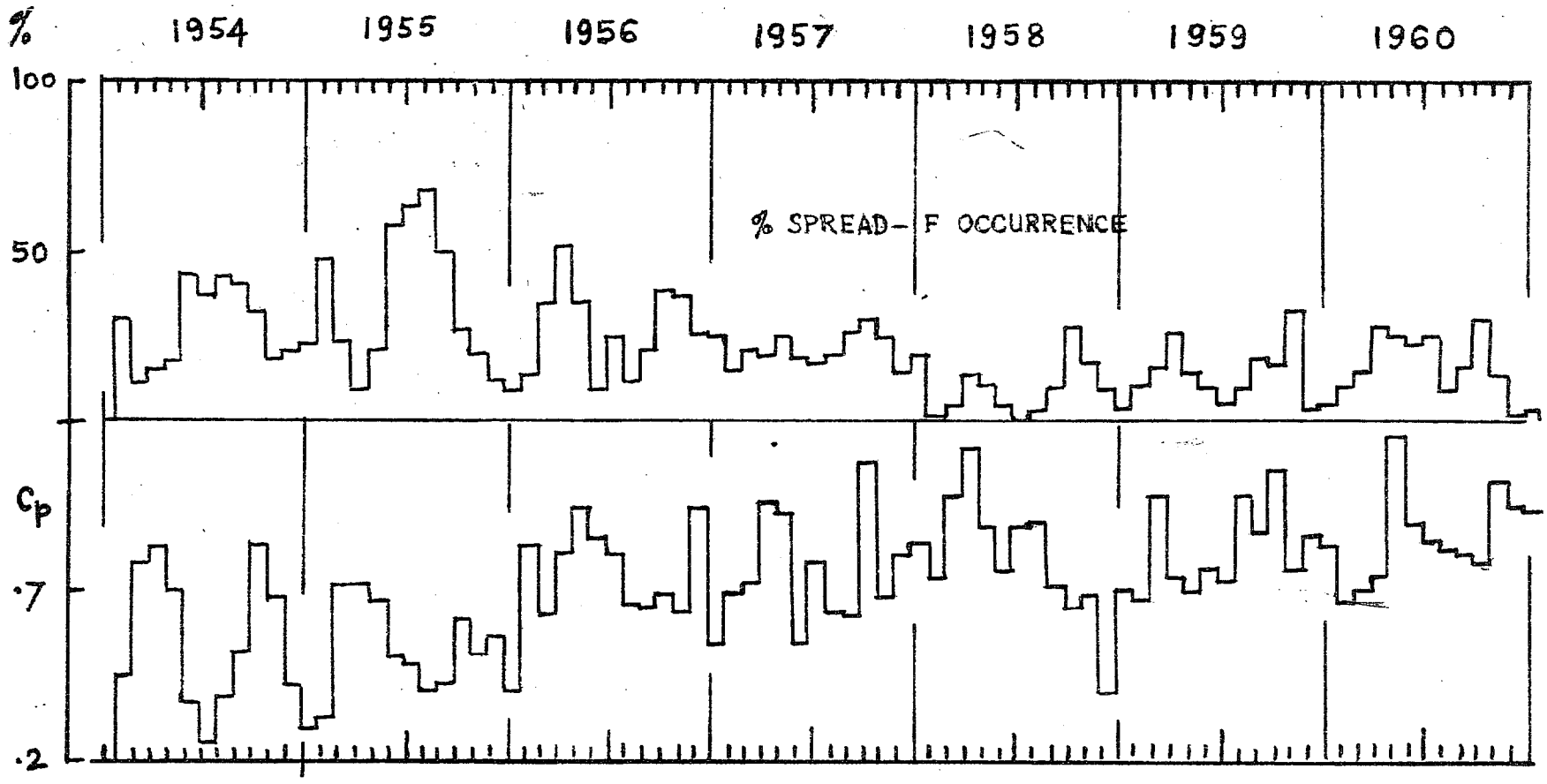

FIG.17-PERCENTAGE SPREAD-F OCCURRENCE BETWEEN 20-06 HRS AT AHMEDABAD AND MONTHLY MEAN MAGNETIC CHARACTER FIGURE Cp

Diffuse echoes indicate that the reflecting region is not uniformly stratified but contains inhomogeneous clouds of varying electron density. Dieminger (1951) studied different types of F-scatter and concluded that the F-scatter was mainly due to irregularities in the layer itself. There are a few instances of spread F occurrences at Ahmedabad during daytime upto 10 hrs, but it is rather uncommon.

Kotadia (1959) studied the diurnal, seasonal and the annual variation of the percentage frequency of spread F occurrences during night at Ahmedabad in the years 1954-57. We have extended the analysis to include the later period 1958-60 and represented the results of the annual variation of spread F in the whole period 1954-60 in Fig.1.7. The percentage frequency of spread F occurrence was calculated in each month between 20 and 05 hrs and a histogram drawn. The monthly mean magnetic character figure Cp is also shown in the figure. The following are its main features :-

(1) The seasonal variation of spread F showed maximum in summer in low sunspot years; minimum in summer and maximum in equinoxes in high sunspot years.

(2) The lowest spread F activity was in 1958, and the highest in 1955 exceeding 60 % in the summer of that year.

(3) It can be seen from the figure that the spread F activity at Ahmedabad decreases with increase in

SPREAD-F ON MAGNETICALLY QUIET AND DISTURBED DAYS AT AHMEDABAD

(AFTER KOTADIA)

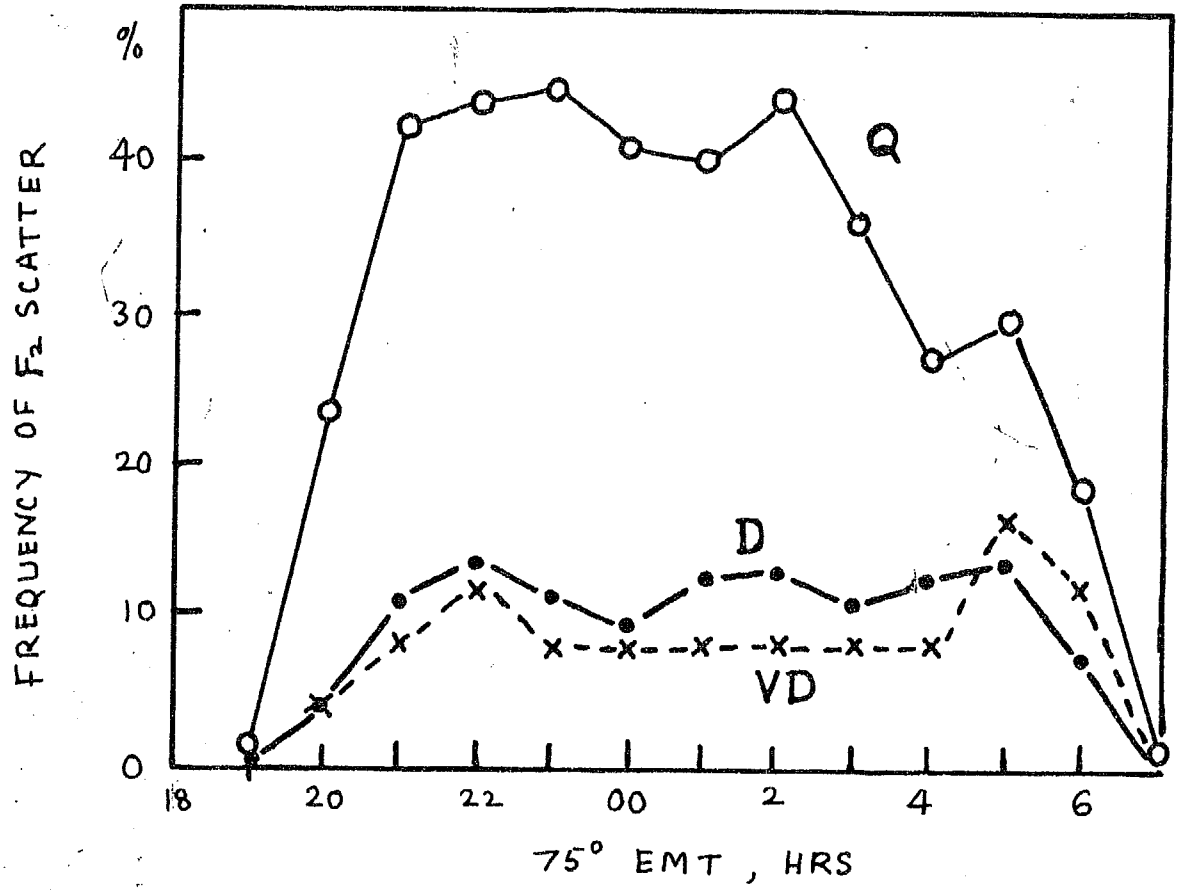

Q : QUIET DAYS, $\Sigma K < 15$, 118 DAYS

D : DISTURBED DAYS, $\Sigma K \geq 25$, 132 DAYS

VD : VERY DISTURBED DAYS, $\Sigma K \geq 35$, 25 DAYS

(1956-57)

FIG. 1·8

magnetic activity. This is in agreement with that found at Ibadan and is opposite to that found in middle latitudes (Wright et al 1956). Fig.1.3 shows more clearly the percentage variation of F2 scatter on magnetically quiet, disturbed and very disturbed days during 1956-57 at Ahmedabad.

Bebor (1951, 1956) postulated the existence of a spread F equator, a line of demarcation between those places which experience an occurrence minimum in the northern summer solstice and those which experience a minimum in the southern summer solstice. At medium and high latitudes, the diurnal variation of spread F occurrence has a maximum soon after midnight, whereas in low latitudes like Ahmedabad, the hour of maximum occurrence of spread F shifts from post-midnight hour in low sunspot years to a pre-midnight hour in high sunspot years. At equatorial latitudes, it occurs most frequently around 21 hrs local time. Thus, the spread F variation at Ahmedabad is more like that of equatorial stations like Kodaikanal in high sunspot years (Bhargava 1958). The changeover from low latitude type to middle latitude type of variation of spread F takes place at about 32° geomagnetic latitude in the northern hemisphere (Kotadia 1959). Singleton (1960) has studied a possible influence of solar and geomagnetic control on spread F at equatorial, middle and auroral zones and reported a certain symmetry of spread F occurrence about the geomagnetic equator rather than about the geographic or dip equators.

3. EFFECT OF GEOMAGNETIC STORMS ON THE EQ LAYER

3.1 General

Disturbances in the geomagnetic field are of frequent occurrence in years of high solar activity. These disturbances known as magnetic storms are caused directly or indirectly by the arrival of streams of charged particles emitted by the sun. Some magnetic storms are preceded by a solar flare by some 20-40 hours. Weak storms have a tendency to recur at 27-day intervals, which is also the solar rotation period, particularly in years of low solar activity; they are presumed to originate from what are called M-regions on the sun. The sudden commencement of a magnetic storm is a worldwide phenomenon which occurs simultaneously within a few seconds all over the globe. In the trace of the horizontal component H of the geomagnetic field in low latitudes, H is above normal for two to three hours in the initial phase of the storm. This is followed by a large decrease in H in the main phase of the storm, afterwhich starts a period of slow recovery which lasts for a few days. Magnetic storms are classified as slight moderate, moderately severe and severe depending upon the deviation of H from its mean value. At equatorial stations, a storm with ΔH between 250 and 400γ is termed moderately severe and with $\Delta H > 400\gamma$, severe. The list of principal magnetic storms recorded at the Kodaikanal Observatory are published regularly in the Indian Journal of Meteorology and Geophysics.

3.2 Magnetic storms and the ionosphere

During magnetic storms, solar charged particles arrive at outer boundary of the earth's atmosphere and generate X-rays and possibly shock waves or hydro-magnetic waves in the atmosphere, particularly in the auroral zone. Ionospheric storms may be caused by these, either directly or indirectly. The intimate connection between magnetic storms and the parameters of the F2 region at high latitudes was discovered by Appleton and Ingram (1936) from their observations during the 1932 Polar Year. At Slough, the F2 layer critical frequency was reduced during magnetic storms, while Berkner and Seaton (1940b) found that foF2 at Huancayo increased with increase of geomagnetic activity. An exception to this general behaviour at Huancayo occurred during large SC magnetic storms on 16-4-1933 and 24-3-1940 when the foF2 at Huancayo suffered large scale decreases within an hour after the SC (Berkner and others 1939, 1940a). Lejay (1943) found that midday values of foF2 at Washington and Slough often changed in opposite directions on magnetically disturbed days.

Since 1940 more detailed investigation of these phenomena have been carried out by many workers. From a study of the changes of the noon values of Δ foF2 (departures of foF2 from monthly mean noon values) during magnetic storms, Appleton and Piggott (1950, 1953) found that the depression in noon foF2 increased with latitude and that the depression was more in high sunspot years than in low. They discussed also

the diurnal control of ionospheric storminess. Rawer (1952) showed from a study of large number of magnetic storms that the effect on the F2 layer depended also on the season. Martyn (1953) obtained the disturbance daily variation (S_p) and storm-time variations (D_{st}) of Δ foF2 and Δ h'F2 for seven ionospheric stations and tried to explain the results by the drift theory. A review of this work and of the Japanese contribution was made by Maeda and Sato (1959). Matsushita (1959) carried out a more thorough investigation into the morphology of ionospheric storms utilizing data from 33 ionospheric stations over a ten-year period. He confined his study to the foF2 variation during magnetic storms and did not treat the virtual height h'F2 or hpF2 as they differ markedly from the true heights.

3.3 F region during magnetic storms at Ahmedabad

Kotadia (1960) studied the S_p and D_{st} variations of the F2 layer at Ahmedabad on the lines of Martyn (1953) and extended the analysis to other low latitudes stations Kodaikanal, Singapore, Delhi and Kolabanji. Kotadia and Ramanathan (1959) reported the results of their studies of storms during 1953-57 based on the analysis of 65 storms irrespective of their intensities. They grouped the storms according to their commencement time in four quarters of the day : (i) 00-05, (ii) 06-11, (iii) 12-17 and (iv) 18-23 hrs local time. The S_p variation in each storm was calculated in terms of a ratio of disturbed foF2

S_D VARIATION OF f_0F_2 AT AHMEDABAD (1953-57)

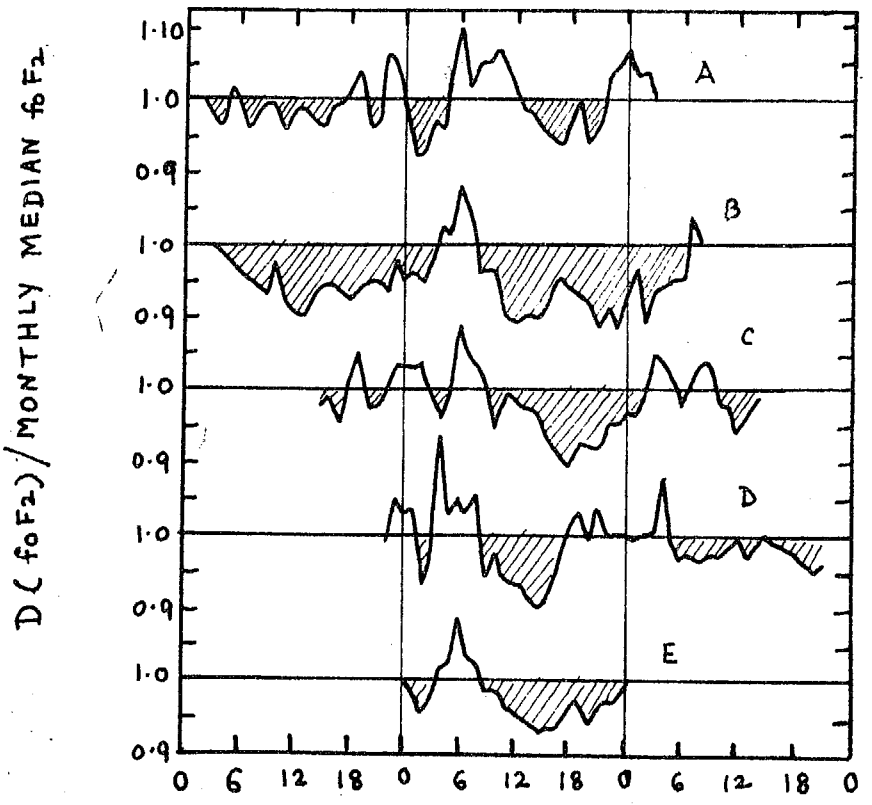

A : SC BET. 00-05 HR, 16 STORMS

B : SC BET. 06-11 HR, 15 STORMS

C : SC BET. 12-17 HR, 20 STORMS

D : SC BET. 18-23 HR, 14 STORMS

E : AVERAGE ON A DAY FOLLOWING THE SC (65 DAYS)

(AFTER KOTADIA AND RAMANATHAN)

FIG. 1·9

to the monthly median foF2. Fig.1.9 which is reproduced from their paper gives a summary of their results. The curve begins at a time around which the commencements were most frequent in the particular quarter. The last curve shows the mean variation of the ratio D(foF2)/median foF2 for one day following the SC. It can be seen that all the curves show a morning rise at about 06 hrs and daytime depressions on the day following the SC.

In order to study the effect of individual severe magnetic storms on the F region, we found Δ foF2 (foF2 on the disturbed day minus the corresponding monthly mean foF2) for one day prior to the SC and followed it up to 48 hours after the SC. We then grouped the storms which commenced in the forenoon and in the afternoon hours and taking nearest integral hour to the commencement time as zero, we plotted Δ foF2 for one day backwards and two days after the zero epoch day. These are shown in Fig.1.10 and 1.11 with times in 75° EMT. There were 3 severe storms in 1958 and 5 each in 1959 and 1960 as listed by the Kodaikanal Observatory. However, ionospheric data were not available for all the storms due to equipment failure and hence only the storms for which data were available are presented here. We have included also two severe storms in September 1957 for comparison. In all five storms which commenced before noon and six storms which commenced in the afternoon are shown in the figure. They are arranged with hours of commencement at increasing hours of the day. To distinguish the Sq variation from the Dst variation we have marked the

midnight hour of the day (00 hr) by the vertical lines.

The biggest storm in this series was on 11-2-53 with $\Delta H = 813\ \gamma$. The largest depressions in foF2 were caused by a storm on 31-3-50. The following main points emerge from the present study :-

(1) All severe storms do not produce the same kind of depression in foF2 in the first 24 hours after the SC.

(2) The majority of the storms commencing in the afternoon hours produced maximum depression in foF2 within 6 to 9 hours after the SC. In the case of forenoon storms, the depression in foF2 occurred mostly on the second day after the SC.

(3) It is interesting to note that in the case of severe magnetic storms, maximum depression occurred during night hours centred around midnight except in a few cases where the depression was a maximum in the evening.

(4) The rise in foF2 at about 03 hrs on the following morning after the SC was not evident in the case of afternoon storms.

9. SUMMARY OF AHMEDABAD RESULTS

We shall summarise in this section the important results obtained at Ahmedabad during the course of this investigation :-

(1) Owing to the favourable position of Ahmedabad (34° dip) near the peak of the latitudinal distribution of F ionization, large changes are observed with variation in solar activity.

(2) Seasonally, foF2 was minimum in summer and maximum in winter and equinoxes in both low and high sunspot years.

(3) Diurnally, foF2 was minimum at about 05 hrs and maximum between 14-16 hrs local time. The sharp daytime peak in the afternoon in low sunspot years was replaced in high sunspot years by a broad daytime plateau and an evening peak.

(4) With rise in sunspot activity, large changes occurred in the midnight value of foF2 with strong seasonal variation.

(5) The height of maximum density in the F2 layer was generally higher in summer than in winter.

(6) The sub-solar frequency of the E layer showed high correlation with the 2800 Mc/s solar radiation flux.

(7) The seasonal variation of the percentage frequency of spread F occurrence at Ahmedabad showed a maximum in summer in sunspot minimum, and in equinoxes in sunspot maximum. The spread F activity decreased with increase in magnetic activity.

(8) The effect of geomagnetic storms of severe type on foF2 was different in different storms. It was found that the maximum change in H did not always produce corresponding maximum changes in foF2.

(9) Maximum depression occurred within 6 to 8 hours after the onset of a severe magnetic storm which commenced in the afternoon hours and on the second day in the case of forenoon storms. The depressions took place mostly during night.

(10) The peak in foF2 at about 00 hrs in the morning on the day following the SC was not evident in the case of severe storms.

10. Discussion

From the study of the global distribution of the parameters of the F region, it is known that there are many anomalies which cannot be explained on the basis of Chapman's classical theory. For example, it is established that the F2 region is unsymmetrical about the geographic equator but is more symmetric about magnetic equator. Further it is found that a belt of low foF2 at noon (well marked in equinoxes) exists at or near the magnetic equator (Appleton 1946). This is known as the noon 'bite-out'. The bite-out effect is more pronounced in sunspot minimum during day time, whereas in sunspot maximum, the effect though smaller persists until about midnight (Martyn 1950). Associated with this effect are two anomalously

high peaks of foF2 in the afternoon lying about 15-20° on each side of the magnetic equator. In winter these two peaks appear to occur rather earlier towards noon.

Apart from this latitudinal anomaly, there is a distinct seasonal anomaly in foF2 in that at all places noon foF2 values in winter are greater than the summer ones particularly during high sunspot years. In the daily variation of foF2, it reaches a peak value not at local noon but 2-3 hrs afternoon. In addition to the above anomalies, there is, (i) a sunrise anomaly peculiar to winter and to equatorial latitudes in all seasons, consisting of a large decrease of foF2 before sunrise and an enhanced increase in the morning hours; (ii) an enhanced diurnal range of foF2 in winter and a reduced range in summer; and (iii) a tendency for the occurrence of more marked abnormalities in the daily variation of foF2 at sunspot minimum (Allen 1954).

Recently, Rastogi (1959) pointed out that discrepancies in the latitudinal variation of noon foF2 in low latitudes disappeared when true magnetic latitude of the station was considered instead of its geomagnetic latitude. Further, it was shown that at medium latitudes the seasonal variation of foF2 in low sunspot years was not similar in the two hemispheres. foF2 in the southern hemisphere showed maximum in summer and minimum in winter, while it showed minimum in summer and maximum in equinoxes in the northern hemisphere (Rastogi 1959).

From a study of true height profiles made by the Cavendish group of workers ranging from 36° N to 30° S dip, it was found that the electron density at a fixed height was lower in the afternoon than in the forenoon. This asymmetry was particularly marked in the equinoxes in a year of high sunspot number. It was also found that the values of N at different heights when plotted against magnetic dip showed a striking maximum in N at around 70° N (dip) in December and a corresponding one around 70° S (dip) in July (Crom et al 1955, 1960).

Theory of F region

Chapman (1931) showed that the absorption of monochromatic ionizing radiation from the sun would produce in the atmosphere q electrons per cc where q is given by

$$q = q_0 \exp (1 - Z - \sec \chi \, e^{-Z}) \quad \ldots \quad (1)$$

q_0 is the maximum rate of production of electron (and ion) for a vertically overhead sun, Z is height above the level of the maximum production measured in units of scale height H_0, and χ is the sun's zenith distance at the given time.

The mechanism of formation of electrons (& ions) is opposed by processes which result in neutralization of ions. The electron density at any time and height is determined by the continuity equation

$$\frac{dN}{dt} = q - \alpha N^2 \quad (2)$$

where α is the recombination coefficient in $cm^3\ sec^{-1}$ and N the electron density. Thus the Chapman model supposes that the level of maximum electron density is formed near the level of maximum electron production.

Apart from minor deviations this theory accounts in a general way for the global morphology of E and F1 regions but fails to explain the morphology of the F2 region.

Bradbury (1938) advanced an hypothesis to explain the formation of the F2 region. He suggested that for this region, α was inversely proportional to N, the rate of electron loss being βN where β was a coefficient of attachment of electrons to neutral atoms and that β decreased with height. He considered that the F2 region was a part of the F1 region lying above hmF1 and the observed increase in N was due to a substantial reduction of the effective coefficient of decay. This theory though it accounts better for the observed latitudinal distribution of foF2 fails to account for the observed rate of foF2 variation with sunspot cycle which is much larger than that of foF1. This suggests that the relation responsible for F2 ionization differs to some extent in quality from that which produces F1.

In an attempt to account for the peculiar morphology of the F2 region, Martyn (1947) introduced the concept of ionization transport and he revised the continuity equation as

$$\frac{dN}{dt} = q - \beta N - \mathrm{div}\ (\vec{v}\, N) \qquad (3)$$

where $\vec{v}$ is the transport velocity of electrons (and ions). Martyn stressed that the tidal forces, both solar and lunar, influence to some extent the daily variation of F2 except near the magnetic equator. Shimazaki (1959) extended Chapman's theory to include variable scale height, non-uniform recombination coefficient and motion of ionized medium and concluded that the Bradbury model for the F2 region was better than Chapman's if a positive gradient of temperature was taken into in the former.

Recently, there have been direct measurements of solar ionizing radiations by rockets in the spectral region below 1000 Å. Havens et al (1953) worked out the theory of the F2 region from observations of the solar spectrum from 8 to 100 Å by rockets and by extrapolating the data concerning both the atmosphere and the solar spectrum from 100 to 1000 Å and by assuming that the ionization is caused by the absorption of the solar radiation in the upper atmosphere. The picture depicted is as follows : the E region is caused by wavelengths shorter than about 100 Å, the ionization between E and F2 by wavelengths from about 100 to 200 Å, and F2 by resonance lines of He 304 and 584 Å.

From further rocket data, it became clear that the ionizing radiations were comprised primarily of the Lyman continuum, the He II resonance line at 304 Å and the X-ray spectrum below 100 Å (Friedman 1959). Rose and Benso (1959) found the intensity of the He II 303.8 Å emission line to be

quite high at 200 km. If it is assumed to be true, then the He II line may prove to be an important source of ionization in the F region.

It is difficult at this stage to formulate a general theory of the F region without adequate knowledge of the variation of the parameters through a sunspot cycle. More direct results from satellites are expected.

-:ooOOOoo:-

CHAPTER II

METHODS OF FINDING TRUE HEIGHTS OF REFLECTION OF RADIO WAVES IN THE IONOSPHERE FROM VERTICAL SOUNDING RECORDS. SCHMERLING'S METHOD

1. INTRODUCTION

The ionogram obtained by means of a vertical incidence sounding recorder represents the virtual height frequency curve. Recently, methods have been developed to derive the true heights of reflection of radio waves in the ionosphere.

These methods can be divided into two groups; (i) model methods and (ii) integral methods. The model methods were the outcome of earlier attempts by Appleton (1937), Appleton and Beynon (1940) and Booker and Seaton (1940). Ratcliffe (1951) developed a quick method of analysing ionospheric records, and in 1955, Beynon and Thomas suggested a modification in the original Appleton and Beynon method. All these models assumed some law of distribution of electrons with height in the ionosphere, usually a parabolic distribution. From Chapman's theory (1931) an expression for the electron density variation could be easily derived as

$$N(o;\ h, \chi) \approx (f_n\ (o;\ \chi)\ \left[1 - \frac{p^2}{d\eta^2(x)} \right] \qquad (1)$$

where $Y = h - h_m$ and $\tau = 2Y_2$, the semithickness of an equivalent parabolic region. Except for the lowest end of the Chapman's distribution curve, the portion below the level of maximum electron density can be approximated to a parabola. We shall summarise the different methods.

2. MODAL METHODS

2.1 Appleton and Beynon's method

The basic equation connecting virtual height h'(f) and the group refractive index μ' is

$$h'(f) = \int \mu' (f, f_N) dh \qquad (2)$$

f_N, the plasma frequency, is related to N through

$$N = 1.24 \times 10^4 \ f_N^2$$

where f_N is in Mc/s, for the ordinary ray.

Appleton (1937) showed that equation (2) may be integrated to obtain

$$h'(f) = h_0 + \frac{\tau}{2} (f/f_0) \log_e \left(\frac{f_0 + f}{f_0 - f} \right) \qquad (3)$$

where f_0 is the critical frequency of the layer; h_0, the height of the bottom of N-h parabola and τ, the semithickness.

Now, from an ionogram, the critical frequency of a particular layer (E, F_1 or F_2) can be found and one can also

compute, from a set of values f_1, f_2, ... etc. corresponding to virtual heights h'_1, h'_2, ... etc., the ratios f_1/f_0, f_2/f_0, and so on. Thus the function

$$1/2(f/f_0) \log_0 \left(\frac{f_0 + f}{f_0 - f} \right)$$

can be evaluated.

If we put $f/f_0 = \zeta$ and

$$\psi(\zeta) = \psi(f/f_0) = 1/2(f/f_0) \log_0 \left(\frac{1 + f/f_0}{1 - f/f_0} \right) \qquad (4)$$

we have a linear relation between $h'(f)$ and $\psi(\zeta)$ viz.,

$$h'(f) = h_0 + \tau \cdot \psi(\zeta) \qquad (5)$$

If we plot h' against $\psi(\zeta)$, the intercept on the height axis gives h_0 and the slope of the line the semithickness τ. If in this graph all points lie on a straight line, it means that the layer is parabolic. This method provides an useful test for parabolicity.

2.3 Booker and Seaton's work

Booker and Seaton (1940) gave a table of values of the function

$$(f/f_0) = \frac{1}{2}(f/f_0) \log_0 \left(\frac{1 + f/f_0}{1 - f/f_0} \right) - 1 \qquad (6)$$

This function is similar to the function $\gamma(\xi)$ which is equal to $1 + \phi(\xi)$. They tabulated values of $\phi(\xi)$ when ξ goes from 0 to 2. A rather remarkable result emerges and that is, at a frequency 0.334 f_0, the virtual height is equal to the height of the electron peak. This is usually tabulated as $h'F_2$ for the F_2 region in the routine scaling of the ionograms. This "frequency factor" affords a rough but quick method for estimating the height of the peak electron density. The following table shows some of the values of $\phi(\xi)$ given by Booker and Seaton.

Table 1.

ξ	0	0.648	.735	.757	.334	.837	.901	.925	.969
$\phi(\xi)$	-1	- 1/2	-1/3	-1/4	0	1/4	1/3	1/2	1

According to Booker and Seaton, the equation for $h'(f)$ becomes

$$h'(f) = h_m + \tau \cdot \phi(\xi) \qquad (7)$$

Using the values given in Table 1, one can calculate h_m and τ by solving a set of simultaneous equations. τ is also given by $(h_p - h_0)$.

It is seen, therefore, that the methods of Appleton and Beynon, and Booker and Seaton provide us the basic parameters of the electron distribution, namely, h_0, h_m, τ.

2.3 Method due to Ratcliffe

Ratcliffe (1951) gave a method for a quick reduction of ionograms. The analysis consists in constructing a set of h'f curves based on equation (3) for different values of semithicknesses on a transparent scale and finding the best fit with the observed records. This is possible since the function $\gamma(\xi)$ is known for various values of ξ from Booker and Seaton's table, and assuming different values of one can evaluate h(f) from (5) for any defined value of h_0.

For a Chapman layer, the integration in (3) cannot be performed analytically. But it has been done numerically by Pierce (1947) who tabulated the results similar to Booker and Seaton's. For a Chapman layer, the height of the maximum electron density is given by the virtual height at a frequency of 0.311 f_c. Ratcliffe (1951b) used linear and square-law profiles in addition to the parabolic model and employed a curve-matching technique.

A useful result obtained by Ratcliffe was an expression for the retardation of a radio wave due to its passage through a lower ionised region.

We have seen that equation 3 is true for all values of f and f_c. It gives the virtual height of reflection for a wave of frequency f less than f_c. If f is greater than f_c, the wave will penetrate the region and get reflected from a higher region which lies beyond the height of maximum electron

density of that region. The equivalent height of reflection in the latter case will, therefore, be much larger than when no layer is present below. If we denote the increase in virtual height by $\Delta h'$ then

$$\Delta h' = \tau[\gamma(\zeta)-1] = \tau \cdot \phi(\zeta) \qquad (3)$$

This group retardation formula is true only when the pulse traverses a semi-parabolic distribution completely. Ratcliffe has also given an expression for the retardation when a pulse passes through a part of a parabolic region.

Ratcliffe has introduced another useful parameter n_T, the total electron content in a column of unit cross-section of the ionosphere upto the level $h_m F_2$. This is given simply by

$$n_T = \frac{2}{3} \tau \cdot N_m$$

$$= \frac{2}{3} \cdot \tau \cdot (1.24 \times 10^4) f_0^2 \quad \text{el/m}^2 \text{ col.}$$

2.4 Beynon and Thomas' method

Beynon and Thomas (1956) have extended the application of Appleton and Beynon's method to cases of reflection from contiguous parabolic sections and have given an expression for the variation of virtual height with frequency in terms of the layer parameters and various degrees of truncation between the ionospheric layers. This method could be used in places where the correction to geomagnetic effect is very small.

To sum up: Appleton and Beynon's method tells us whether there is any deviation from parabolicity of the ionospheric regions. It is known that there are deviations and therefore the model methods cannot be applied to the regions other than parabolic. Another series defect in the model methods is the neglect of the effect of the magnetic field.

3. SHIMI AND WHILE'S WORK

There have been attempts to modify the model methods by taking into account the effect of the geomagnetic field. Shimi and While (1953) and Shimi (1953) computed h'-f curves for parabolic and linear profiles by integrating equation 2 numerically for various magnetic parameters applicable to different geographic locations. Their results can be applied to any one of the methods described in section 3.

4. GENERAL REMARKS ON MODEL METHODS

It is found in practice that actual N-h profiles seldom conform well to the simple shapes postulated in the model methods. This makes model methods unsuitable for detailed profile analysis. They are, however, useful for obtaining quick estimates of layer height and layer thickness. The method of estimating $h_F f_0$ based on a frequency factor $0.834\ f_0$ is very rough as it depends very much on the layer shape.

It is possible by the model methods to evaluate the

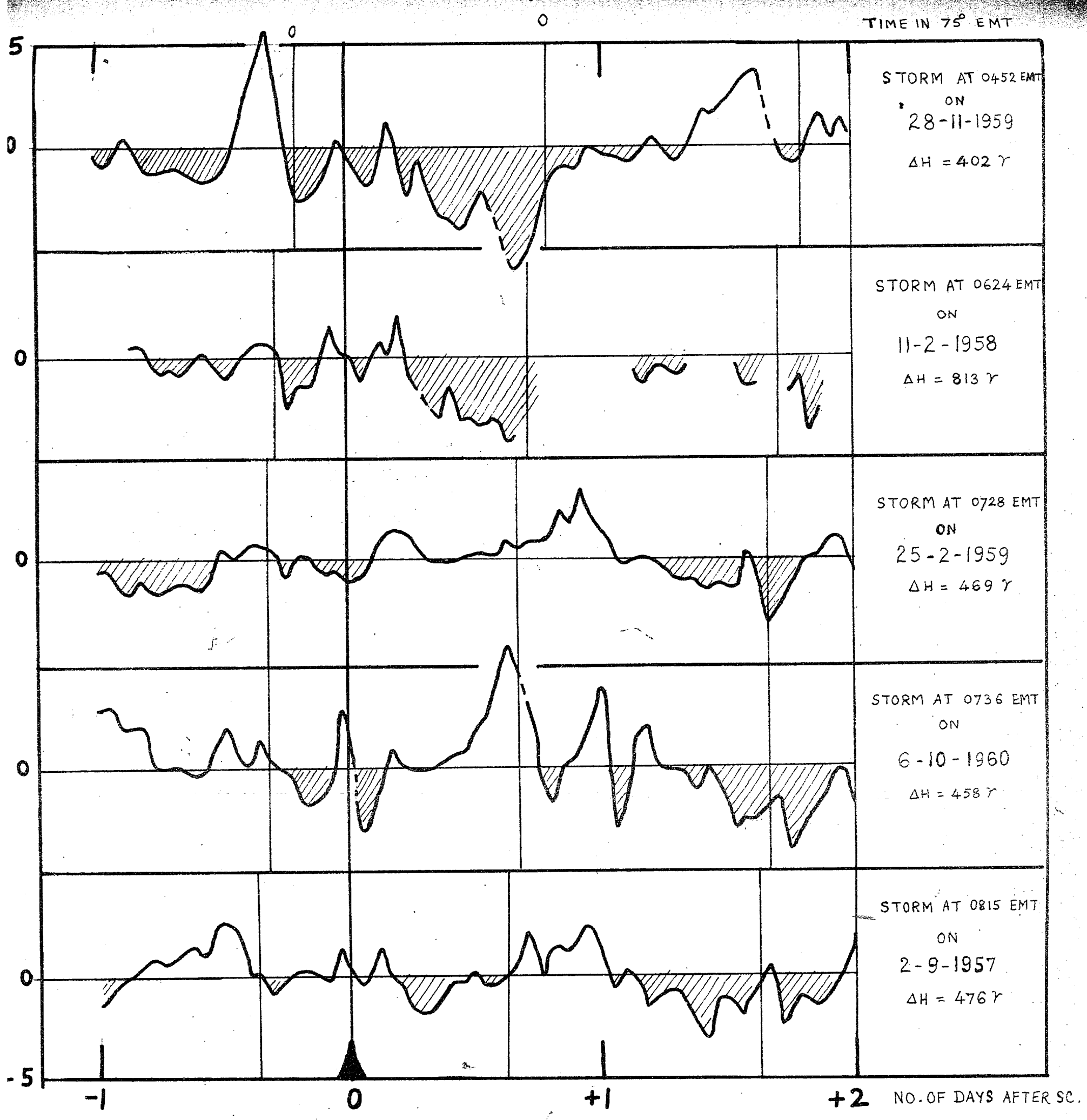

FIG. 1·10 STORM-TIME VARIATION OF f_0F_2 AT AHMEDABAD DURING SEVERE FORENOON MAGNETIC STORMS IN 1957-60

(MIDNIGHT 00 HR IS MARKED BY THIN VERTICAL LINE)

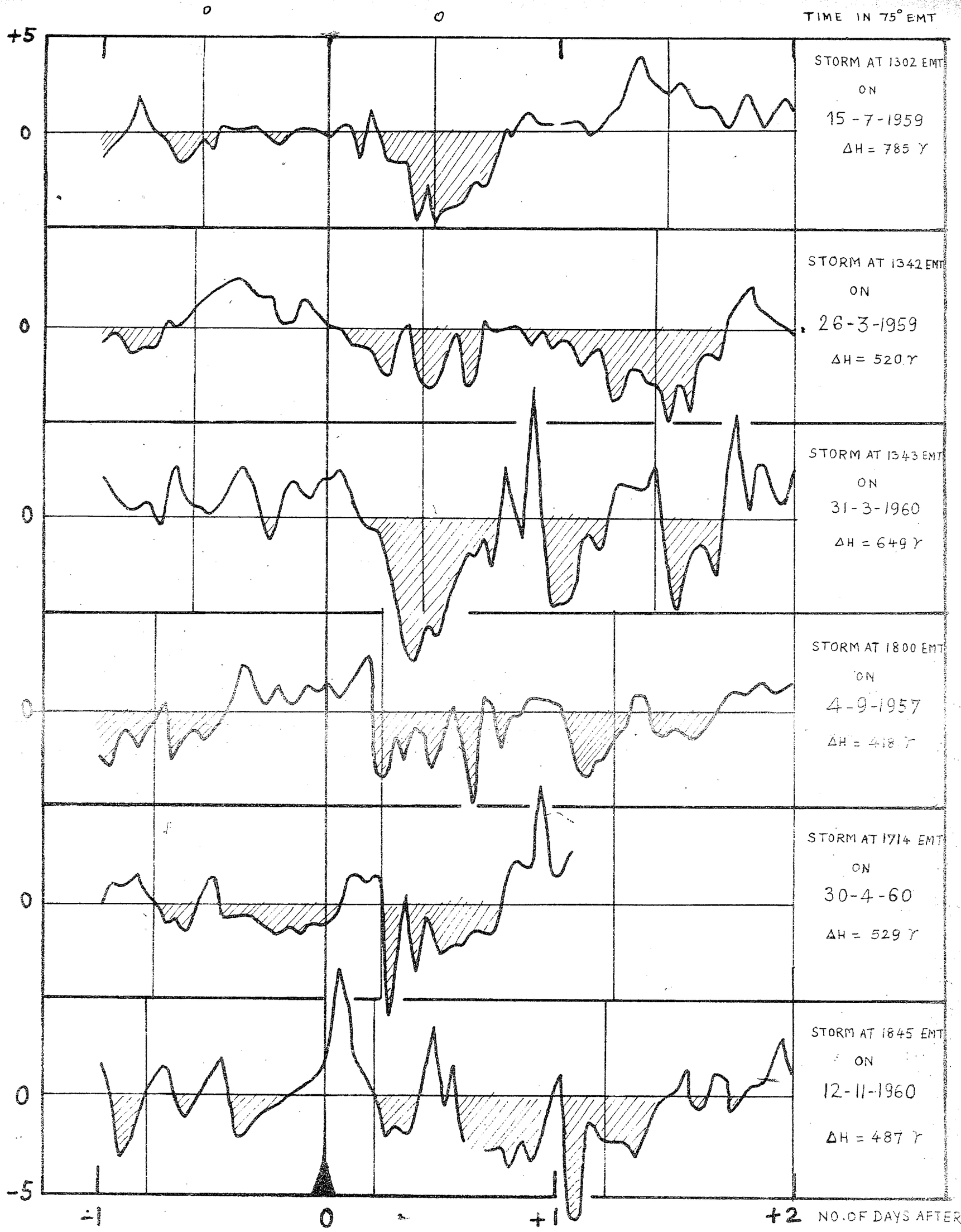

FIG. 1·11 STORM-TIME VARIATION OF f_0F_2 AT AHMEDABAD DURING SEVERE AFTERNOON MAGNETIC STORMS IN 1957-60

(MIDNIGHT 00 HR IS MARKED BY THIN VERTICAL LINE)

retardation of a pulse which completely penetrates lower half of a layer and is reflected back from a higher level. There is a drawback in such a method since no estimate of retardation suffered by a wave in the upper half of the layer was made. The h'-f curve which results from several layers of known shapes may be analysed by performing the analysis for the lowest layer first and then subtracting the retardation produced by this from the remainder of the h'-f curve before proceeding further with the analysis. Sreenivasan (1953) adopted such an approach for the analysis of some h'-f curves at Ahmadabad. We shall come to his method later. Such analysis is correct if the layer shapes between maxima of f are known fully. If the layer shape is Chapman-like, it is to be noted that it is asymmetrical and contains about twice as many electrons above the peak as below. It is not therefore justified to apply the retardation correction only to the lower half of the parabola.

6. INTEGRAL EQUATION METHODS

There was a constant urge to find more appropriate integral methods to overcome the two serious drawbacks of the model methods, namely, i) the 'a priori' assumption of a parabolic distribution of electron density, and ii) the neglect of the influence of the earth's field on the height distribution calculation.

We shall first review the attempts made ignoring the field and then the effects of the inclusion of the field.

5.1 Neglecting the geomagnetic field

Appleton (1930) showed that equation 2 may be inverted if the magnetic field is ignored. The result is

$$h(f_N) = \frac{2}{\pi} \int_0^{f_N} \frac{h'(f)}{\sqrt{f_N^2 - f^2}} \qquad (9)$$

Manning (1947) gave another method of deducting this result based on Laplace transform.

Evaluation of integral in (9) is facilitated if one makes the transformation, $f/f_N = \sin\theta$, since $f \leq f_N$; so that (9) reduces to

$$h(f_N) = \frac{2}{\pi} \int_0^{\pi/2} h'(\theta)\, d\theta \qquad (10)$$

For each point required on the N-h profile, the h'-f curve must be plotted in a scale $\theta = \sin^{-1}(f/f_N)$ and the area found with a planimeter. This frequent replotting makes the analysis lengthy and tedius. Pokoris (1940), Rydbeck (1940) and Manning (1947) analysed a few isolated h'-f curves by this method.

5.1.1 Kelso's method

Kelso (1952) used the Gaussian-Christoffel quadratures

to evaluate the integral (3) by numerical analysis. He showed that replotting can be avoided by performing the integration numerically and merely sampling the h'-f curve at predetermined multiples of f_y. These multiples are chosen to be equal increments of θ on the $h - \theta$ curve, so that Kelso's method is equivalent to stepwise integration under the $h' - \theta$ curve.

Kelso's method can be applied in a rapid manner by replotting each h'-f curve, one only, on a logarithmic frequency scale. The sampling points can be picked out by using a slider marked with the frequency ratios. Schmerling and Thomas (1956) used this method to obtain the electron distribution in undisturbed F2 layer. Sreenivasan (1958) applied the Gauss-Mehler quadrature to the no field case of true height determination for his analysis of Ahmedabad records during 1954-56.

5.3 Including the earth's magnetic field

Neglect of the earth's magnetic field was a serious limitation at places other than on the magnetic equator. Kelso (1954) and Budden (1955) showed how to calculate the true height distribution of electrons without assuming special form for the distribution and with due allowance for the magnetic field.

In this case, the generalised refractive index formula given by Appleton has to be used instead of that simple Sellmeyer formula. Neglecting electron collisions, the formula can be written as

$$\mu^2 = 1 - \frac{2x\,(1-x)}{D} \qquad (11)$$

where $x = \frac{f_N^2}{f^2} = \frac{Ne^2}{\pi m f^2}$; f_N, the plasma frequency.

N = number density of electrons

e, m = charge and mass of electron

f = exploring frequency of the wave packet

$D = 2(1-x) + 2 - Y^2 \sin^2\theta$

$Y = \frac{f_H}{f}$

$f_H = \frac{He}{2\pi mc}$, the gyrofrequency of the electron

H = total field intensity of the earth's magnetic field in Oersted

θ = propagation angle i.e. angle between the direction of the earth's field and the wave normal

$= 90 - \phi$ where ϕ is the dip angle

$S = \pm\sqrt{Y^4 \sin^4\theta + 4Y^2(1-x)^2 \cos^2\theta}$

c = velocity of light in free space in cm/sec.

The positive sign for the radical in the expression for S is for the ordinary component and the negative sign for the extra-ordinary component of the radio wave.

It is well known that the group velocity and hence the group height of reflection depends on the strength and direction of the magnetic field at a particular place. It is to be noted that equation 11 is for μ, the phase refractive index and the group refractive index μ' can be obtained from

$$\mu' = \mu + f\frac{\partial \mu}{\partial f} \qquad (12)$$

Thus μ is a function of x, Y and θ . Equation 11 can be written as

$$(\mu^2-1)\, Df^2 = 2x(1-x)f^2 \qquad (13)$$

Differentiating and simplifying this, we get

$$(\mu\mu' - \mu^2)\, D = 2\left[1-\mu^2-x^2+\frac{1}{S}(1-\mu^2)(1-x^2)\, Y^2\cos^2\theta\right] \qquad (14)$$

From (14), we can get $\mu\mu'$ and knowing μ, μ' can be calculated from (12). This formula is convenient and is accurate for the computation of μ'. Sreenivasan carried out this task of tabulating μ' for different values of f for the dip angle of Ahmedabad and plotted curves of (μ' . t) versus t, where $t = \sqrt{1-x}$, for the ordinary ray.

It is interesting to compare the effect of the magnetic field on μ, $\mu\mu'$ and μ' - (see Table 2).

Table 2.

	Zero field	With field
(1)	$\mu^2 = 1-\frac{f_N^2}{f^2} = 1-x$	$\mu^2 = 1-x\left[\frac{2(1-x)}{D}\right]$
(2)	$\mu\mu' = 1$	$\mu\mu' = \mu^2+\frac{2}{D}\left[1-\mu^2-x^2+\frac{(1-\mu^2)(1-x^2)}{S}Y^2\cos^2\theta\right]$
(3)	$\mu' = \frac{1}{\mu}$	$\mu' = \mu+\frac{2}{\mu D}\left[\quad,,\quad\right]$

3.3 Eidon's work

Although Shinn and Bhula were the first to reveal

the effect of the magnetic field on the electron distribution, the presumption of the parabolic model by them still remained. Budden (1955) could overcome this difficulty by solving the integral (3) by treating it as a limit of a matrix equation. Later, Schmerling (1957) and Thomas et al (1963) applied Budden's method to analyse ionospheric records.

Equation 2 may be rewritten as

$$h'(f) = \int_0^f \mu'(f, f_N) \frac{dZ(f_N)}{df_N} df_N \qquad (15)$$

To invert this equation, it must be assumed that Z and hence $\frac{dZ}{df_N}$ are monotonic functions of f_N in the range $0 \leq f_N \leq f$. Let h', Z and f now be considered as sets of discrete values, at equal increments Δf of f, such that

$$h'(n\,\Delta f) = h'_n$$
$$Z(n\,\Delta f) = Z_n$$
$$n\,\Delta f = f_n$$

where n is an integer. $\frac{dZ}{df_N}$ may be taken as fairly constant within each interval Δf, so that

$$\frac{dZ}{df_0} = \frac{Z_m - Z_{m-1}}{\Delta f}, \qquad (m-1)\Delta f \leq f \leq m\Delta f \text{ and } m \leq n$$

Equation 15 can now be replaced by a summation over a finite number of strips n as

$$h'_n = \sum_{m=1}^{n} (Z_m - Z_{m-1}) \int_{(m-1)\Delta f}^{m\Delta f} \frac{\mu'(n\Delta f, f_N)}{\Delta f} df_N \qquad (16)$$

$$= \sum_{m=1}^{n} (Z_m - Z_{m-1})\, M_{nm} \qquad (17)$$

where $M_{nm} = \frac{1}{\Delta f} \int_{(m-1)\Delta f}^{m\Delta f} \mu'(n\Delta f, f_N)\, df_N$

$= 0$ for $n > m$

$= 1$ for $n = 1$

Equation 17 can be written in the form of column and square matrices. Symbolically it has the form

$$h' = \underline{M}\,\underline{Z} \qquad (18)$$

Knowing h' from the ionogram, $\underline{M}$ can be evaluated after computing the elements M_{nm} by numerical integration. What we want is Z, the true height, and it can be solved by inverting the matrix $\underline{M}$. That is

$$Z = (\underline{M})^{-1} h' = \underline{L}\, h' \qquad (19)$$

The coefficients of matrix L need be calculated once for all for any given magnetic latitude and are then available for reduction of any number of records. As the method of analysis has assumed that h' is known down to zero frequency, some assumption must be made about the missing portion of the h'-f trace. The h'-f records usually terminate between 1-3 Mc/s at the low frequency end. It can be assumed with little harm that h' is constant down to zero frequency with a value equal to that at f_{min}.

Budden's method is best suitable for programming and feeding to an electronic digital computer. Thomas and Vickers (1953) have given details of programming. In laboratories where the electronic computer facilities are not available, this method is laborious. Schmerling (1953) has given an easy method for reduction of h'-f curves to N-h profiles including the effects of the earth's field and without the use of computing aids. It is of great practical value for workers who want to do the analysis manually.

6. MANUAL METHOD OF SCHMERLING

There are some methods which do not require the aid of a digital computer. See for example Jackson (1956), Kelso (1954, 1957) . These methods are more lengthy in execution and hence require considerable time for routine work.

Schmerling's method is closely similar to original Kelso method but is modified to include automatically the effect of the earth's magnetic field. Initially a computer is needed to prepare a set of frequencies at which the h'-f records are to be sampled. These sampling frequencies have to be computed specifically for the dip angle of a station from which the records are to be analysed. Once the sampling frequencies are found then they can be used to reduce any number of h'-f records to N-h profiles. Recently Schmerling and Ventrice (1959) have given tables of ratios of sampling frequencies to f_N applicable to any station with dip angle

lying between 0 and 30° on either side of the magnetic equator.

We can write equation 9 as

$$h(f_N) = \int_0^{f_N} g(f_N, f)\, h'(f)\, df \qquad (20)$$

where $$g(f_N, f) = \frac{2}{\pi \sqrt{f_N^2 - f^2}} \qquad (21)$$

If we substitute

$$\theta\ (f_N, f) = \frac{2}{\pi} \arcsin (f/f_N) \qquad (22)$$

then (20) reduces to

$$h(f_N) = \int_0^1 h'(\theta)\, d\theta \qquad (23)$$

θ is considered here as a function of f at a fixed value of f_N. The integration can be performed numerically without actually transforming the h'-f curves. If the area under each h'- θ curve is imagined to be divided up into K equal strips, the trapezium rule gives, approximately,

$$h(f_N) = \frac{1}{k} \left\{ h'(\theta_0) + h'(\theta_1) + \cdots h'(\theta_r) + \cdots h'(\theta_{k-1}) \right\} \qquad (24)$$

where $$\theta_r = \frac{2r+1}{2K} \qquad (25)$$

and r is an integer ranging from 0 to K-1. Then the true height can be obtained by averaging K values of h' read from

h'-f curve at specified frequencies given by the solution of (25) and (28). The accuracy increases with K_j but experience has shown that five or ten values are adequate in practice depending upon the smoothness of the h'-f curve.

If the field is included, $G(f_j, f)$ will have to be evaluated numerically and sampling frequencies can be obtained in a similar way.

Titheridge (1959) worked out a method which can be applied to both ordinary and extra-ordinary traces on the ionogram. The method is more lengthy and difficult in application for day to day analysis of large number of records though this gives somewhat better accuracy. More recently, Titheridge (1961) has outlined another method for the reduction of ionograms on the assumption that the complete real height curve can be represented by a single polynomial in f. This requires the aid of a digital computer and also has some disadvantages which he has discussed.

7. METHOD ADOPTED AT AHMEDABAD

We have used the method of Schmerling utilising Schmerling and Ventrice coefficients appropriate to our station (34° dip) and slightly modifying it to suit our requirements (Deganker 1961). The table of coefficients used in the analysis at Ahmedabad are given in a paper, a reprint of which is appended at the end of the chapter.

7.1 The procedure for reduction of ionogram

The procedure can be stated as follows :-

(1) Each h'-f curve was plotted in all its details on a logarithmic scale of frequency. The height scale was taken as 1 cm = 50 km. This gave sufficient magnification to reduce errors in reading heights.

(2) An extra-polation of the virtual height graph to low frequency (f = 0) becomes necessary, since the trace on the ionogram cannot be seen below 1.5 or 1 Mc. It was assumed that the minimum virtual height of the F2 layer at night was constant down to zero frequency. This will not introduce much error except at sunrise and sunset and in cases of night E. Normally, at sunrise and sunset, the h'-f curve was extended to zero frequency (if the lower layers were absent) taking into consideration the slope of the curve at f_{min}.

(3) During daytime, the minimum virtual height of E layer was taken as the bottom of the ionosphere. Large gaps in the h'-f curve due to deviative absorption was filled in by a reasonable estimate of the curve. If the E trace was invisible on the ionogram, due to ionospheric absorption or other causes, it was sketched in on the graph paper by using monthly median values. If the record at an integral hour was not available, the one nearest to that was taken for reduction.

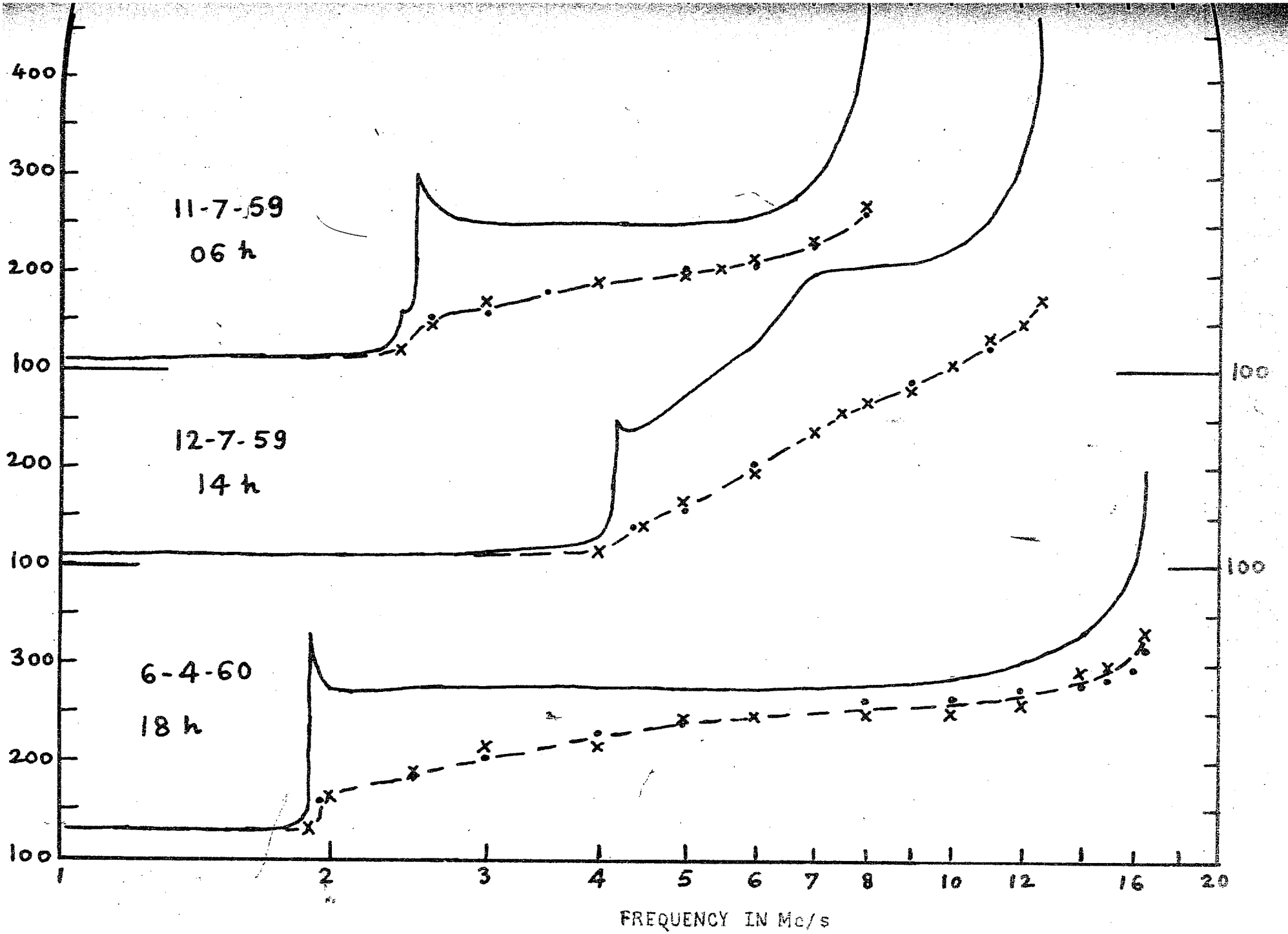

FIG. 2·1 TRUE HEIGHT PROFILES BY 10 POINT (...) AND 5 POINT (x x x) METHODS AT AHMEDABAD

(4) Parts of the virtual height curve obscured by blanketing E_s were filled in with a reasonable curve. The E_s trace itself was not considered while calculating the N-h profile.

Once the h'-f trace is transferred on a logarithmic graph paper, use of sampling frequency table is made. To obtain true height at some frequency, say, 10 Mc/s is to add up the virtual heights at the five frequencies given opposite the value fo = 10 Mc/s (see Appendix) in the table and to divide it by five. We should mention here that sufficient accuracy could be obtained by using 5 point method. Both 5 point and 10 point analysis were tried for a few h'-f curves and we found that they did not yield significantly different results. This is shown in Fig.8.1. A table of sampling frequencies in 1 Mc step for both 10 point and 5 point analysis is given in the Appendix.

7.2 Transparent overlays

Sometimes it is desirable to find true heights at small frequency intervals. This was done easily by preparing transparent overlays.

Three transparent overlays were prepared for use in the frequency range centred at 4.5, 10.5 and 16.5 Mc/s with f/f_0 marked on them in the same logarithmic scale as that of frequency on the graph paper. By sliding the overlay in a particular frequency range, one can determine the true height

at any desired frequency on the h'-f curve. Mean of the five (or ten) virtual heights scaled at intersections of the h'-f curve with each of the sampling points marked on the overlay gives the true height at that point. To obtain h_mF, the index line has to be aligned with f_oF_2. In this way complete true height profile was obtained from f_N = 1 to $f_N = f_oF_2$. From this true height curve, f_N values were read off at each 20 Km height interval from the bottom of the layer to h_mF. The f_N values thus obtained were converted to N values from the relation $N = 1.24 \times 10^4 f_N^2$. A final table giving N at each hour at each 20 Km height interval from 120 Km to h_mF during day and from the base of the F layer to its h_m during night was prepared. This has now become a standard practice of representing N(h, t) data. h_mF, N_mF, h_o, N_o and y_m could also be tabulated at each hour. A sample table is shown in Appendix II. This complete process took about 20 minutes per record. We shall report in the following pages the results of our true height calculations.

Reprinted from the "Proceedings of the Indian Academy of Sciences," Vol. LIV, 1961

CHANGES IN THE ELECTRON DENSITY DISTRIBUTION IN THE IONOSPHERE OVER AHMEDABAD ASSOCIATED WITH SOLAR FLARES AND MAGNETIC STORMS

Part I. July 10–19, 1959

By
S. S. Degaonkar

Reprinted from "The Proceedings of the Indian Academy of Sciences", Vol. LIV, No. 1, Sec. A, 1961

CHANGES IN THE ELECTRON DENSITY DISTRIBUTION IN THE IONOSPHERE OVER AHMEDABAD ASSOCIATED WITH SOLAR FLARES AND MAGNETIC STORMS

Part I. July 10–19, 1959

BY S. S. DEGAONKAR

(*Physical Research Laboratory, Ahmedabad*)

Received January 5, 1961

(Communicated by Dr. K. R. Ramanathan, F.A.SC.)

INTRODUCTION

THE present paper contains data of electron density distribution in the ionosphere over Ahmedabad in a highly disturbed period in July 1959 and a brief discussion of the findings. From the vertical soundings made at the Physical Research Laboratory, the true heights of reflection of the various frequencies were calculated using the tables of Schmerling and Ventrice (1959) and modifying them for the magnetic latitude of Ahmedabad (Dip 34°). As is well known, what we get from the soundings are the virtual heights of reflection h' of pulses of different frequencies where

$$h' = \int_0^{h_0} \mu'(f, f_0)\, dh. \qquad (1)$$

In equation (1), μ' refers to the group refractive index for ordinary waves of frequency f, h is the height above ground, h_0 is the height of reflection of waves of frequency f_0; and f_0 is related to the electron density N by the relation

$$N = 1{\cdot}24 \times 10^4 f_0^2$$

where N is expressed as the number of electrons per cm.^{3}, and f_0 as Mc./sec.

μ' is a complicated function of f and N and the strength and direction of the earth's magnetic field. Knowing h' for different frequencies, we have to determine the values of the geometric height h. The equation can be solved only by numerical analysis, using a lamination method in which the integral is replaced by a discrete sum over a number of suitable strips (*see* Thomas and Vickers, 1958).

Equation (1) can be written as

$$h'(f) = \int_0^{f_0} \mu'(f, f_0) \frac{dh}{df_0} df_0. \qquad (2)$$

The integral equation (2) can be treated as the limit of a matrix equation $h' = \mathrm{MD}h$.

The coefficients in the matrix equation can be solved either by inverting the matrix, or by a step-by-step solution for each strip. The accuracy can be increased as much as we desire by choosing sufficiently small intervals. For rapid reduction this method requires a digital computer which was not available.

The manual method of Schmerling (1958) allows for the effect of the earth's magnetic field, assumes only that the electron density increases monotonically with height and is convenient to use and sufficiently accurate. The true height corresponding to the frequency f_0 is given by

$$h(f_0) = \frac{1}{n} \sum_{1}^{i=n} h'(f_i) \qquad (3)$$

where h' is measured in kilometers and the f_i^s are the frequencies at which the virtual heights are read to give $h(f_0)$. The frequencies f_i depend on the end frequency f_0.

Using this method and the tables of coefficients given by Schmerling and Ventrice (1959) the values of the coefficients for the dip latitude of Ahmedabad which is 34° N. and the gyrofrequency 1·18 Mc./s. were interpolated. For calculating the coefficients, the values of dip angle and the total magnetic field at ionospheric heights are required to be known accurately. Schmerling's table provides the coefficients only up to 13·5 Mc./s. but since at Ahmedabad, the F_2 layer critical frequencies often go beyond 16 Mc./s. it became necessary to extend the column of coefficients to 16·5 Mc./s. by extrapolation. These coefficients which are in the form of ratios f_i/f_0 for given values of f_0, within the ranges given, define the sampling frequencies f_i at which h' are to be read from the h'–f curve to give $h(f_0)$. The sampling frequencies can be chosen either at 10 points or 5 points. We compared the results by both the 10-point and the 5-point methods and since they were found to agree well, we decided to adopt the 5-point analysis generally and use the 10-point method at frequencies near which there were rapid changes of h'. Table I gives the coefficients used.

TABLE I

10 *coefficients for calculating* h *from* h'f *over Ahmedabad*

	f_0 Mc./s.								
	16·5	13·5	12·0	10·5	9·0	7·5	6·0	4·5	3·0
f_i/f_0 ..	0·995	·995	·995	·995	·995	·995	·995	·994	·993
..	·965	·965	·965	·965	·965	·964	·963	·963	·962
..	·914	·912	·911	·910	·909	·908	·906	·905	·906
..	·841	·839	·838	·836	·835	·833	·830	·827	·824
..	·750	·748	·747	·745	·743	·741	·737	·733	·727
..	·641	·639	·638	·637	·635	·632	·629	·624	·616
..	·517	·515	·514	·513	·511	·509	·506	·501	·496
..	·380	·378	·377	·376	·375	·373	·370	·367	·366
..	·230	·230	·230	·229	·228	·227	·226	·225	·226
..	·077	·077	·077	·077	·077	·076	·076	·077	·078

TABLE II

5 *coefficients for calculating* h *from* h'f *over Ahmedabad*

	f_0 Mc./s.								
	16·5	13·5	12·0	10·5	9·0	7·5	6·0	4·5	3·0
f_i/f_0 ..	0·985	·984	·984	·984	·983	·983	·983	·982	·981
..	·880	·878	·877	·875	·874	·872	·870	·868	·867
..	·700	·696	·694	·693	·691	·688	·685	·680	·673
..	·450	·448	·447	·446	·444	·442	·440	·435	·432
..	·154	·154	·154	·153	·153	·152	·152	·152	·153

Tables of sampling frequencies f_1, $f_2 \ldots f_{10}$ for the 10-point method and of $f_1, f_2 \ldots f_5$ for the 5-point method were prepared by multiplying the

frequencies from 1 Mc./s. to 20 Mc./s. at 0·5 Mc./s. intervals by the above coefficients in the appropriate frequency ranges. To obtain the true height at a particular frequency f_0, the virtual heights at 10 (or 5) frequencies indicated opposite the value of f_0 in the table (not given here) are added up and their average found.

Later on, a procedure was adopted for the rapid reduction of h'-f curves to N(h) profiles. Each h'-f trace was sketched on a simple log graph paper with frequencies on a logarithmic scale. Three different transparent sliders were prepared with sampling ratios marked on them in the same scale for datum f_0 frequencies of 4·5, 10·5 and 16·5 Mc./s. Within the range of accuracy of the slider, it was then only necessary to align the datum with the frequency on the record for which h is required, to read off h' at marked points on the slider and to take the mean. This procedure is quicker and has the advantage that it serves to obtain the true height at any desired frequency on the h'-f curve.

The data presented here relate to the period when solar activity was exceptionally high. There were as many as seven solar flares of major importance between the 10th and 17th July 1959 and three great magnetic storms were associated with them. Table III lists the solar flares with their occurrence times in 75° E.M.T. and in Table IV are listed the three magnetic storms.

TABLE III

Short wave fade-outs

Date	Time of commencement	Importance	Ionospheric effects
10–7–1959	0710	3+	Slow
	1014	3+	G
13–7–1959 ..	0252	3	G
14–7–1959 ..	0825	3+	S
	1900	3+	Slow
16–7–1959 ..	1808	3	S
17–7–1959 ..	0214	3+	S

G—gradual; S—sudden

(From the *Transactions of American Geophysical Union*, 1960, 41, 87.)

TABLE IV

Date	Start of SC at Kodaikanal 75° E.M.T.	Date	Approx. end of storm 75° E.M.T.	Intensity	H in γ
11–7–1959	2128	12–7–1959	19xx	*m*	168
15–7–1959	1302	17–7–1959	04xx	*s*	785
17–7–1959	2138	19–7–1959	16xx	*ms*	327

—(From the *Indian Journal of Met. and Geophy.*, 1960, **11**, 86.)

Due to the kindness of the Director of the Alibag Observatory (Dr. P. R. Pisharoty), we are enabled to reproduce the H magnetograms of Alibag on these days (Fig. 1).

It can be seen that the storm on the 15th was of very severe type.

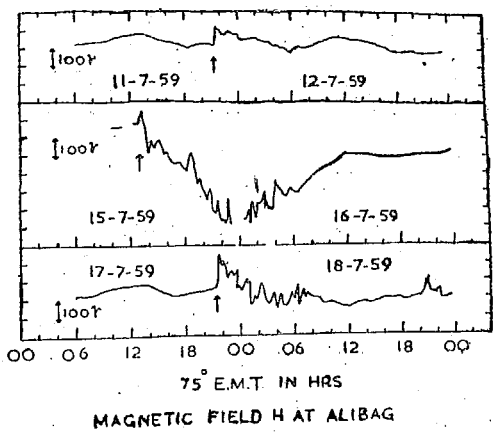

FIG. 1.

Results of true height analysis.—In Figs. 2 and 3 are plotted the electron densities at every 10 km. interval starting from the bottom of the E-layer during day, and of the F-layer during night. Lines of equal density were drawn at intervals of 2×10^5 el./c.c. Such a representation shows up the true changes of the heights of particular density levels. These results are based on the reduction of all hourly h'-f records. Some half-hourly records too were utilised, particularly when they showed somewhat different characteristics in comparison with the neighbouring hourly records. When an hourly record was missing, the one nearest to that one was taken for

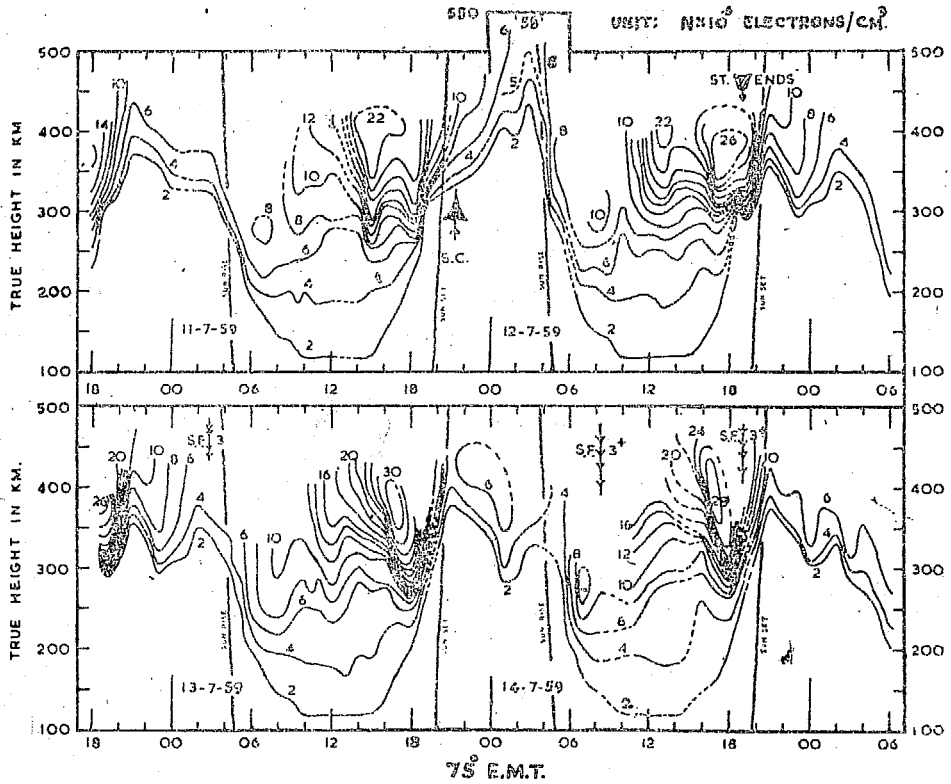

ELECTRON DENSITIES OVER AHMEDABAD 11 TO 14 JULY 1959

FIG. 2.

reduction. Whenever E-region cusps were not visible on the ionograms (due to absorption or other causes), the E–F transition was sketched in from the monthly median values of f_0E. As the F-layer is most sensitive to magnetic disturbances, it is believed that the present study will be able to throw some light on their characteristic features. We shall now discuss the results.

I. The storm on the 11th was preceded by a flare on the 10th. It was of the SC type and moderate in character. The time of onset of the storm at Alibag is marked on the diagram by a big arrowhead. The storm occurred at night and the oscillations built up in the F-region can be clearly seen. The peak oscillation took place at about 03 hrs. on the 12th, nearly 5½ hrs. after the onset of the storm. If we compare particular density levels on this night with those on the previous and the following night, we can see that the levels had gone up by more than 100 km. at 03 hrs. on the 12th.

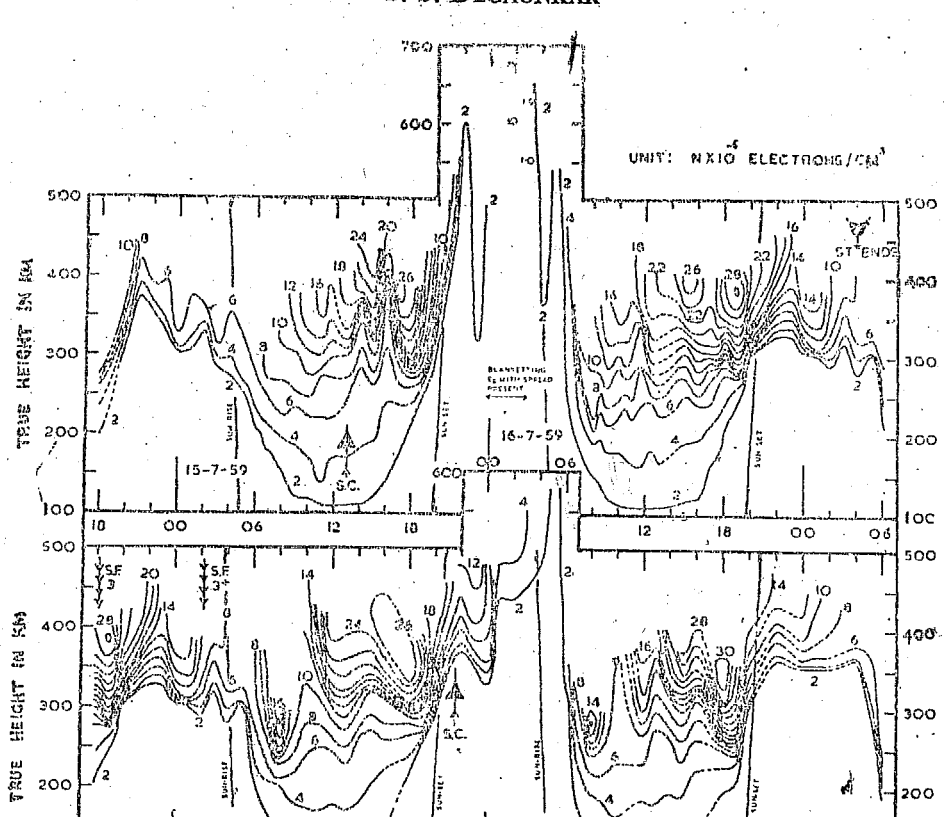

ELECTRON DENSITIES OVER AHMEDABAD 15 TO 18 JULY 1959

FIG. 3.

The rise in height was associated with a fall in electron density. The storm ended at about 19 hrs. on the 12th.

The variation is better appreciated when we compare the density distribution on the 13th which was a magnetically quiet day. The distribution on the 14th was more or less similar to that on the 13th.

Another big solar flare was observed at 0825 hrs. on the 14th. This flare produced a sudden short-wave fade-out for over an hour and during that period, ionosondé records could not be obtained. It would be of interest to know whether the flare caused any immediate enhancement of ionization in the F-layer. However, radio pulses of relatively small power are inadequate to probe this.

Yet another solar flare occurred at 19 hrs. (about sunset) on the 14th but this could not be observed at Ahmedabad; it would have certainly caused changes in the ionosphere in the sunlit portions of the atmosphere.

II. The intense magnetic storm which commenced at 1302 hrs. on the 15th induced perturbations within an hour of its onset. The undulations were built up with increasing amplitude, the peak occurring sometime between 00 and 02 hrs. on the 16th. The exact peak intensity of the oscillations could not be followed owing to two reasons: (1) an unusually strong blanketing type of E_s occurred with multiple reflections and spread echoes in the ionograms, and since the maximum electron densities were low, the E_s partly blanketed the trace. (2) As the layer heights were very great, the trace might have gone beyond the scale of the record which was nearly 900 km. In any case it is evident that the amplitude of the oscillations were of the order of 300 km. The whole layer was dilated and this was accompanied by a steep fall in electron densities. The period of oscillations was roughly 2 hrs. in the beginning. It is curious to note that between 21 and 23 hrs., the $f_{\text{min.}}$ trace suffered group retardation because of the presence of low-level ionization below the F-layer. The distribution of electrons below the F-layer could not however be determined with exactness.

The storm continued to influence the ionosphere till 19 hrs. on the 16th. Once its influence weakened, the electron densities increased and the layer heights dropped to 300–350 km.

III. Before discussing the last storm, we should like to make a remark on the high electron concentrations observed at relatively low levels between 250 and 280 km. at about 08 hrs. on the 17th and at about the same time on the 18th. We have calculated the total electron content n_T up to $h_m F_2$ at each hour on all these days. (These are given in the Appendix in units of 10^{11} el./cm.^{2} col.) The total electron content also shows peaks in the early morning hours on the 17th and 19th. The peak electron density of 26×10^5 el./cm.^{3} at 12 hour on the 17th was exceptionally high for July at that hour.

The storm which commenced at 2138 hrs. on the 17th showed similar perturbations but of less amplitude. The peak oscillation occurred at about 05 hrs. on the 18th, and the undulations continued till 16 hrs. on the 19th. The period of the oscillations was about 3 hrs. to start with.

The following points stand out:

(1) The perturbations produced by magnetic storms in low latitudes are mainly in the F-layer. The ionosphere below 200 km. remains relatively unaffected.

(2) During a magnetic storm the layer heights go up, accompanied by sharp falls in electron densities. There is comparatively little or no F-scatter.

(3) The total electron content also undergoes wide fluctuations during a storm. The daytime peak of n_T splits into several maxima as compared to a single peak on an undisturbed day. There is a tendency for the total content to be subdued during daytime when a magnetic storm is in progress.

(4) It is interesting to note that the daytime h_mF is definitely lower than h_pF_2 both on quiet and disturbed days (Figs. 4 *a* and 4 *b*). The difference

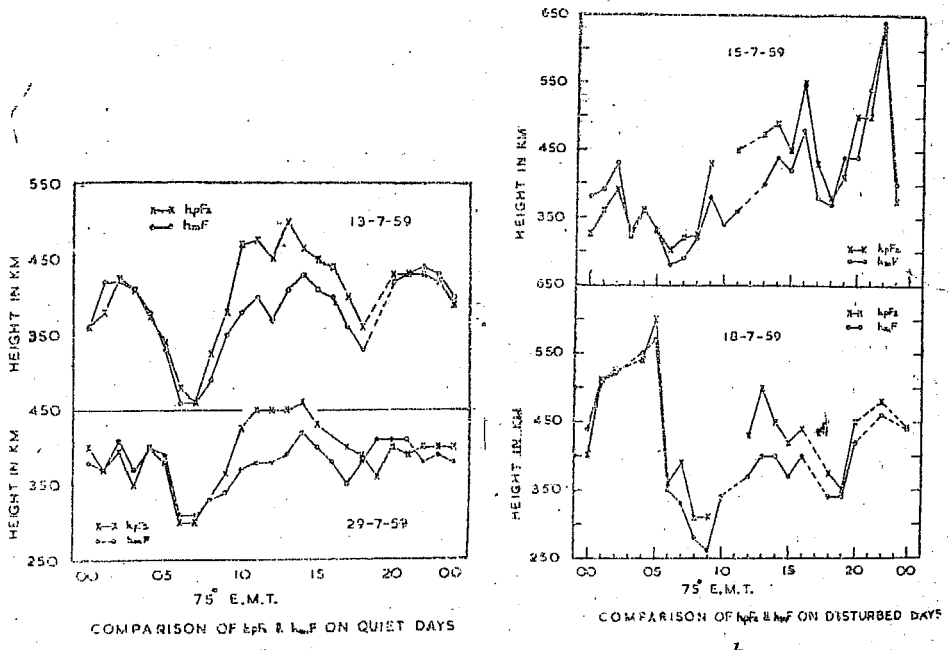

FIG. 4.

between h_pF_2 and h_mF is not great at night hours, but during daytime h_mF is lower by 50–60 km. than h_pF_2. It may be remembered that h_pF_2 is based on the assumption of a parabolic model taking the actual height to be the virtual height at 0·834 of the critical frequency of the F_2 layer.

SUMMARY

The paper discusses the results of calculation of electron density—height profiles of the ionosphere in a highly disturbed period in July 1959 from the vertical soundings made at Ahmedabad. After a brief account of the method

of calculation (following Schmerling and Thomas), tables of coefficients for calculating the true heights from the h'-f curves of Ahmedabad are given. Charts of equal electron density at intervals of 2×10^5 electrons/c.c. are presented for each day during the period 10 to 19 July.

An appendix is added giving the hourly values of maximum electron density NmF and total electron content n_T for all the days.

ACKNOWLEDGEMENTS

A good amount of preliminary work required for calculating electron density profiles was done by Dr. S. R. Sreenivasan. The thanks of the author are due to him for making available his working papers and thesis.

The author also wishes to express his thanks to Prof. K. R. Ramanathan under whose guidance the present study was carried out.

REFERENCES

1. Schmerling, E. R. and Ventrice, C. A. — *J. Atmosph. Terr. Phys.*, 1959, **14**, 249.
2. Thomas, J. O. and Vickers, M. D. — *D.S.I.R. Radio Research, Special Report No.* 28, 1958.
3. Schmerling, E. R. .. *J. Atmosph. Terr. Phys.*, 1958, **12**, 8.
4. Sreenivasan, S. R. .. *Ph.D. Thesis*, Gujarat University, 1958 (Unpublished).

APPENDIX—*July* 1959

Time \ Day	10		11		12		13		14	
E.M.T. 75°	N_m	n_T	N_m	n_T	N_m	n_T	N_m	n_T	N_m	n_T
0	59	47	68	55	75	28	70	28	61	31
1	..	..	..	37	60	53	61	53	61	33
2	..	..	61	44	58	32	52	32	52	38
3	61	49	66	53	58	32	56	32	55	38
4	48	48	75	42	58	28	52	28	..	..
5	61	59	65	57	89	34	51	34	37	30
6	88	41	79	..	..	38	74	38	64	47
7	116	61	85	61	84	56	92	56	114	83
8	..	..	72	118	116	94	100	94	85	79
9	..	..	85	70	83	143	105	143	..	..
10	..	..	104	163	90	170	112	170	..	..
11	..	..	..	172	127	213	164	213	179	235
12	..	..	140	212	194	219	170	219	164	207
13	206	232	..	272	226	272	194	272	179	224
14	215	279	226	207	194	297	226	297	216	275
15	226	269	243	253	210	285	261	285	..	..
16	194	191	216	234	243	282	298	282	279	283
17	179	192	223	222	279	249	314	248	287	211
18	159	119	..	..	..	180	272	180	261	152
19	134	90	194	172	261	..	..	..	..	..
20	96	85	150	155	194	86	115	86	137	118
21	64	47	..	100	124	24	56	24	59	22
22	74	47	81	76	107	39	72	39	70	49
23	74	54	81	62	92	42	72	42	64	53

N_mF in 10^4 electrons/c.c.
n_T in 10^{11} electrons/cm.^{2} col.

APPENDIX—*July* 1959 (*Contd.*)

Time \ Day	15		16		17		18		19	
E.M.T.	N_m	n_T	N_m	n_T	N_m	n_T	N_m	n_T	N_m	n_T
0	70	50	..	..	147	91	98	79	127	84
1	63	43	15	13	140	62	25	27	100	61
2	79	63	..	..	100	67	46	35	90	47
3	64	18	15	14	90	61	..	..	..	..
4	61	43	25	12	79	60	32	23	70	34
5	61	44	20	21	61	14	16	19	61	36
6	62	43	45	62	79	79	21	30	81	63
7	96	70	100	79	121	141	88	91	100	107
8	103	112	114	136	179	114	150	96	150	129
9	137	195	150	163	100	81	84	68	194	168
10	147	175	179	216	137	254	79	125	164	193
11	164	201	179	317	194	268	..	..	179	266
12	..	..	..	..	261	352	164	208	210	221
13	194	249	226	318	243	319	179	210	279	327
14	243	330	..	..	243	340	254	295	279	295
15	261	315	261	276	261	333	279	272	202	275
16	206	304	243	251	261	231	299	277	294	240
17	279	230	226	248	..	..	..	..	..	..
18	243	230	279	279	279	187	317	225	279	210
19	164	240	298	275	143	164	261	214	210	172
20	100	103	243	213	150	127	150	114	164	119
21	88	92	210	122	137	101	..	..	150	116
22	27	16	194	146	124	115	134	91	124	86
23	49	33	137	73	124	109	..	..	..	..

N_mF in 10^4 electrons/c.c.
n_T in 10^{11} electrons/cm.^{2} col.


BANGALORE
PRESS
LAKE VIEW
MYSORE RD
BANGALORE
CITY

APPENDIX I(A)

Ten sampling frequencies from f_0 = 1 to 25 Nc/s for Ahmedabad (based on Schmerling coefficients).

f_0	f_1	f_2	f_3	f_4	f_5	f_6	f_7	f_8	f_9	f_{10}
1	.99	.98	.91	.92	.78	.62	.50	.37	.23	.08
2	1.90	1.92	1.81	1.65	1.45	1.23	.99	.78	.45	.16
3	2.88	2.89	2.72	2.47	2.20	1.85	1.49	1.10	.68	.23
4	3.93	3.85	3.62	3.31	2.93	2.50	2.00	1.47	.90	.31
5	4.97	4.82	4.52	4.13	3.67	3.12	2.51	1.83	1.12	.39
6	5.97	5.73	5.44	4.93	4.42	3.77	3.01	2.22	1.36	.46
7	6.97	6.73	6.35	5.83	5.19	4.42	3.56	2.61	1.59	.53
8	7.95	7.71	7.28	6.66	5.93	5.06	4.07	2.98	1.82	.61
9	8.96	8.70	8.18	7.53	6.69	5.71	4.60	3.38	2.05	.69
10	9.98	9.65	9.10	8.36	7.45	6.37	5.13	3.78	2.30	.77
11	10.95	10.61	10.01	9.20	8.20	7.00	5.64	4.14	2.52	.85
12	11.94	11.58	10.93	10.06	8.93	7.60	6.17	4.52	2.76	.92
13	12.94	12.54	11.86	10.91	9.72	8.31	6.70	4.91	3.00	1.00
14	13.93	13.51	12.77	11.75	10.47	8.95	7.21	5.29	3.23	1.08
15	14.93	14.48	13.68	12.59	11.22	9.59	7.72	5.67	3.45	1.16
16	15.92	15.44	14.62	13.46	12.00	10.23	8.27	6.03	3.68	1.23
17	16.92	16.41	15.54	14.30	12.75	10.90	8.79	6.46	3.91	1.31
18	17.91	17.37	16.45	15.14	13.50	11.54	9.31	6.84	4.14	1.39
19	18.91	18.33	17.37	15.98	14.25	12.18	9.82	7.23	4.37	1.46
20	19.90	19.30	18.28	16.82	15.00	12.82	10.34	7.60	4.60	1.54
21	20.90	20.27	19.19	17.66	15.75	13.46	10.86	7.98	4.83	1.62
22	21.89	21.23	20.11	18.50	16.50	14.10	11.37	8.36	5.06	1.69
23	22.89	22.20	21.02	19.34	17.25	14.74	11.89	8.74	5.29	1.77
24	23.88	23.16	21.94	20.18	18.00	15.38	12.41	9.12	5.52	1.85
25	24.88	24.12	22.85	21.02	18.75	16.02	12.92	9.50	5.75	1.92

APPENDIX I(B)

Five sampling frequencies from f_N = 1 to 25 Mc/s for Ahmedabad (based on Schmerling coefficients).

f_N	f_1	f_2	f_3	f_4	f_5	N x 10^{-3}/cc.
1	0.98	.87	.64	.43	.16	0.12
2	1.96	1.73	1.35	.86	.31	0.50
3	2.94	2.60	2.02	1.30	.48	1.11
4	3.93	3.47	2.72	1.74	.61	1.93
5	4.91	4.34	3.40	2.17	.76	3.10
6	5.89	5.22	4.11	2.64	.91	4.46
7	6.88	6.10	4.81	3.09	1.06	6.08
8	7.86	6.98	5.50	3.54	1.21	7.94
9	8.85	7.87	6.22	3.99	1.38	10.04
10	9.84	8.75	6.93	4.46	1.53	12.40
11	10.82	9.63	7.68	4.91	1.68	15.00
12	11.81	10.52	8.33	5.36	1.85	17.85
13	12.79	11.41	9.05	5.82	2.00	20.95
14	13.77	12.29	9.74	6.27	2.15	24.30
15	14.76	13.17	10.44	6.72	2.31	27.90
16	15.74	14.05	11.14	7.17	2.46	31.74
17	16.73	14.93	11.83	7.61	2.62	35.84
18	17.71	15.80	12.53	8.06	2.77	40.19
19	18.70	16.68	13.22	8.51	2.92	44.76
20	19.68	17.56	13.92	8.96	3.08	49.60
21	20.66	18.44	14.62	9.41	3.23	54.68
22	21.67	19.33	15.40	9.90	3.39	60.02
23	22.66	20.24	16.10	10.35	3.54	65.60
24	23.64	21.12	16.80	10.80	3.69	71.42
25	24.62	22.00	17.50	11.25	3.85	77.50

APPENDIX II

AHMEDABAD, March 30, 1950.

10^3 electron/cc

Km.	00	01	02	03	04	05	06	07	08	09	10	11	12
320													2905
300	2574												2610
340	2430					333						2136	2163
320	1736	2430				375						1941	1643
300	794	2136		1190	477	322			1643	2065	2034	1536	1240
280	27	1370	1343	1119	446	251	493	988	1557	1941	1736	1240	1004
260		310	1643	1004	333	127	446	375	1370	1643	1370	1050	915
240			715	935	310	27	310	772	375	1119	1027	875	772
220				603	193		169	603	644	794	715	715	603
200							60	375	446	553	493	541	432
190							43	193	235	361	333	413	346
180							45	119	139	240	261	310	293
140							38	96	142	139	193	250	240
120							21	65	389	157	169	193	203
$h_m F$	360	320	290	310	300	340	290	290	300	300	310	350	330
$(hM)F$	2574	2430	1010	1215	477	338	493	960	1643	2065	2036	2236	2344
h_0	290	255	225	205	210	240	115	110	110	110	110	110	110
f_0	27	50	27	50	27	27	12	12	27	27	50	50	50
n_p	1362	936	333	940	307	253	876	303	1921	1601	1635	2252	3070

APPENDIX II (contd.)

AHMEDABAD, March 30, 1960.

10^3 electron/cc

Km.	1330	14	15	16	17	18	19	20	21	22	23
380		4013					3543	2754			2363
360	3753	3301	3375				3174	2538	2713		2129
340	3174	3420	3534	3379		3301	2700	2096	2430	3060	1941
320	2829	2700	3037	3020	3379	3174	2163	1240	1972	2700	1448
300	1643	1041	2430	2430	2982	2003	1443	603	1313	2263	697
280	1100	1432	1643	1729	2253	1396	603	50	603	1240	27
260	360	1050	1073	1036	1240	1004			50	310	
240	735	794	875	875	715	446					
220	576	603	630	627	493	193					
200	477	461	493	446	310	77					
180	333	346	346	293	193	45					
160	203	272	250	203	131	33					
140	229	340	198	169	116	30					
120	203	112	169	100	103						
hmF^2	370	330	370	350	320	350	330	370	370	340	330
NmF^2	3974	4013	4013	3534	3379	3333	3534	2754	2700	3060	2363
ho	110	115	110	125	115	125	270	280	280	250	230
No	50	27	27	27	27	12	50	50	50	27	27
Nt	3195	3345	3757	2364	2044	2445	2719	1852	1317	1612	1472

CHAPTER III

RESULTS OF CALCULATION OF VARIATION OF ELECTRON DENSITY WITH THE HEIGHT

1. INTRODUCTION

We described in the preceding chapter the method adopted for the reduction of h'-f records to true height profiles at Ahmedabad. It is essentially a method of integration and is sufficiently accurate and rapid in application. The assumption of electron density N increasing monotonically with height appears to be justified and the results agree well with those obtained from rockets and satellites. A summary of rocket and satellite results can be found in Friedman (1959), Seddon and Jackson (1958, 1961), Krassovsky (1961) and some others. We enumerate here the important conclusions arrived at by these direct observations.

(1) The ionosphere below the F region has no strongly pronounced layers. It is characterized by many small maxima with a continuous increase of electron density from the bottom upto the F2 layer maximum.

(2) The height of peak electron density and the ionization below the F region is in general 50-100 Km lower than is apparent from h'-f records.

(5) The ionization above h_{max} decreases very slowly with height indicating very large scale height for ionised particles of the ionosphere.

The last conclusion is important in the interpretation of ionospheric attenuation of cosmic radio noise. It is dealt with in Chapter V.

We shall describe the results of N(h) distribution over Ahmedabad.

2. EARLIER WORK AT AHMEDABAD

We have mentioned previously that regular ionospheric data are available in our laboratory since February 1953. To reduce all h'-f records to true height profiles manually will take a very long time. We have for the present to restrict ourselves to analyse a few days records in each season and study the nature of the variations. A first attempt was made by Sheriff (1956) of this laboratory who analysed h'-f records on three quiet and three disturbed days in each month during 1953-54. He employed the curve matching technique of Ratcliffe and studied the seasonal variation of the parameters of the F region. Though this gave a general picture of the type of variation, the method used was only an approximate one. Sreenivasan started work on the systematic study of the fine structure of the ionosphere over Ahmedabad in 1956 and worked out a 5-point method of analysis similar to that of Kelso.

He analysed a number of records on magnetically quiet and disturbed days during 1954-56. Initially, he calculated the electron distribution neglecting the effect of the earth's magnetic field. Later, he found that the heights calculated by ignoring the field were higher by about 6.2 β at Ahmedabad. In Greenivasan's method of approach, each of the layers E, F_1, $F_{1.5}$ and F_2 was considered to be parabola and by applying the parabolicity test given by the Appleton-Beynon method corrected for group retardation in the underlying layer as suggested by Ratcliffe. This is not quite correct since we know that there are large deviations of the ionospheric layers from parabolicity, especially during daytime and in magnetically disturbed periods. Consequently, the F region heights calculated by him were exaggerated by 50-100 Km during the day. This difficulty could be avoided by applying the integral method from the bottom of the ionosphere to the peak density level as is done here.

3. RESULTS FROM THE PRESENT ANALYSIS

We report here the results of true height analysis on some selected days during 1957-60. The following table lists the days on which N(h) profiles were calculated.

It is convenient to group the days according to the geomagnetic activity indices, ΣK_p, for the day as given in CRPL Bulletin, Part B series. The table 2 shows such grouping.

Table 1.

Year	Day	Year	Day
1957	August 31	1959	January 2, 7
	September 1 to 6		April 11, 30
			July 10 to 19, 29
1958	January 1, 4		
	April 25, 27	1960	March 30, 31
	July 11, 19		April 1 to 6
	October 10		November 10 to 17

Total number of days analysed : 44

Total number of ionograms reduced : More than 1000.

Table 2.

ΣK_p	< 20	21-30	31-50	> 50
	4- 1-58	31- 8-57	2- 9-57	3- 9-57
	25- 4-58	1- 9-57	4- 9-57	15- 7-59
	27- 4-58	11- 7-58	5- 9-57	18- 7-59
	9-10-58	7- 1-59	1- 1-58	31- 3-60
	2- 1-59	11- 4-59	12- 7-58	1- 4-60
	20- 4-59	12- 7-59	11- 7-59	13-11-60
	10- 7-59	14- 7-59	16- 7-59	
	13- 7-59	30- 3-60	17- 7-59	
	29- 7-59	4- 4-60	19- 7-59	
	10-11-60	6- 4-60	2- 4-60	
		11-11-60	3- 4-60	
		17-11-60	5- 4-60	
			12-11-60	
			14-11-60	
			15-11-60	
			16-11-60	
	10	12	16	6

In the series of diagrams that follow in this chapter, we have plotted the values of electron density N at fixed heights from 120 Km to hmF at 30 Km interval during daytime and at the same height intervals but from the base of the F layer to its hm during night. The figures are arranged to show the variation on individual days in different seasons, including magnetically quietest days (low ΣK_p) to very disturbed days (high ΣK_p). We have refrained from taking averages of the electron distribution on the days showing the same ΣK_p because the density variations on such days were rarely similar.

It can be noted that on quiet days the pattern of electron distribution in the ionosphere was generally regular with small fluctuations depending on the season. On disturbed days there were irregular changes both in heights and electron densities.

4. DISCUSSION

It is now recognised that information regarding N(h, t) is basic for ionospheric studies. The data tabulated on a routine basis such as foF2, hpF2, h'F2 etc. disguise many facts which are noticeable in N(h) tables. The minimum virtual height h'F2 depends so much on the group retardation lower in the ionosphere that it is not a reliable index of the height variation of the F2 layer. The hpF2 which is the virtual height at 0.834 f_o based on the assumption of a parabolic layer model is higher by 50-80 Km during day as compared to true

height h_m of N_m obtained by the true height analysis.

The true height variation of the electron density at a given height is a quantity of importance for the continuity equation

$$\frac{dN}{dt} = q - \alpha N^2 - \beta N - div(N\vec{v})$$

This can be appreciated when we examine the N(h, t) distribution in winter and equinoxes when we observe large increase in N after sunset and before midnight. Such large value of N in the absence of solar radiation is no doubt connected with drift forces both lateral and vertical.

The time variation of N_mF_2 is less valuable because it represents the plasma frequency at a height which is continually changing. Further, the variation of N_mF_2 and that of N say at 300, 250 or 220 Km are not similar. Knowledge of the variation of N at fixed heights at different places in different seasons and different epochs of the solar cycle are now becoming available. This together with the direct results of electron density measurements from rockets and satellites will undoubtedly lead to a better understanding of the ionosphere.

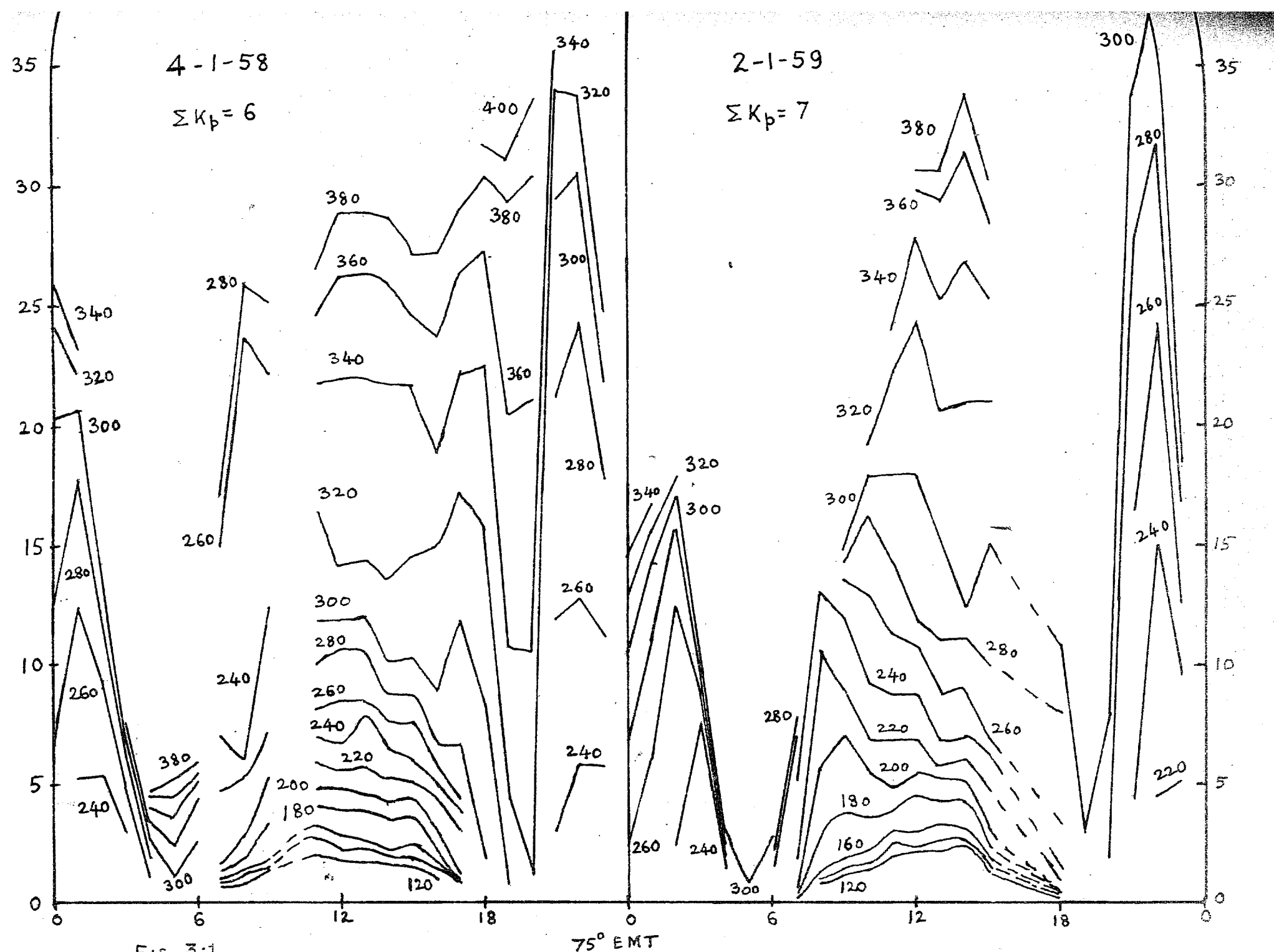

FIG. 3·1

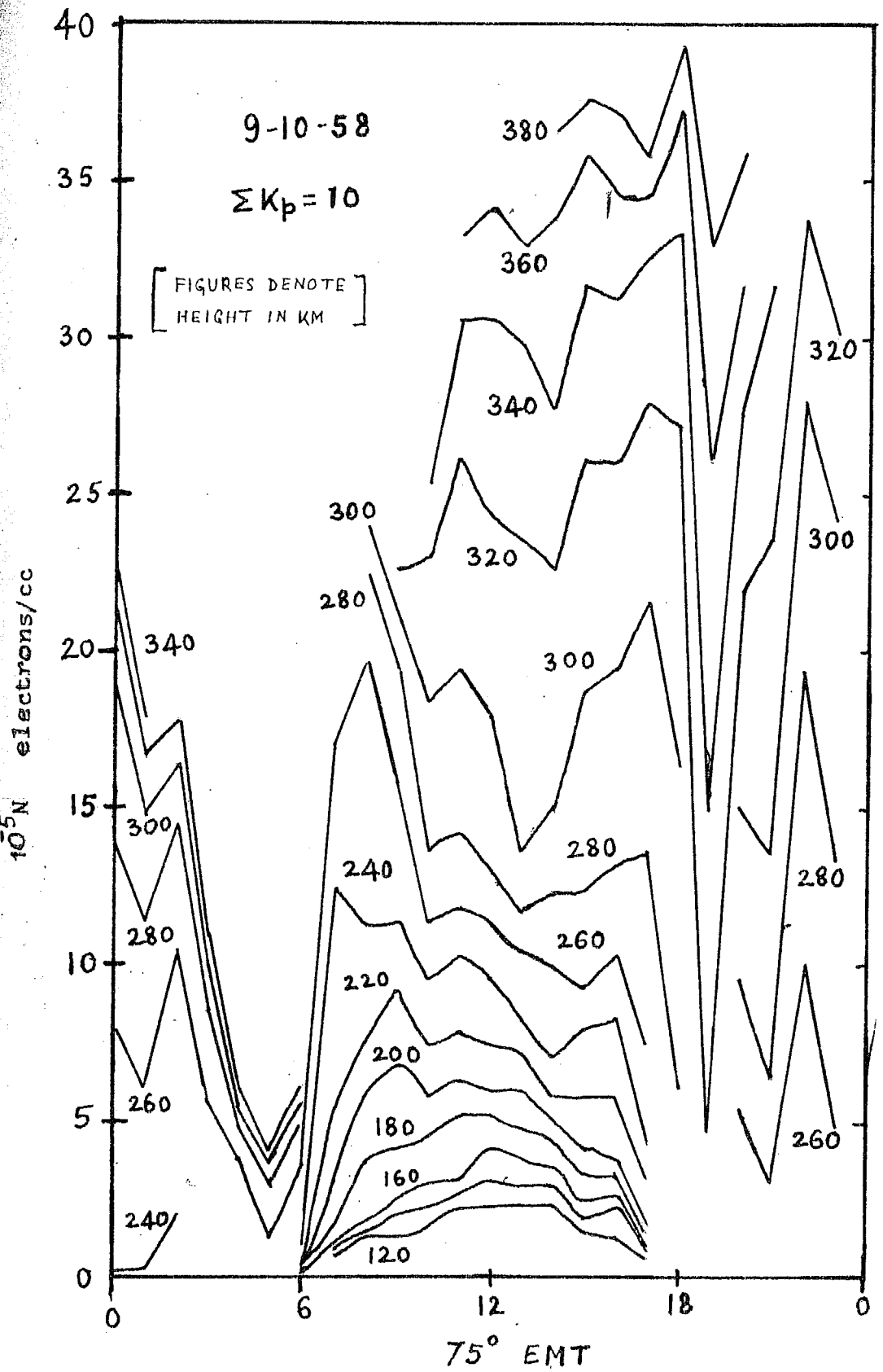

FIG. 3·2 ELECTRON DENSITIES AT FIXED HEIGHTS OVER AHMEDABAD

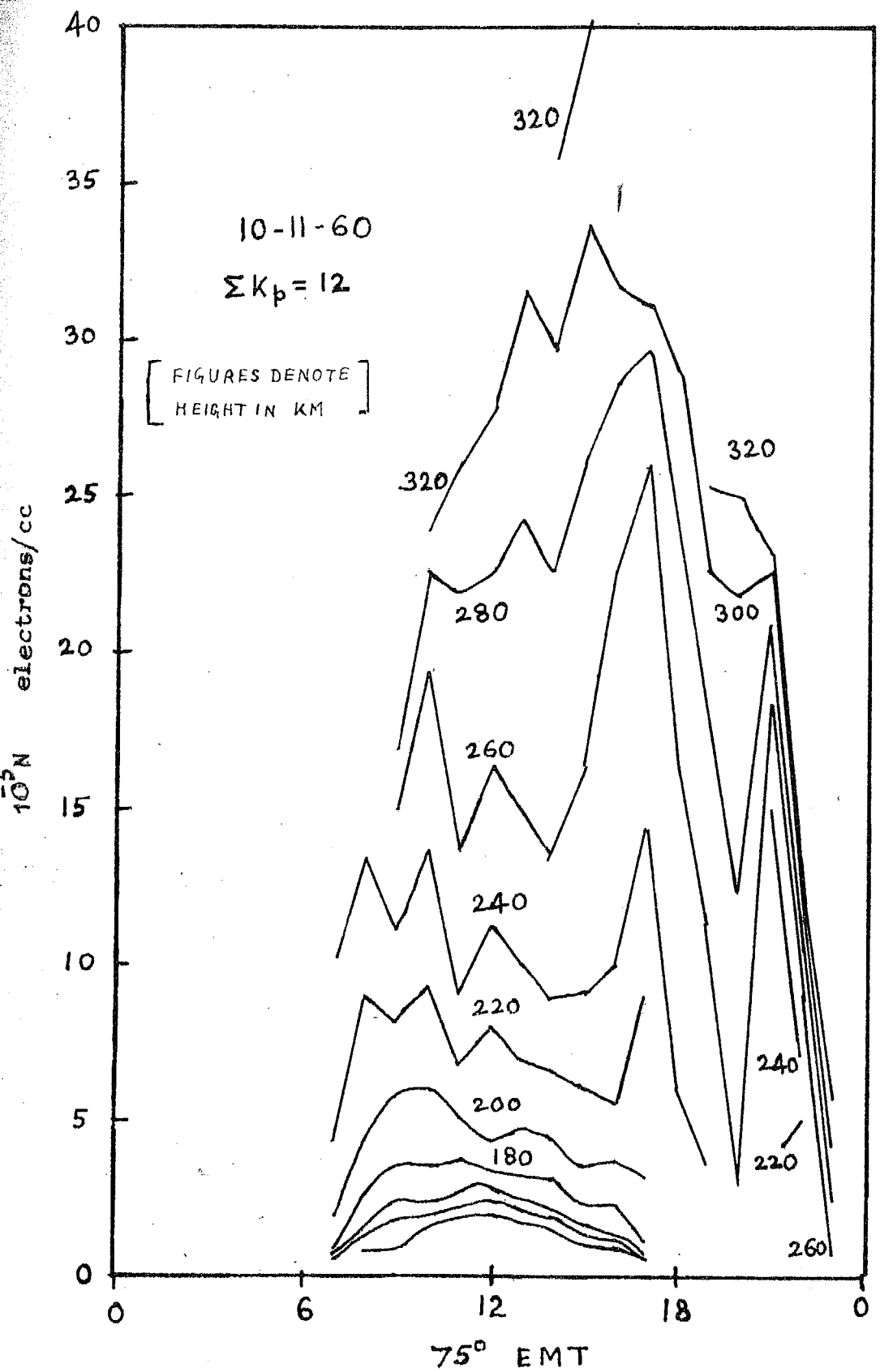

FIG. 33 ELECTRON DENSITIES AT FIXED HEIGHTS OVER AHMEDABAD

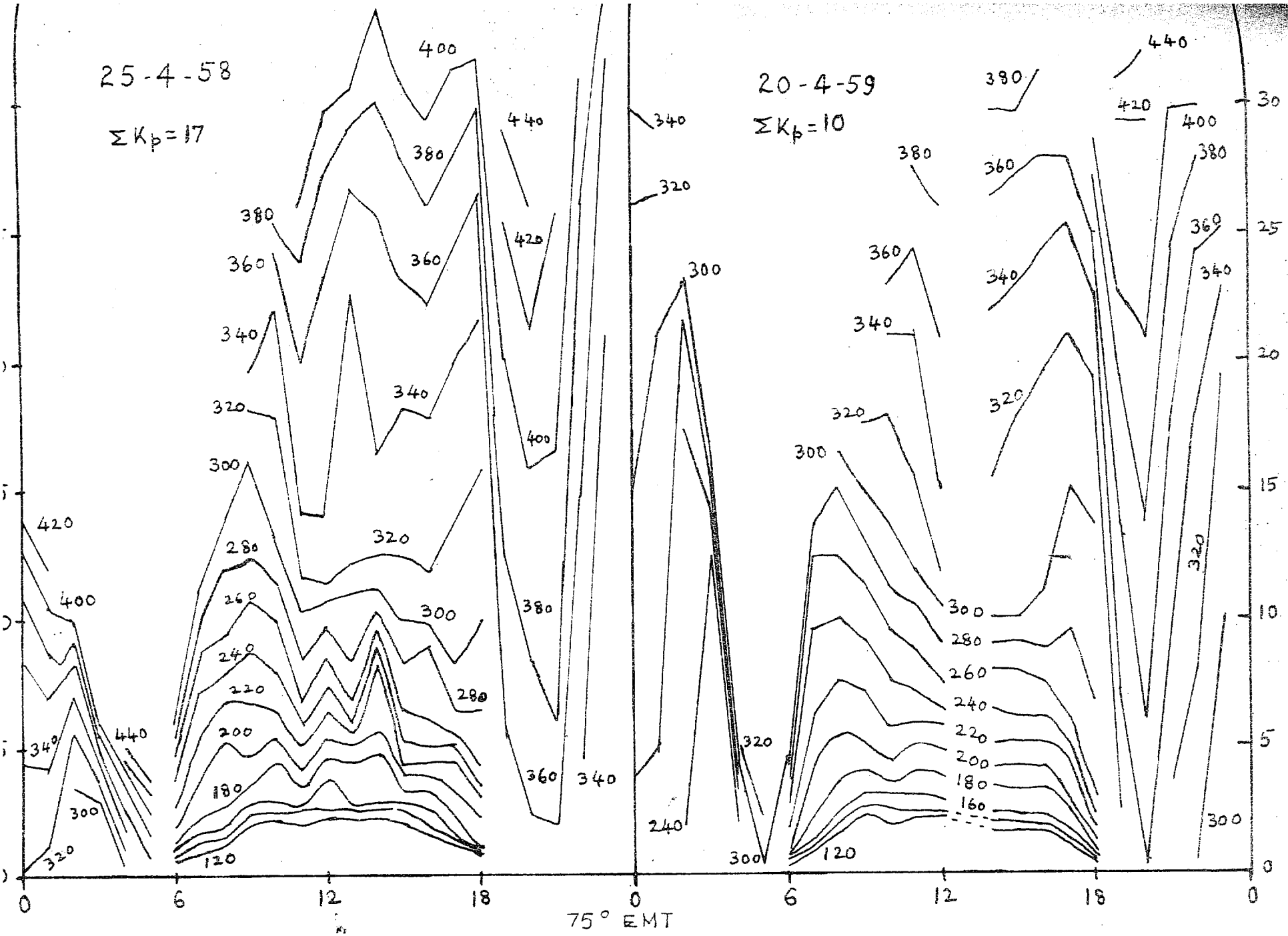

FIG.3·4 ELECTRON DENSITIES AT FIXED HEIGHTS OVER AHMEDABAD

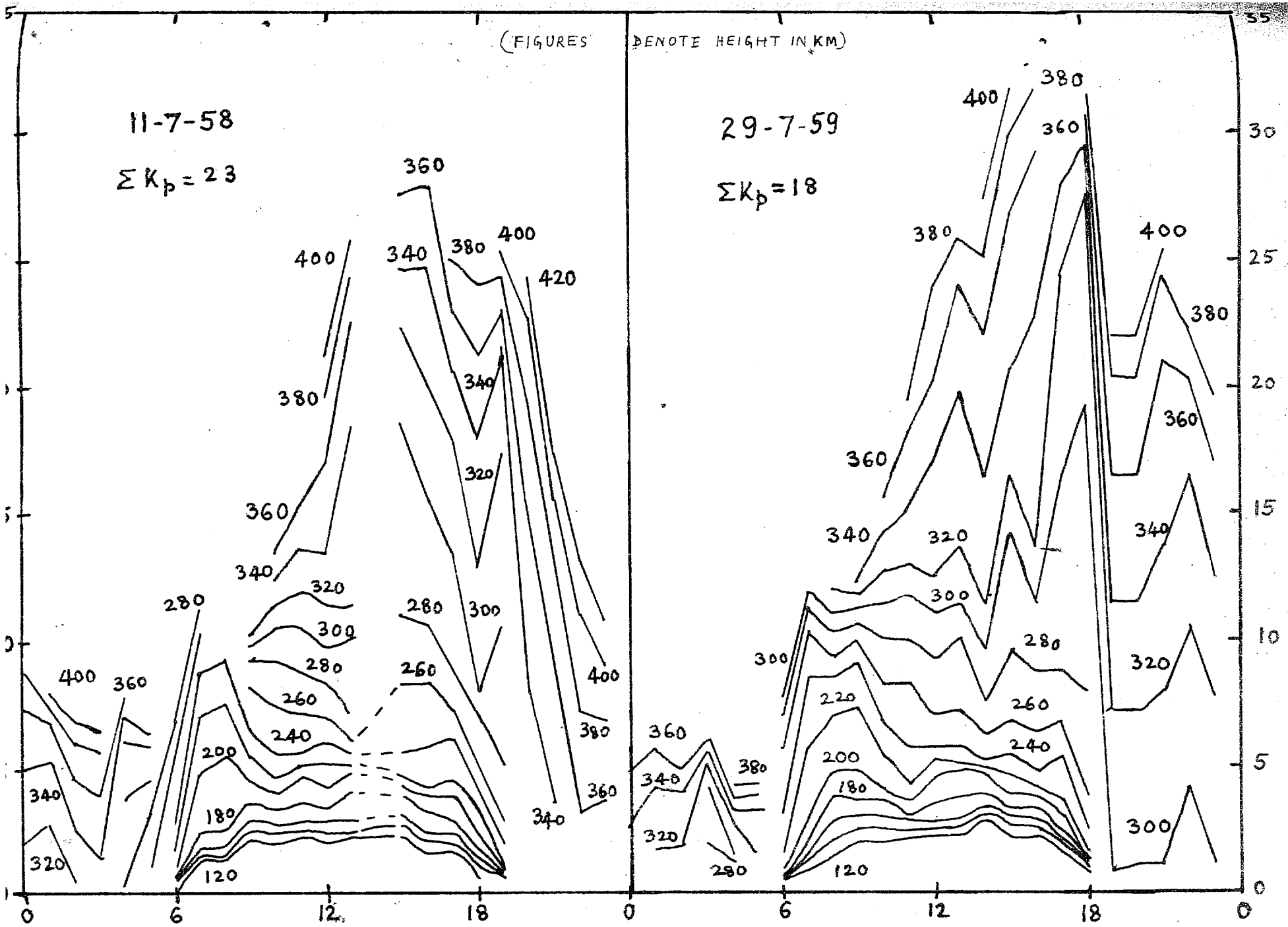

FIG. 3·5 ELECTRON DENSITIES AT FIXED HEIGHTS OVER AHMEDABAD

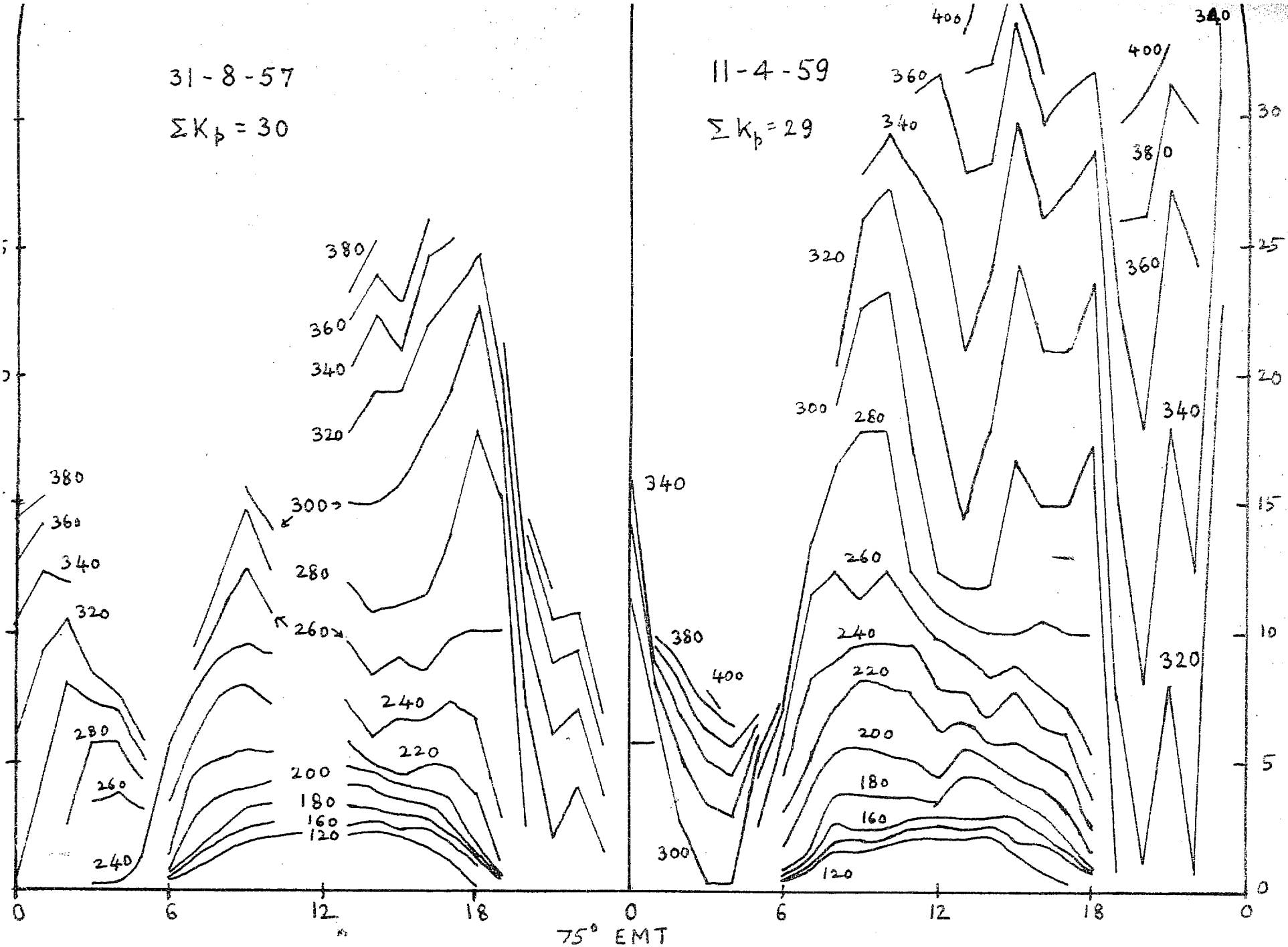

FIG. 3·6 ELECTRON DENSITIES AT FIXED HEIGHTS OVER AHMEDABAD

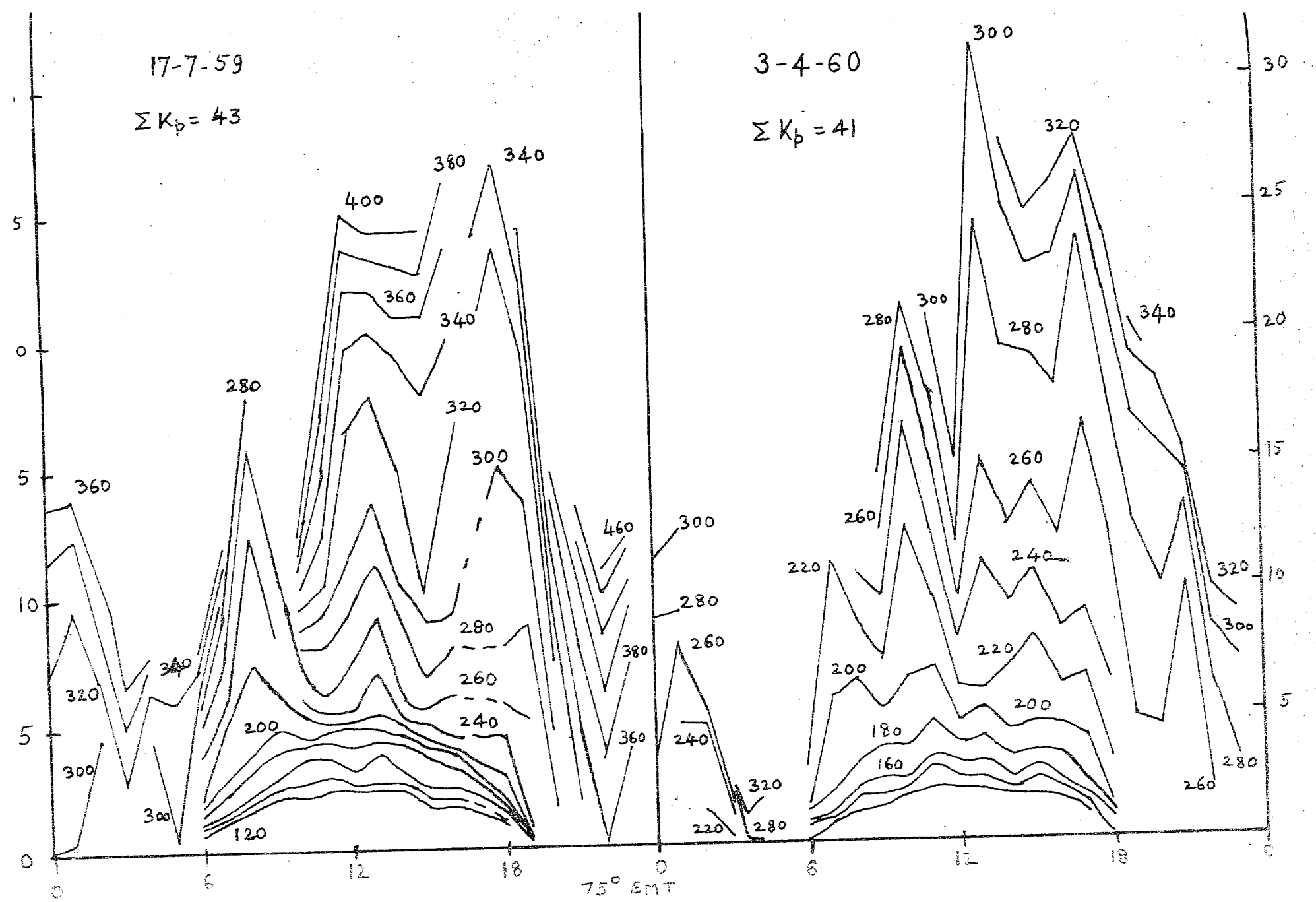

Fig. 2 ELECTRON DENSITIES AT FIXED HEIGHTS OVER AHMEDABAD

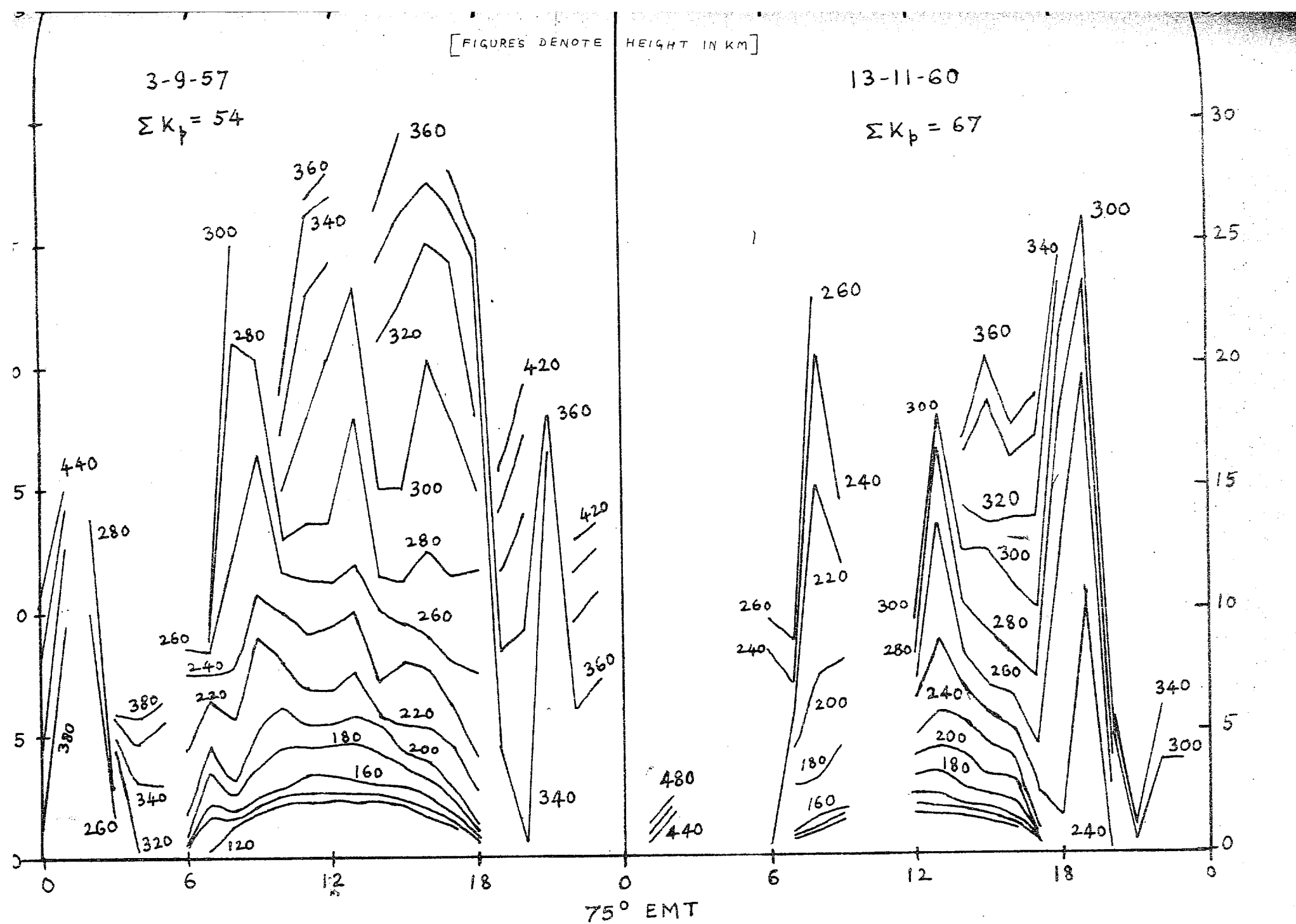

FIG.3.8 ELECTRON DENSITIES AT FIXED HEIGHTS OVER AHMEDABAD

CHAPTER IV

EFFECT OF SELECTED MAGNETIC STORMS ON THE ELECTRON DENSITY DISTRIBUTION

1. INTRODUCTION

In this chapter we shall present the results of our analysis of electron distribution over Ahmedabad in some magnetically disturbed periods. We have seen earlier that at Ahmedabad, a decrease in foF2 and a raising of the ionospheric levels take place during magnetic storms. It is important to know the electron distribution in the ionosphere under such conditions.

2. N(h) DISTRIBUTION DURING HIGHLY DISTURBED PERIODS

Our study relates to the following four groups of events which were very conspicuous. They relate to :

(1) August 30 to September 5, 1957

(2) July 10 to 19, 1959

(3) March 30 to April 6, 1960

(4) November 10 to 17, 1960.

Of these the results of the July 10-19, 1959 events have been published (Deganaker 1961).

We shall discuss the results in each group separately since the conditions in one were not the same in the other.

3.1 August 30 - September 5, 1957

We shall first list the sequence of events in this period. This is helpful, because it enables us to trace the connection between the causative solar phenomenon and its effects on our atmosphere. The solar and magnetic data were taken mainly from the reports of Hiraiso Observatory, Japan in respect of solar flares and from the reports of Kodaikanal Observatory regarding the principal magnetic storms. The list would be lengthy if all solar flares of importance 1, 2 and 3 are included. We restrict ourselves to giving only solar flares of importance 2 and 3.

Table 1.

Date	Onset time, UT	Description
30-8-57	1920	SC magnetic storm, $\Delta H = 178\gamma$
30-8-57	0358	
31-8-57	0245	Class 2 flare
	0543	Class 2 flare
	1310	SC magnetic storm, $\Delta H = 115\gamma$ (Japan)
	2034	Class 2 flare
1-9-57	0304	Class 3 flare
	0950	Class 2 flare
	2000	Class 2 flare
2-9-57	0315	SC magnetic storm, $\Delta H = 470\gamma$
	0407	Class 2 flare
by	2100	Polar cap absorption
3-9-57	0043	Class 3 flare
	0300	Class 3 flare
	1021	Class 2 flare
4-9-57	1300	SC magnetic storm, $\Delta H = 413\gamma$
5-9-57	0000	Class 3 flare
	2053	Class 3 flare.

The SC magnetic storms on 2 and 4 September were of severe type and that on August 31 was moderate.

In Fig.4.1 are drawn the iso-electron density lines from the bottom of the ionosphere to the maximum density level. The lines marked 1, 2, 4, 6, 10 etc. are the iso-dense levels corresponding to 1×10^5, 2×10^5, 4×10^5 etc. electrons per cm^3. After the level marked 6, the levels are drawn at an interval of 4×10^5 el/cc upto h_{max} level. Such a diagrammatic representation brings out vividly the changes in the height of iso-dense lines. We shall adhere to this presentation of diagrams in this chapter. The time scale are Ahmedabad zonal times corresponding to 75^0 EMT which is 5 hours ahead of UT. The occurrence of solar flares are marked by thin arrows at the top and the SC of a magnetic storm is shown at the bottom of the figure. The onset times of events are also in 75^0 EMT, the same as that for the electron distribution.

It can be noticed that following the SC, large changes in height and electron densities occurred. The magnitude of the changes depends on the severity of the magnetic storm. The depression in $foF2$ becomes evident within a few hours of the onset of a moderately severe storm and much quicker in the case of severe storms. It has also been found that the storms which commenced in the afternoon or late in the evening, cause large changes in height and electron densities within 5 to 6 hours of the onset. We have also found from our data that the ionosphere is affected much more during dark hours both in respect of height and densities. The effect of solar flares on the F region

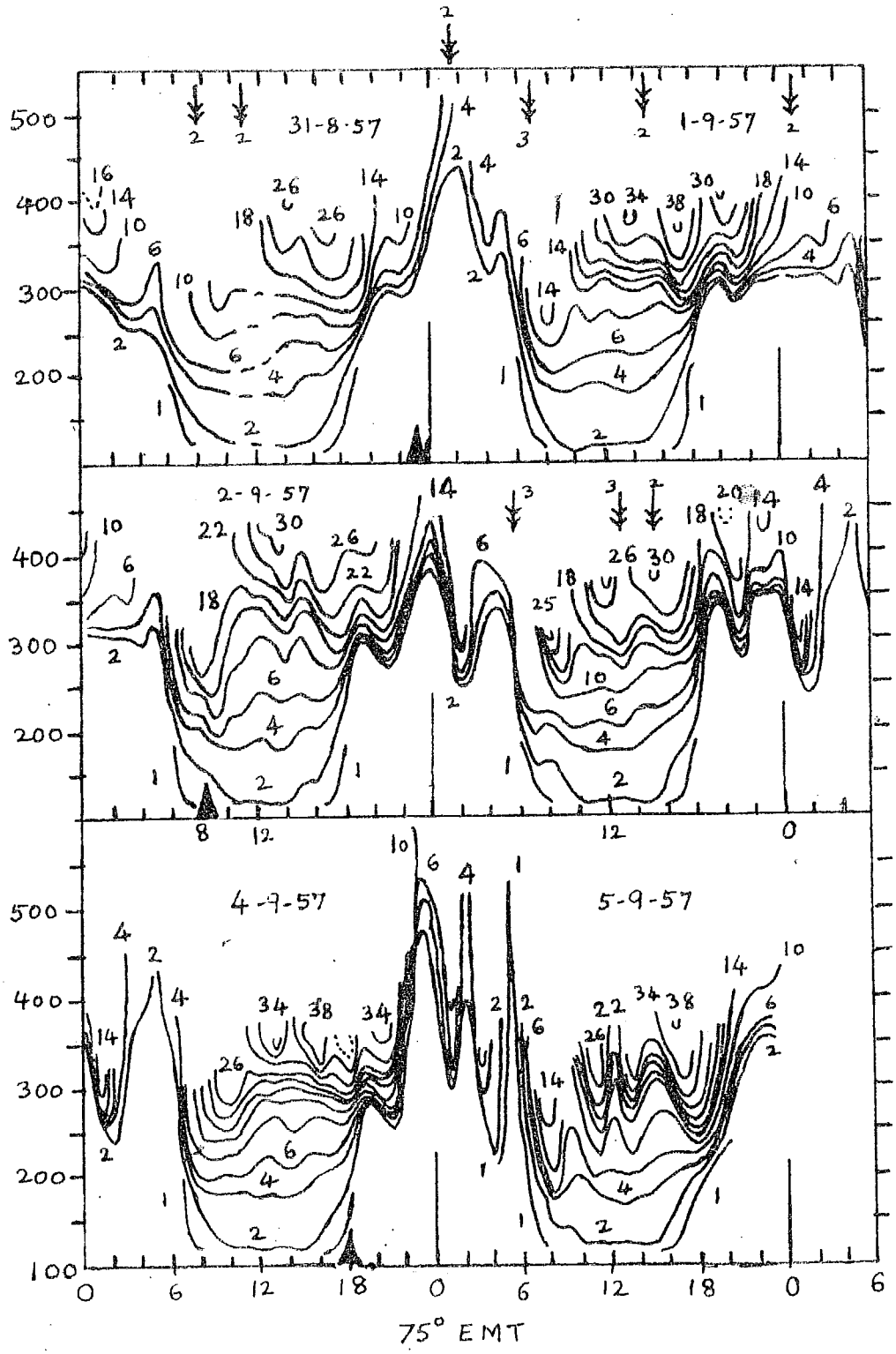

FIG. 4·1 ELECTRON DENSITY DISTRIBUTION OVER AHMEDABAD

31 AUGUST TO 5 SEPTEMBER 1957

↓ SOLAR FLARE ▲ SUDDEN COMMENCEMENT

The severe storm on 4-5-57 produced oscillations in height of the order of 300 Km having a period of about 3 hours. A sharp negative gradient of electron density became evident nearly 4 hours after the SC. The electrons were dispersed quickly within an hour between 22 and 23 hrs. The electron density was reduced further in the night and remained low throughout the next day. The perturbation was confined mainly between 200 Km and $h_{max}F_2$.

A point which deserves particular mention is that strong localised concentration of electrons at about 350 Km take place in the morning hours during the main phase of the magnetic storm. At Ahmedabad, this has been observed in most of storms with a few exceptions.

2.2 July 10-19, 1959

We shall briefly describe the main features in this period to keep up the continuity. There were seven solar flares all of major importance and three magnetic storms of which one was of very severe type. Polar cap absorption which is caused by the bombardment of the atmosphere by the low energy cosmic rays emitted by the sun, was reported on three days in this period. Table 2 gives the list of events.

It may well be remembered that magnetic storms are generally preceded by solar flares with a time delay of 30-40 hours.

Table 2.

Date	Onset time, UT	Description
10-7-59	0210	Class 3+ flare
	0514	Class 3+ flare
	0700	Polar cap absorption (Thule)
11-7-59	1623	SC magnetic storm, $\Delta H = 163\gamma$
12-7-59	2153	Class 3 flare
14-7-59	0325	Class 3+ flare
	by 0700	Polar cap absorption
	1400	Class 3+ flare
15-7-59	0302	SC magnetic storm, $\Delta H = 785\gamma$
16-7-59	1303	Class 3 flare
	2114	Class 3+ flare
	by 2250	Polar cap absorption
17-7-59	1633	SC magnetic storm, $\Delta H = 327\gamma$

Fig.4.2(a) and 4.2(b) show the iso-dense levels of electron density in the ionosphere on these days. Following the storm on July 11, the layer heights went up by at least 100 Km in about 3 hours after the SC. The electron distribution on July 13 and 14 represented quiet day distribution as there was no magnetic disturbance on those days. The intense storm on July 15 induced perturbation at the upper levels in the F-region within an hour after the SC. The magnitude of the perturbation was of the order of 300 Km at its peak and the period was about 3 hours. Between 00 and 02 hrs on the 16th the F layer appeared to be blown off. Intense sporadic E activity was evident during this period and night time E layer with low ionization distribution could be inferred from the

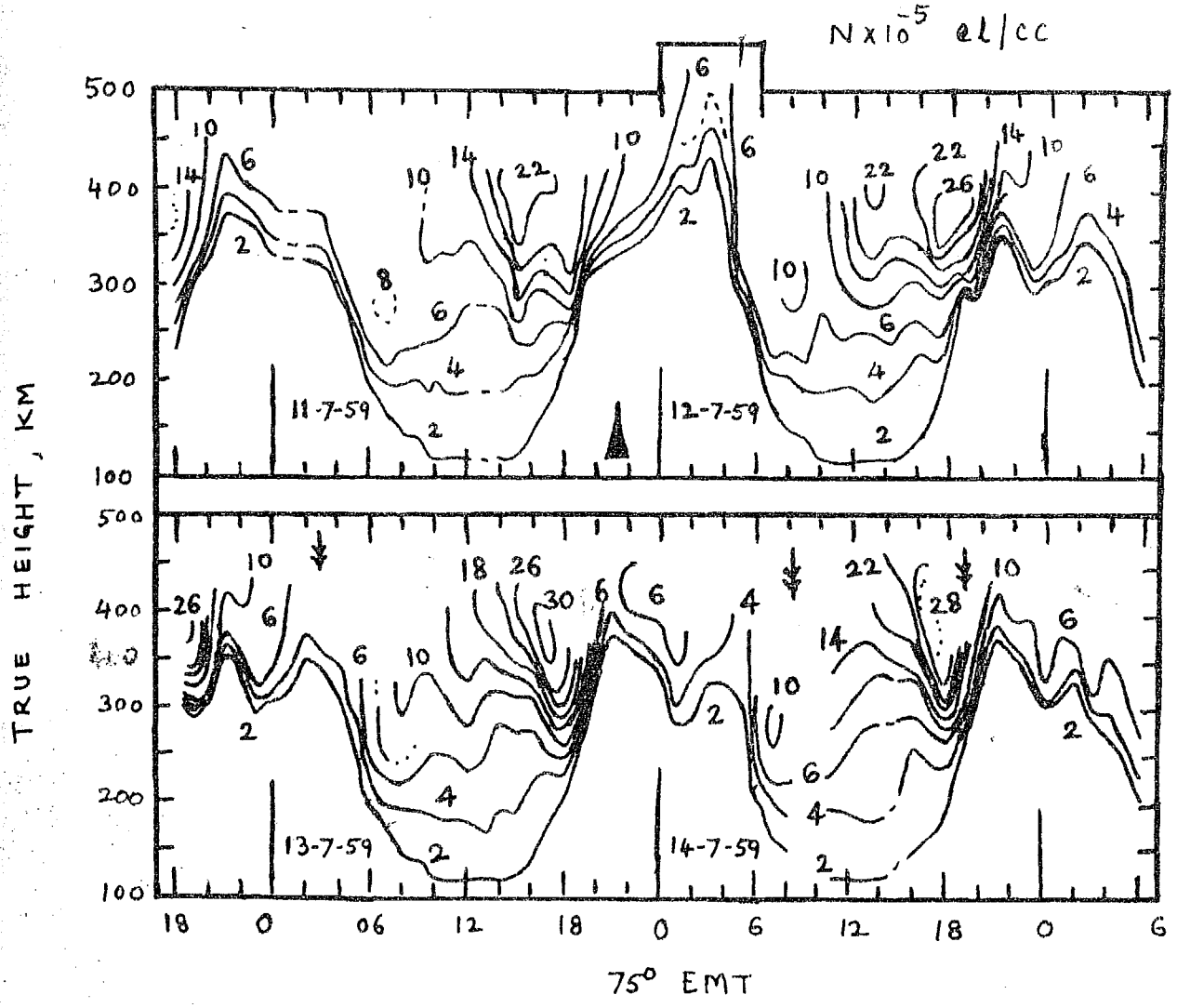

FIG. 4·2(a) ELECTRON DENSITIES OVER AHMEDABAD 11-14 JULY 1959.

↓ SOLAR FLARE ▲ SUDDEN COMMENCEMENT

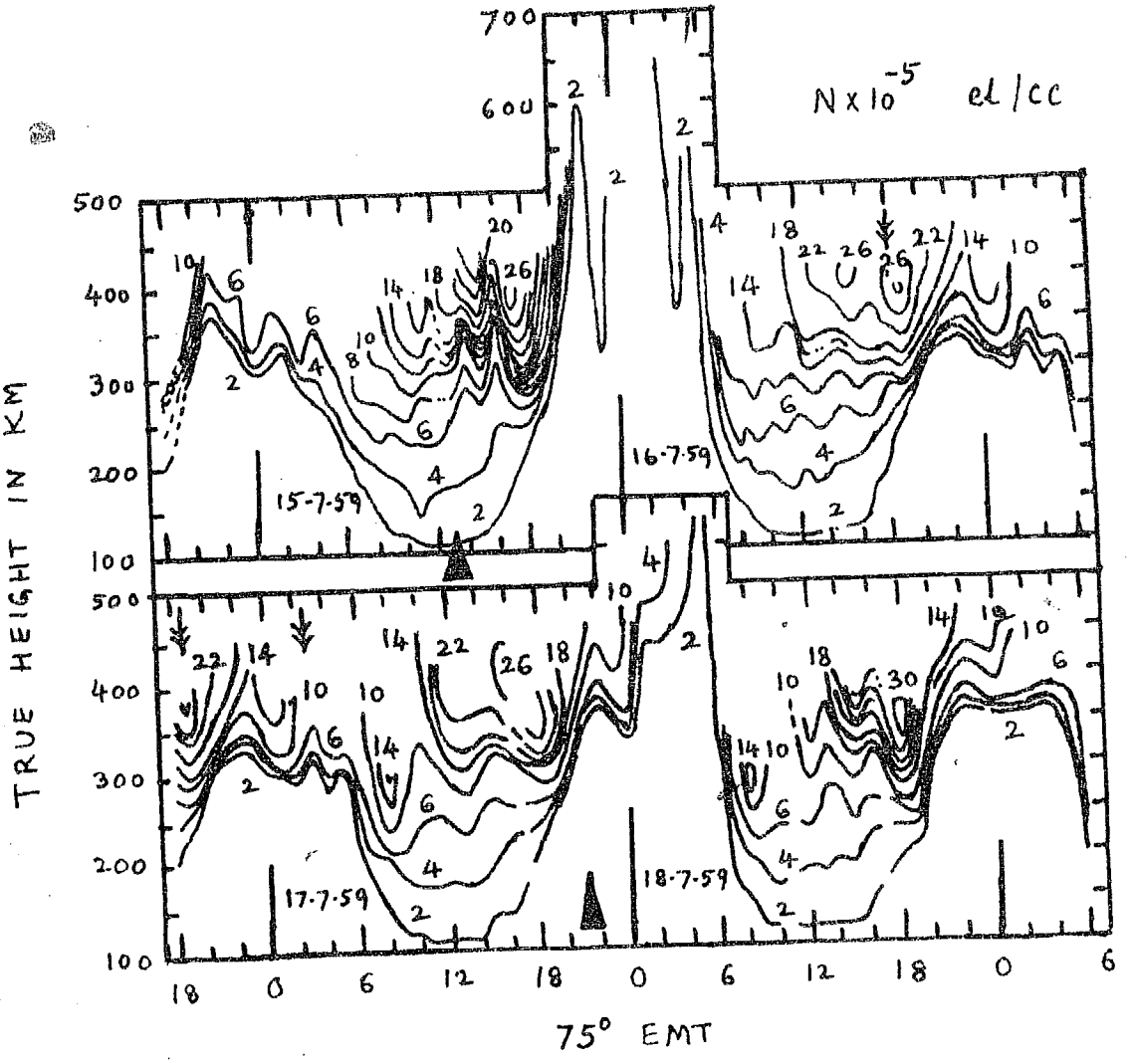

FIG. 4·2(b) ELECTRON DENSITIES OVER AHMEDABAD 15-18 JULY 1959

↓ SOLAR FLARE ▲ SUDDEN COMMENCEMENT

14 - 7 - 1959

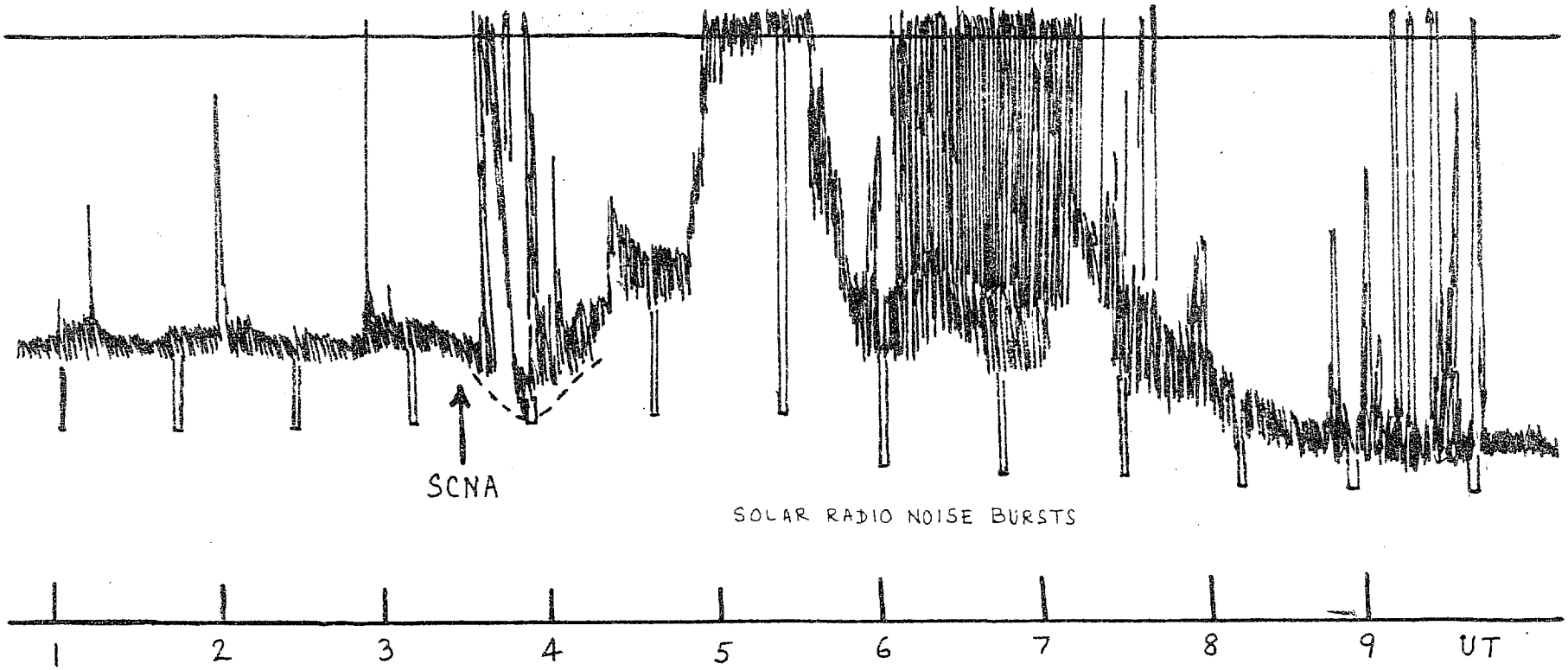

FIG. 4-3 SUDDEN COSMIC NOISE ABSORPTION ON 25 Mc/s & INTENSE SOLAR RADIO NOISE BURSTS AT AHMEDABAD ON 14 JULY 1959

Lonogram since it had produced group retardation at the low frequency end of the F trace. However its density distribution could not be calculated.

The storm on the 17th produced perturbation less intense in character, though small undulations persisted throughout the next day.

It may be mentioned here that localised concentration of electrons in the morning hours occurred on July 12, 14, 17 and 18, but curiously enough not on the 16th.

On July 14, a class 3+ flare occurred and within 4 hours of the occurrence of this flare a polar cap absorption was reported. It may be interesting to see the cosmic radio noise record at 25 Mc/s at Ahmedabad at these hours. We have reproduced in Fig.4.3, a portion of this record. It shows a sudden cosmic noise absorption (SCNA) corresponding to a solar flare at 0325 UT, which produced a maximum absorption of 5 db. Strong solar radio noise bursts lasting for nearly 4 hours can be seen following the SCNA. Even during the SCNA, strong solar radio noise bursts could be recorded.

2.3 March 30 to April 6, 1960

The table below gives the occurrence of solar flares, magnetic storms and polar cap absorption events in this period.

Table 3.

Date	Onset time UT	Description
30-3-60	0633	Class 3+ flare
	2043	Class 2+ flare
31-3-60	by 0730	Polar cap absorption (Thule)
	0343	SC magnetic storm, $\Delta H = 640\gamma$
1-4-60	0330	Short wave fade out and SCNA at 95 Mc/s (Ahmedabad)
	0945	Polar cap absorption (Thule)
2-4-60	2312	SC magnetic storm, $\Delta H = 300\gamma$
3-4-60	0306	Class 3 flare
	0527	Class 3 flare
5-4-60	0140	Class 3+ flare.

The SC magnetic storm on 31-3-60 was very severe. The iso-dense levels of electron density are shown in Fig.4.4 for 4 days from March 30 to April 3, 1960. On the night of 31-1-60, the peak amplitude of the undulation was of the order of 150-200 Km. The first perturbation occurred at about 19 hrs on 31-3-60 after nearly 6 hours after the SC. The height of maximum density went up by 150 Km and the electron density started falling. N_{max} was about 30 x 10^5 el/cc at 20 hrs which came down to 4 x 10^5 el/cc within an hour. On 1-4-60, many unusual things can be noticed. The usual concentration of electrons at 03 hrs at 250 Km is clearly seen. A rapid dispersal of electrons followed. At 10 hrs, the F region appeared to have been pushed up to a height of about 600 Km and the peak electron density at that hour was only 15 x 10^5 el/cc approximately. In the next

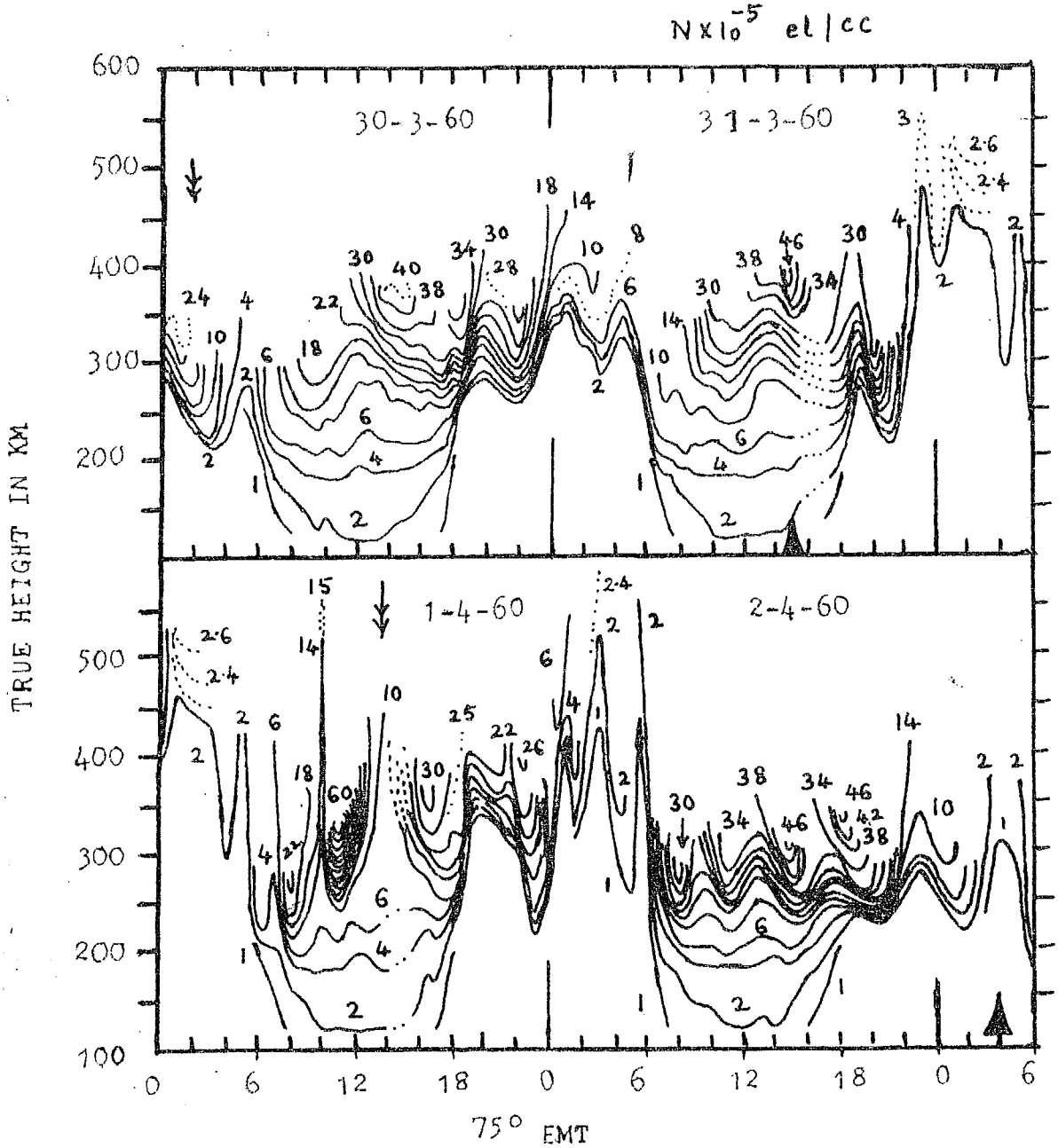

FIG. 4·4 ELECTRON DENSITY DISTRIBUTION OVER AHMEDABAD

30 MARCH TO 2 APRIL 1960

↯ SOLAR FLARE ▲ SUDDEN COMMENCEMENT

15-20 minutes something happened and $h_{max}F_2$ collapsed from 600 Km to about 320 Km and the electron density shot up enormously at 1025 hrs. There was a very high gradient of electron density in a small region between 250 to 320 Km below h_{max}. Above h_{max}, we do not know what the distribution was like. This high concentration of electrons should have been formed by the horizontal transport of electrons from elsewhere followed by a rapid downward transport. It is difficult at this stage to explain the mechanism without examining the data from other stations. It is interesting to note that in about 5 hours after the occurrence of this phenomenon at Ahmedabad, a polar cap absorption was observed at Thule.

The cosmic radio noise record at Ahmedabad is shown in Fig.4.5. It shows that the cosmic radio noise intensity dropped down to a low value at about the same time when high F2 electron density gradients were observed at about 0525 UT. The cosmic radio noise intensity recovered to its original value within the next hour. There occurred an SCNA afterwards at 0350 UT which can also be seen in the figure as the second dip. There was complete shortwave fade out on our ionospheric records taken at 14 hrs EMT; there was however no fade-out at 1025 EMT though the cosmic radio noise intensity was affected in the same manner in both the cases. The former dip was due to high F region attenuation, while the latter was due to enhanced D region absorption as a result of the solar flare at 1350 EMT.

1-4-1960

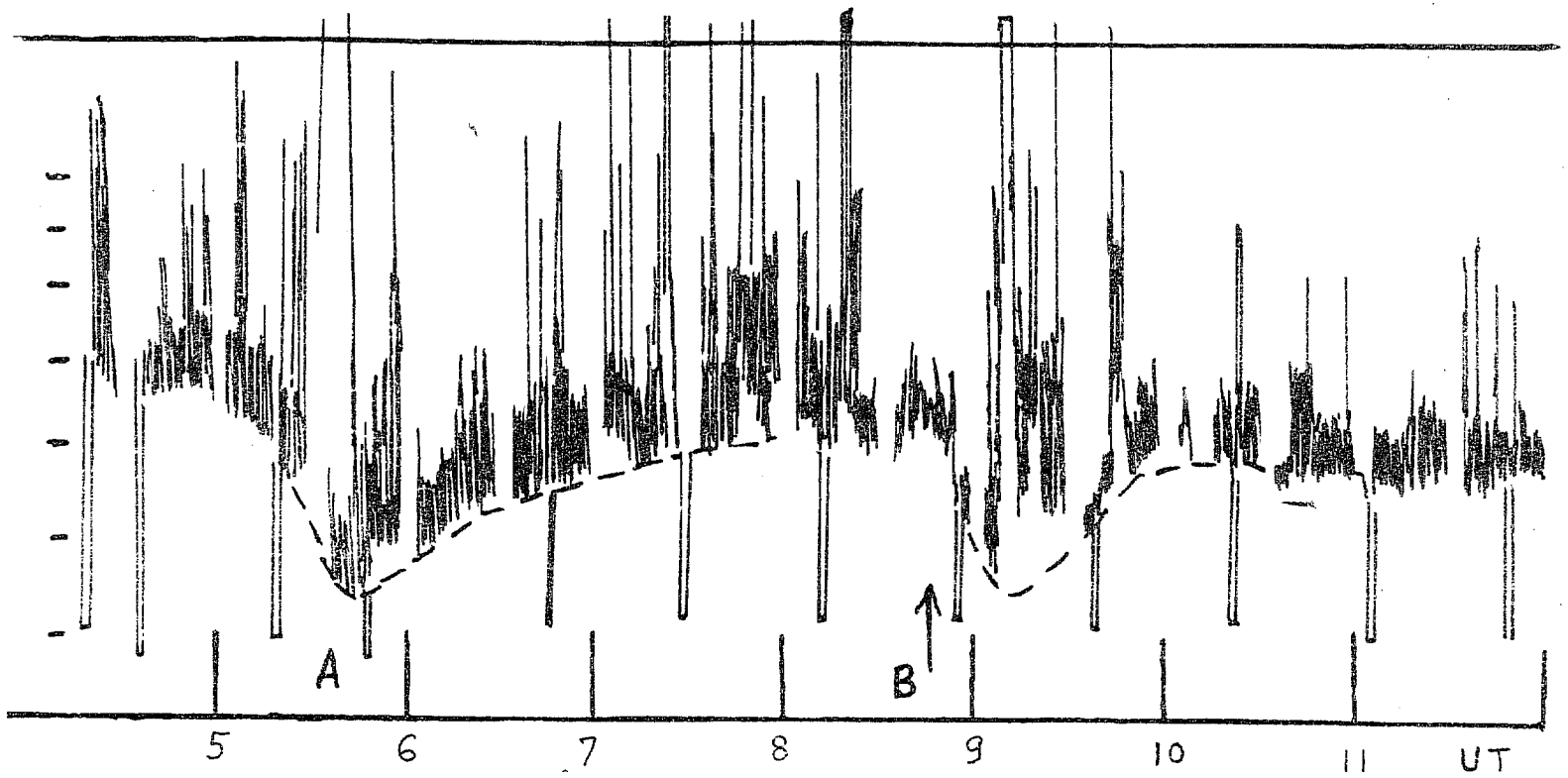

FIG. 4·5 COSMIC NOISE RECORD AT 25 Mc/s AT AHMEDABAD SHOWING ENHANCED ABSORPTION DUE TO STRONG foF2 INCREASE (A) & A SOLAR FLARE (B)

The undulations on the night of April 1-2 were stronger than in the previous night, which indicates that another sudden commencement might have taken place on the afternoon of April 1, though the magnetic observatories have not reported it. It is also probable that the storm on March 31 was exceptionally strong in producing large upheavals in the ionosphere for a longer period.

The electron densities were high throughout April 2 and no large scale oscillations appeared on that day. There were small perturbations following the storm in the early morning hours on April 3.

3.4 November 10-17, 1960

Solar activity was exceptionally high in this period. Increases in cosmic ray intensities were reported from higher latitudes and the polar cap type absorption, which is normally observed beyond 60° geomagnetic latitude under such magnetic disturbances, was reported down to 57° geomagnetic latitude (Ottawa) in this highly disturbed period. (A series of notes appeared in the Canadian Journal of Physics, Vol.39, pp.600-636, 1961 bear out this fact.) We shall first list the events in the following table.

The cosmic ray events are taken from Stoljoo et al (1961) and the polar cap black out data are taken from Campbell and Hubert (1961).

Table 4.

Date	Onset time IST	Description
10-11-60	1000	Class 3 flare (Canada)
11-11-60	0034	SC magnetic storm, $\Delta H = 133\gamma$ (Japan)
	0304	Great solar noise storm (Japan)
	0313	SCNA with solar noise storm (Ahmedabad)
12-11-60	1320	Great solar noise storm (Ottawa)
	1330	Class 3+ flare (Ottawa)
	1343	Neutron increase (Deep River)
	1345	SC magnetic storm $\Delta H = 437\gamma$
	by 1530	Polar black out (Resolute Bay)
	by 1515	Polar black out (Ottawa)
	1900	Secondary neutron increase (Deep River)
13-11-60	1021	SC magnetic storm (equatorial)
14-11-60	0010	Class 3 flare (Japan)
	0300	Class 3+ flare (Japan)
	0300	SCNA at 25 Mc/s (Ahmedabad)
	0320	Class 2 flare (Japan)
15-11-60	0307	Class 3+ flare (Canada)
	0220	Class 3+ flare (Japan)
	0220	SCNA (Ahmedabad)
	0242	Neutron increase (Deep River)
	0430	Polar black out (Resolute Bay)
	1302	SC magnetic storm $\Delta H = 305\gamma$
	1330	Polar black out (Ottawa).

In Fig.4.6, we have shown the iso-dense levels in the ionosphere over Ahmedabad during this period. If we compare the distribution on pairs of days, such as 10 and 11, 12 and 13 and 16 and 17, we would understand the effect of the magnetic storms on the F region better. The distribution on November 10 and 17 could be considered as quiet day distributions.

The storm on Nov.11 being a minor one did not cause any large scale upheavals in the ionosphere. Nonetheless its

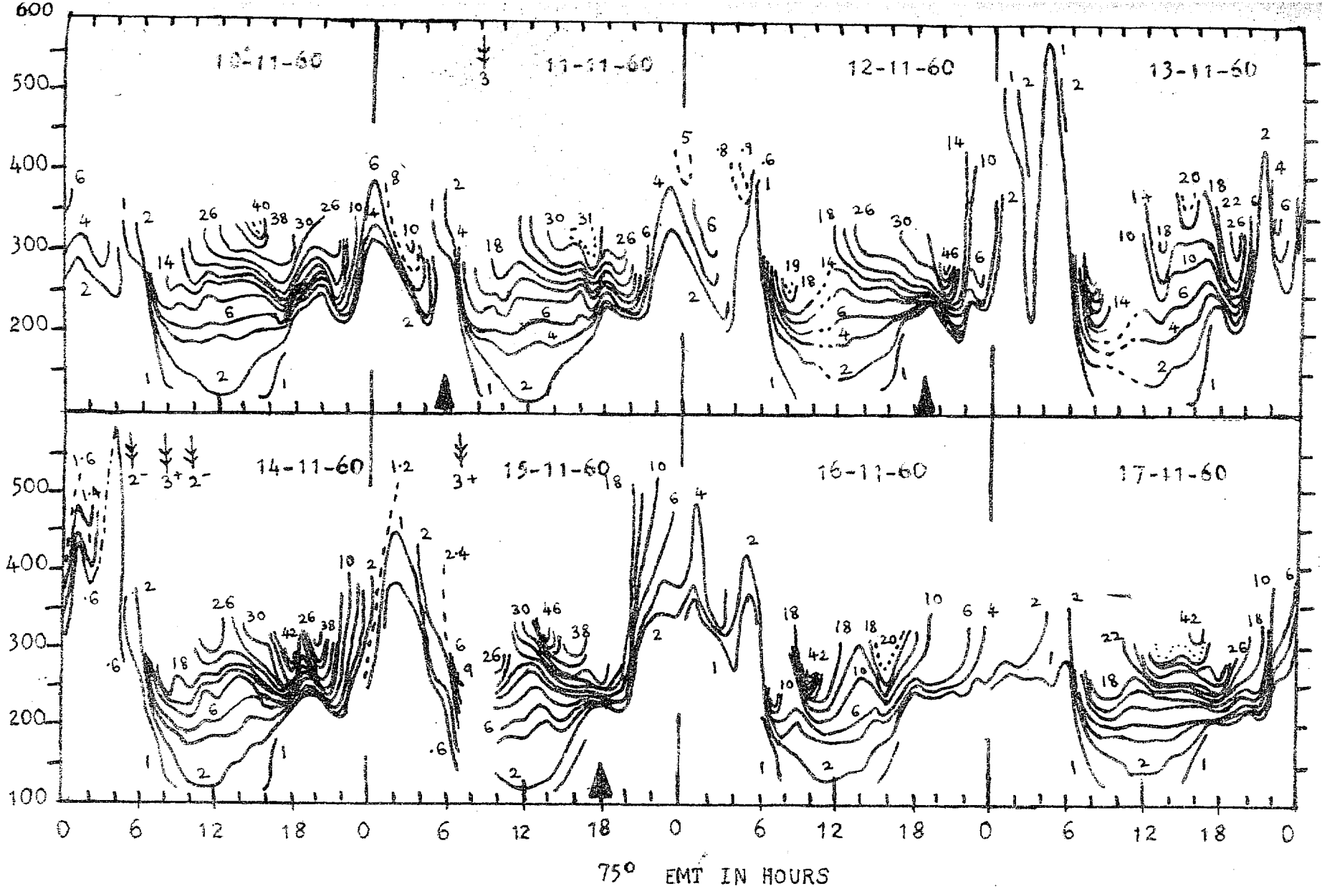

FIG. 4-6 ELECTRON DISTRIBUTION IN THE IONOSPHERE OVER AHMEDABAD DURING NOVEMBER 10-17, 1960

effect can be detected on the afternoon of that day. The storm on Nov.12 was the most severe one in this group. It is interesting to note that unusually large concentration of electrons appeared within an hour after the SC and then disappeared quickly in the next few hours. This high electron concentration caused corresponding large attenuation of the cosmic radio noise intensity at 25 Mc/s at Ahmedabad. The range of height variation on the night of Nov.12-13 was between 300 and 600 Km. The expected morning electron concentration occurred on the 13th morning. Before the ionospheric conditions returned to normal, there occurred another storm on 15-11-60. This caused the ion dense levels to spread out on the 16th. A localised high concentration of electrons can be seen at about 10 HMT on the 16th. This also caused large attenuation of cosmic radio noise intensity at 25 Mc/s at Ahmedabad. The significance of this attenuation and the mode of electron distribution in the ionosphere upto 1000 km are discussed more fully in the next chapter.

2.4.1 Cosmic radio noise record on November 11, 1960

We shall report here an interesting solar event which could not have been recorded elsewhere. Fig.4.7 shows a portion of the cosmic radio noise record at 25 Mc/s on November 11 at Ahmedabad. It shows an SCNA which occurred simultaneously with the solar flare at 0313 UT. It was gradual in development with a duration of about 90 minutes. It caused maximum absorption of 3 db of cosmic radio noise intensity. About two hours after

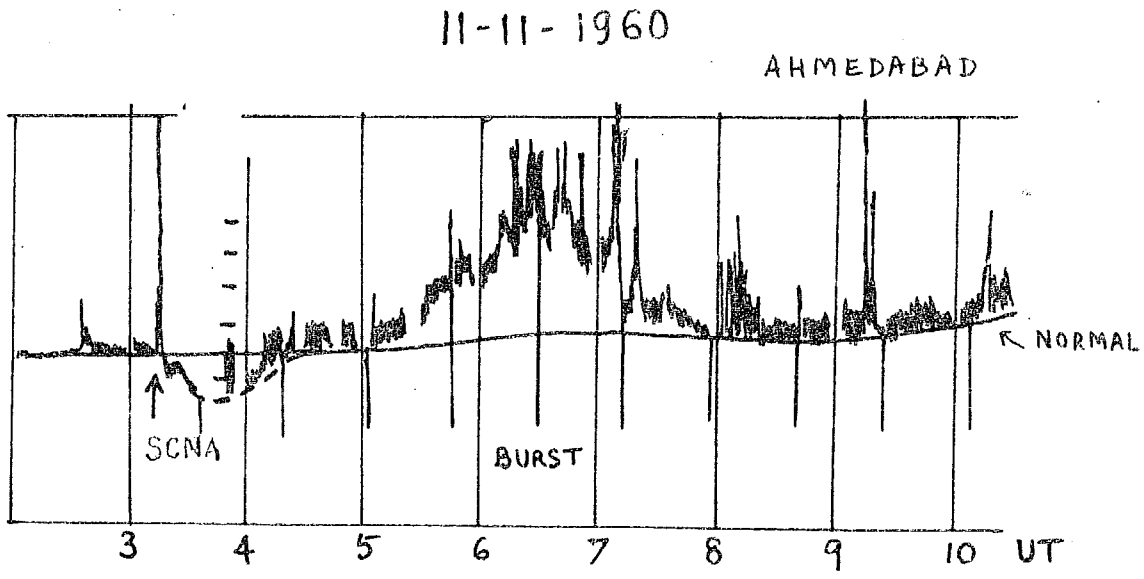

Fig. 4·7(A) COSMIC RADIO NOISE RECORD AT 25 Mc/s AT AHMEDABAD SHOWING AN SCNA AND SOLAR RADIO NOISE BURSTS

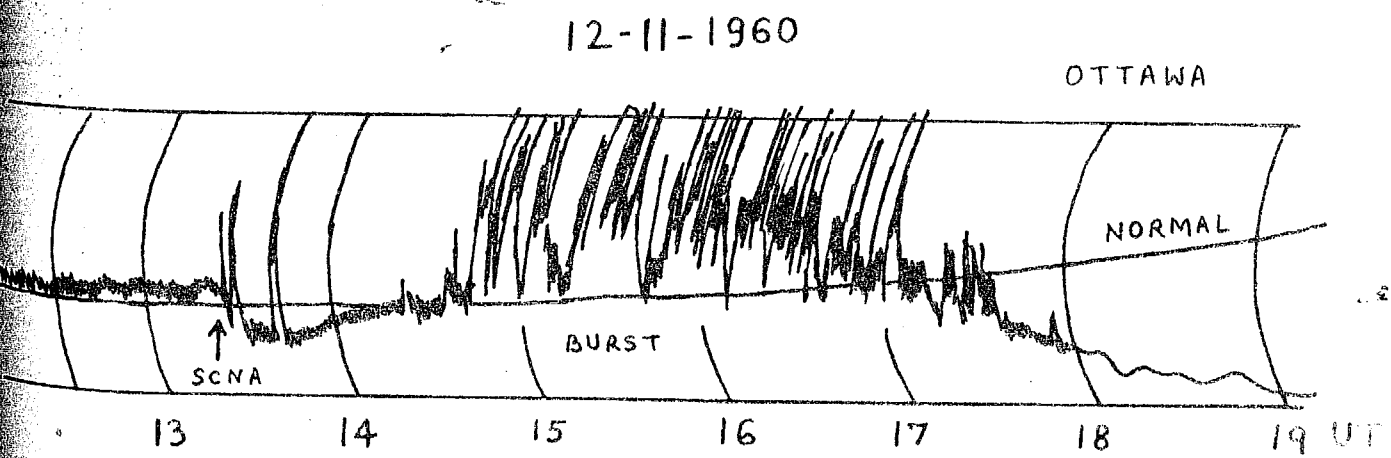

Fig. 4·7(B) RIOMETER RECORD AT 30 Mc/s SHOWING AN SCNA AND SOLAR RADIO NOISE BURSTS AT OTTAWA ON 12-11-60.

(AFTER VOGAN AND HARTZ 1961)

the start of the SCNA, a long duration burst of solar noise of highly variable intensity were recorded. The bursts lasted for nearly three hours. The cosmic radio noise intensity returned to normal at about 03 UT. It is possible that the severe magnetic storm which started at 1345 UT on Nov.12 was an effect of this solar flare and the subsequent intense solar radio bursts. We are led to this conclusion since the time delay between the occurrence of the SCNA on Nov.11 at Ahmedabad and the worldwide sudden commencement on Nov.12 was about 35 hours which is understandable. There was a similar event recorded on a 30 Mc/s riometer at Ottawa on Nov.12 at 1325 UT (Vogan and Hartz 1961) which is reproduced in the same figures for comparison. The SCNA at Ottawa caused a maximum absorption of 1 db and was also followed by irregular long duration solar bursts. In addition, it shows a polar cap type of absorption setting in immediately after the solar bursts.

2.4.2 Latitudinal variation of foF2 during Nov.1960 events

Another important feature in this series is depicted in Fig.4.3, wherein the daily foF2 variations at Ahmedabad (34° dip), Yamagawa (49° dip) and Wakkanai (60° dip) are plotted during 10-17 Nov. 1960. The foF2 variation showed the expected latitudinal distribution with Ahmedabad on the top on all days except on Nov.13 and 16. This means that on days following the severe magnetic storm, the peak foF2 belt gets largely liquidated. Therefore the foF2 variation at Ahmedabad did not

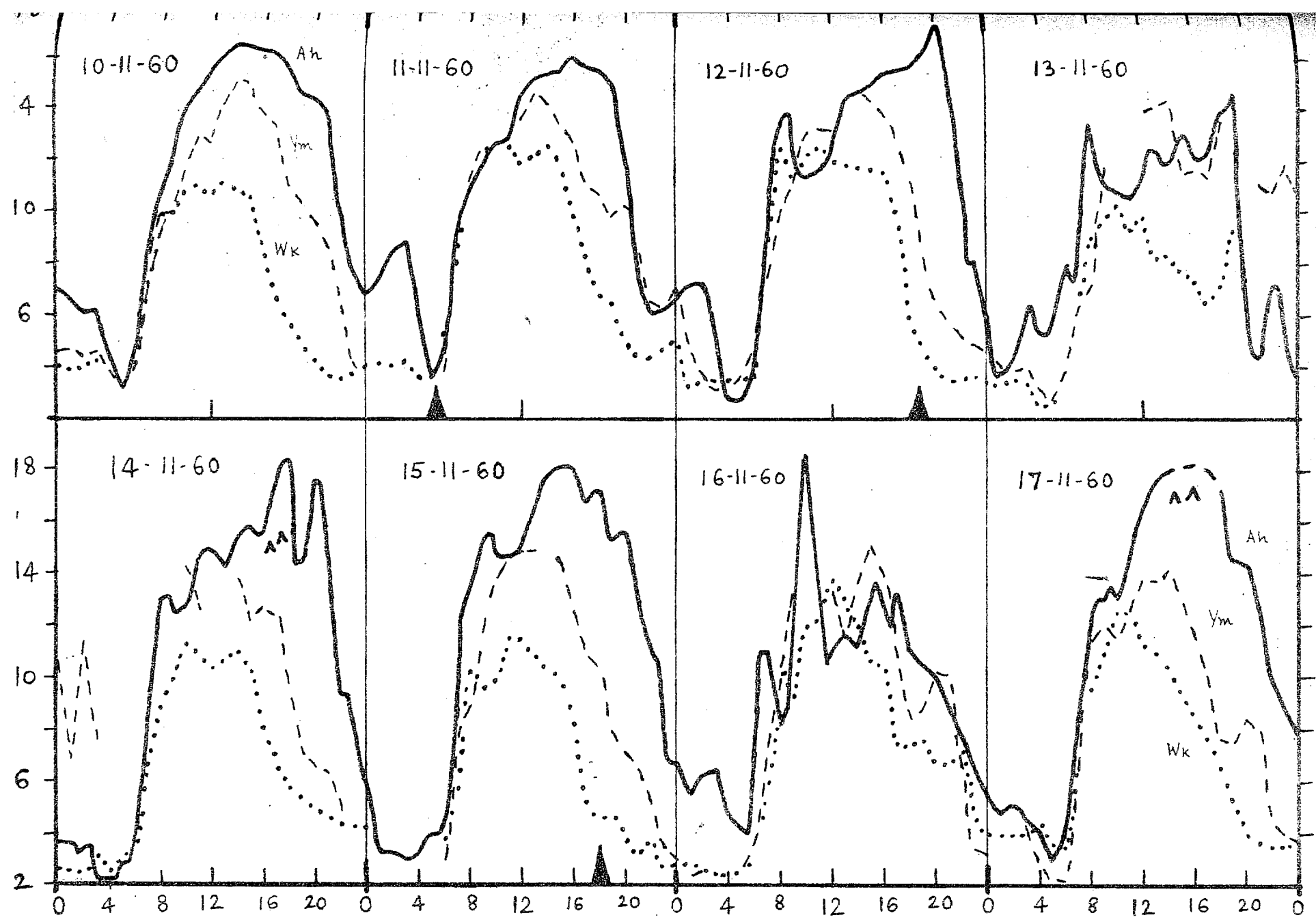

FIG. 48 f_0F_2 VARIATION WITH LATITUDE DURING NOVEMBER 1960 EVENTS AT AHMEDABAD (34° DIP) ——, YAMAGAWA (48° DIP) – – –, & WAKKANAI (60° DIP) . . .

differ much from that at higher latitudes. Once the influence of the storm receded, Ahmedabad regained its position near the peak foF2 belt. It would be interesting to study the global distribution of foF2 on these days.

A gist of the results during November 1960 events at Ahmedabad was submitted in a paper sent to the International Conference on Cosmic Rays and the Earth Storm held at Kyoto, Japan in September 1961. An abstract of the paper is appended at the end of this chapter (Degaonkar and Bhonsle 1961).

3. DISCUSSION

3.1 Variation of N_m, nT and h_m

It is interesting to compare the variation of the maximum electron density N_m, the total electron content in a column of unit cross-section nT and the height of maximum electron density h_m during magnetic storms. We calculated the total electron content upto h_m from N(h) data by the trapezium rule from the base of the E layer during day and from the base of the F layer during night. N_m is obtained from foF2 by the relation $N = 1.24 \times 10^4 f_0^2$. N_m is expressed in 10^5 el/cc and nT in 10^{13} electrons per cm^2 col so that both these amounts become comparable with only a difference in their units. The results are shown in Fig.4.9.

On examining the nature of variation of N_m and nT at

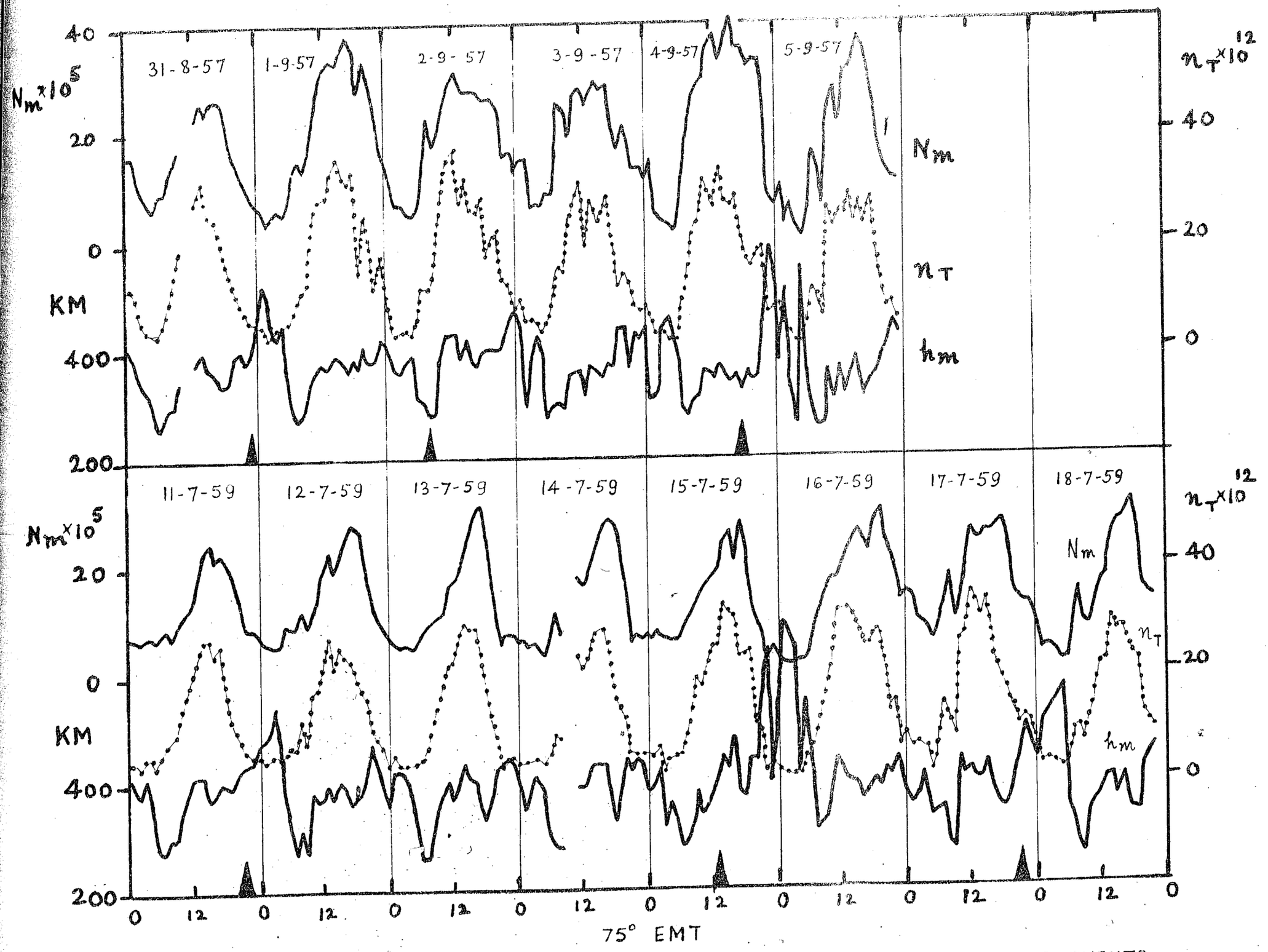

FIG. 4.9 Nm, n_T & hm, VARIATION AT AHMEDABAD DURING SEPT. 1957 & JULY 1959 EVENTS

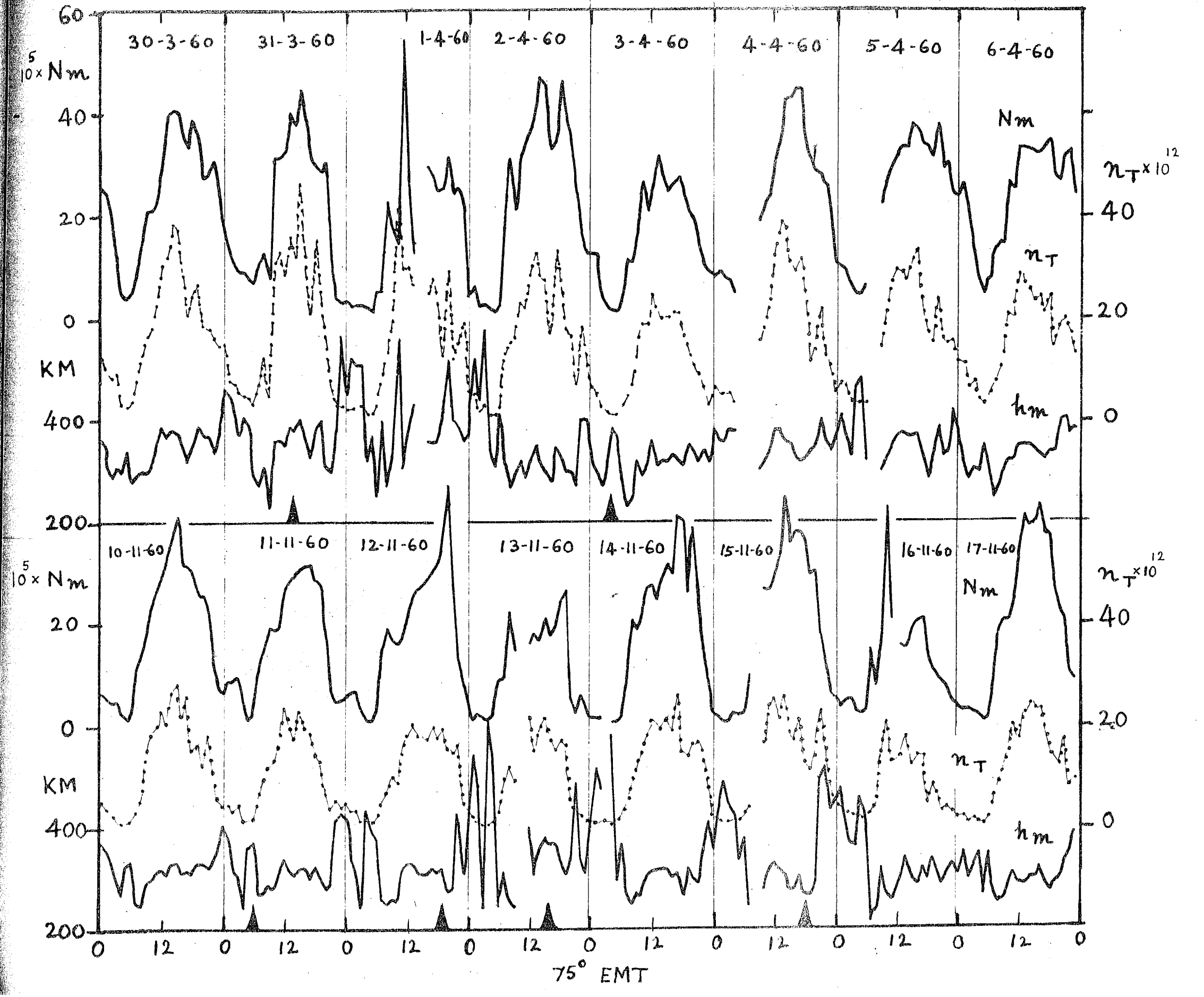
30-3-60
31-3-60
1-4-60
2-4-60
3-4-60
4-4-60
5-4-60
6-4-60
10^5 × Nm
60
40
20
0
KM
400
200
Nm
n_T
$n_T \times 10^{12}$
40
20
0
hm
10-11-60
11-11-60
12-11-60
13-11-60
14-11-60
15-11-60
16-11-60
17-11-60
10^5 × Nm
20
0
KM
400
200
Nm
n_T
$n_T \times 10^{12}$
40
20
0
hm
0
12
0
12
0
12
0
12
0
12
0
12
0
12
0
12
0
75° EMT

Ahmedabad in all the four groups of events, we find that their variation is fairly smooth on quiet and slight disturbed days with a maximum occurring between 14-15 hrs and a minimum early in the morning. It is wellknown that N_m does not obey cos χ law, and it can be seen here that n_T also does not vary with $\cos^n \chi$ strictly though it tends to have a closer dependence on cos χ than N_m. Sheriff (1956) arrived at a similar conclusion from the study of Ahmedabad records during 1953-54.

During the main phase of a magnetic storm of high intensity, N_m and n_T both undergo rapid changes. At Ahmedabad, N_m gets depressed within a few hours after the SC and from Fig.4.9 and 4.10 it can be seen that n_T also is reduced during the main phase. This lends support to the ionization drift theory.

If we look at the results on the seasonal basis, we find that N_m and n_T are less in July than those in equinoxes and winter months. Similarly, the magnetic storm affects the ionospheric parameters much more in winter and equinoxes. It may be noted that N_m and n_T do not undergo similar variation all the time; large N_m does not necessarily mean large total content n_T. because heights are involved in the calculation of n_T.

The variation of h_m is also shown in Fig.4.9 and 4.10. It can be observed that large changes in h_m took place during dark hours following the SC. The nighttime change in h_m was of the order of 300 Km. During daytime, the changes in h_m were quite small.

3.3 Results obtained elsewhere

The height h_m did not differ much during day from that during night on quiet days at Ahmedabad. It, however, showed a dip in the morning hours. At Slough and Watheroo, Thomas (1959) found that h_m was lower by 50-100 Km at midday than at midnight both in low and high sunspot years. At Maui, the variation of h_m is more like that at Ahmedabad.

Thomas (1959) has also studied the latitudinal variation of h_mF_2 at midday and midnight during summer and equinoxes and at different epochs of the solar cycle. It is clear that h_mF_2 near magnetic equator is higher at midday than at midnight in all seasons. At moderate to high latitudes, noon h_mF_2 is about 330 Km and at midnight 300-350 Km in summer. The seasonal variation is opposite to that predicted by the Chapman theory. At Ahmedabad, in years of high solar activity, the average value of h_m is between 300-350 Km with small fluctuations.

4. SUMMARY OF THE RESULTS

We summarise the main points from the study of the electron density and height distribution at Ahmedabad under magnetically disturbed conditions.

(1) Large depressions in electron densities and elevations in height take place most significantly during night hours after the SC of a severe magnetic storm.

(2) Electron densities remain low on the day following the SC. On the third day of the storm, the electron densities are more than restored above their normal values.

(3) The total electron content in a column of unit cross-section upto h_m suffers considerable reduction during severe magnetic storms occurring in winter and equinoxes.

(4) Localised high concentration of electron density at a height of about 250 Km are formed at 08-09 hrs in the morning after the SC. Large irregular concentrations of very high density were found in the March-April and November 1960 events.

(5) Large perturbations in height of the order of 300 Km are induced by severe storms.

(6) The latitudinal peak of F2 near the latitude of Ahmedabad apparently gets dilated during large disturbances.

-:oooOOOooo:-

Ionospheric disturbances and changes in Cosmic Radio Noise Absorption on 25 Mc/s at Ahmedabad associated with some Solar events and geomagnetic storms in November 1960

By

S.S.Degaonkar and R.V.Bhonsle

Physical Research Laboratory, Ahmedabad, India.

SUMMARY

The paper describes the results of analysis of N(h) profiles and the changes in the observed total attenuations of 25 Mc/s cosmic radio noise recorded at Ahmedabad during 10-17 November 1960, a period of high solar activity.

Using N(h) data and tentative models of electron density variation with height above h_{max}, calculations of ionospheric attenuation on 25 Mc/s cosmic radio noise were made and compared with the observed total attenuation of cosmic radio noise. It is shown that a substantial part of the attenuation takes place above h_{max} and that during magnetic storms, the attenuations are greatly reduced.

(Presented at the International Conference on Earth Storm held at Kyoto, Japan in September 1961)

CHAPTER V

CALCULATION OF IONOSPHERIC ATTENUATION AT 25 MC/S COSMIC RADIO NOISE AT AHMEDABAD ON THE BASIS OF $\int N\nu\,ds$

1. INTRODUCTION

A cosmic radio noise recording equipment at 25 Mc/s was set up by Dr.R.V.Bhonsle at the Physical Research Laboratory in 1956 and data have been collected since then. The records have provided valuable information on some aspects of ionospheric physics in low latitudes. The results have been analysed and partly discussed (see references at the end). Among the problems studied have been :

(a) The diurnal and seasonal variations of total ionospheric attenuation of cosmic radio noise at 25 Mc/s.

(b) Sudden ionospheric disturbances (SID's) associated with solar flares. These show up as sudden cosmic noise absorptions (SCNA's).

(c) Changes in ionospheric attenuation in geomagnetically disturbed periods.

The main points that have emerged from the study are :

(1) The monthly mean diurnal curves of the total attenuation exhibited either one hump or two humps. The humps were more prominent in equinoxes than in summer and winter.

(2) The first hump occurred in most of the months between 14 and 16 hr local time.

(3) Whenever the second hump occurred, it did so in the early part of the night. It was most frequent in equinoxes and in some winters in the high sunspot period.

(4) The total attenuation could be divided into two components : (i) a daytime symmetrical component about noon and (ii) a residual non-symmetrical component. Unambiguous correlation of the non-symmetrical component with the critical frequency, f_0F_2, of the F2 layer showed that the major part of it originated in the F region, though there might be residual effects originating above the level of F2 peak ionization.

(5) The magnitude of total attenuation observed at Ahmedabad during 1957-59 was much higher than that observed by Mitra and Shain (1953) in Australia. This high value of attenuation at Ahmedabad was partly expected because Ahmedabad is situated near the latitude of peak F2 ionization.

(6) The D region absorption at Ahmedabad was never greater

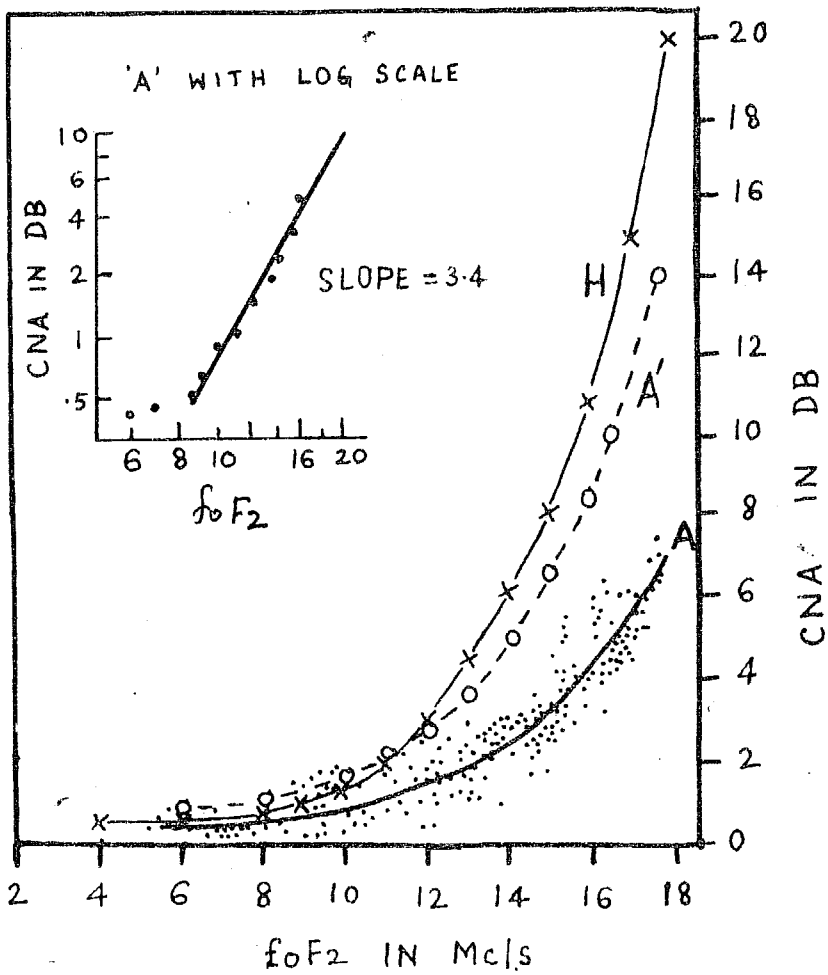

COSMIC NOISE ABSORPTION AGAINST foF_2

A – 25 Mc/s AHMEDABAD, 1958-59

A' – 18 Mc/s CALCULATED FROM 'A'

H – 18 Mc/s HAWAII, NOVEMBER 1958 (STEIGER & WARWICK)

FIG 5·1

than 3 db even in summer, while high F2 attenuation exceeding 6-7 db have been observed frequently (Bhonsle and Ramanathan 1953). This is in contrast with that reported by Mitra and Shain from the observations in Australia, where they found that the major contribution to the total absorption came from the D region with a small portion in the F2 region depending on its critical frequency.

Fig.5.1 shows a mass plot of the mean hourly values of cosmic radio noise absorption at 23 Mc/s at Ahmedabad against foF2 in each month during 1958-59. The mean curve drawn on logarithmic scale is shown at the left hand top corner. It can be seen that there is approximately a linear relationship between log(foF2) and log(D) for foF2 $>$ 3 Mc/s. The attenuation under this condition can be expressed as

$$D = K + \lambda (foF2 - 3)^{3.4} \qquad (1)$$

The significance of the exponent is discussed in a paper by Ramanathan, Bhonsle and Deganker (1961).

2. EFFECT OF GEOMAGNETIC STORMS ON COSMIC RADIO NOISE ABSORPTION

In a study of the effect of magnetic storms on the total attenuation of cosmic radio noise, Bhonsle and Ramanathan

(1950) found that the total attenuation became abnormally low on the first two days after the sudden commencement of the storm but increased to values above normal on the third day after the commencement. The observed changes in attenuation associated with magnetic storms were tentatively explained as being due to changes in foF2 and F scatter.

It was thus clear that the region F both above and below its peak density play an important role in producing high attenuation observed in these latitudes. As we have a long series of ionospheric and cosmic noise data, it was considered that it would be useful to calculate the ionospheric attenuation at 25 Mc/s from N(h) profiles, for a few interesting events at least, in order to estimate the electron distribution in the outer ionosphere. In the following pages we shall describe the method of calculation and discuss the results.

3. THEORY OF IONOSPHERIC ABSORPTION

The ionosphere contains free electrons and ions which are set in vibration by the passage of an electromagnetic wave. The ions being more massive, their accelerations and velocities will be much less than those of the electrons. If each electron is assumed to be free, it will execute regular periodic oscillations so long as the wave is passing through the ionised cloud. The oscillating electrons scatter some of the incident radiation and the scattered wavelets add up with the incident radiation

causing a change of phase of the transmitted wave and the intensity of the incident wave also suffers some attenuation due to scattering. On the whole no nett work is done on the electron since the electron re-radiates what it receives. If, however, the electrons are not entirely free to execute oscillations as they collide with ions and neutral particles which are present, in the ionosphere, they change the energy of oscillatory motion into the kinetic energy of random movement. The energy is then lost from the point of view of the passing wave and therefore the wave gets attenuated. The overall attenuation per unit path length will depend on the product of electron density N and the electron collision frequency, ν and inversely on the angular frequency of the wave, ω . This means that if $\omega >> \nu$, then the attenuation decreases as the frequency increases. In the atmosphere, it should be noted that N and ν are functions of height. The attenuation per unit path length depends on the product $N\nu$.

The magneto-ionic theory shows that provided the direction of phase propagation is not perpendicular to the magnetic field, the absorption coefficient K is given by [see Mitra (1952) or Ratcliffe (1959)] .

$$K = \frac{2\pi e^2}{mc} \frac{1}{\mu} \frac{N\nu}{(\omega \pm \omega_L)^2 + \nu^2} \qquad (2)$$

where the symbols have their usual meanings, ω_L is the angular gyrofrequency corresponding to the longitudinal

component of the earth's magnetic field. The two signs indicate the ordinary (+) and the extra-ordinary (-) component of the wave. Two types of absorption generally occur in the ionosphere, namely, i) non-deviative and ii) deviative.

We are mainly concerned with non-deviative type of absorption here, since it can be assumed that $\nu^2 << (\omega \pm \omega_L)^2$ and $\mu \approx 1$ if the critical frequency of the region is not too close to the operating frequency.

Therefore equation (2) becomes

$$K = \frac{2\pi e^2}{mc} \frac{N\nu}{\nu^2 + (\omega \pm \omega_L)^2} \qquad (3)$$

and the total attenuation can be evaluated by

$$\int K \, ds = \frac{2\pi e^2}{mc} \frac{1}{(\omega \pm \omega_L)^2} \int N\nu \, ds \qquad (4)$$

The non deviative absorption of radio waves of high frequency f in the vertical direction in the ionosphere can be calculated from equation 4 if we know the distribution of N and its collision frequency. The equation can be further simplified since $\omega_L << \omega$ and therefore ω_L can be neglected (Chapman and Little 1957). The equation 4 then becomes

$$\int K \, ds = \frac{e^2}{2\pi mcf^2} \int N_e \nu \, ds \qquad (5)$$

or it can be written as

$$D = \frac{A}{f^2} \qquad (6)$$

where D is expressed in decibels and f in Mc/s, and

$$A = 1.17 \times 10^{-14} \int_0^H N_e \nu \, dh \qquad (7)$$

where N_e is the number density of electrons, ν its effective collision frequency, and H is the maximum height to which integration is taken.

4. EFFECTIVE COLLISION FREQUENCY OF ELECTRONS

In calculating ionospheric absorption collision frequencies of electrons with ions and with neutral particles have both to be considered.

For levels below 100 Km where the air is not appreciably dissociated, the collision frequency ν_{en} of electrons with neutral particles (atoms and molecules) is given by (Nicolet 1950).

$$\nu_{en} = 5.4 \times 10^{-10} N_n T^{1/2} \qquad (8)$$

where N_n is the number density of neutral particles. ν_{en} decreases with height since N_n also decreases.

Cowling (1945) showed that when an electron moves through an atmosphere containing uncharged atoms and molecules and comparatively few ions, the effective cross-section for collision between an electron and an ion is much larger than that for a collision between an electron and a neutral particle. In D and E regions of the ionosphere, ν_{en} predominates, while

in the F region ν_{ei} becomes important. The electron-ion collisions in the higher regions of the ionosphere become particularly important in latitudes where medium densities are high. This has been clearly brought out by Ramanathan et al (1961).

Gouling's expression for the collision frequency of electrons with positive ions as revised by Nicolet (1953) is given as

$$\nu_{ei} = \left[34 + 4.18 \log_{10} \left(\frac{T^3}{Ne} \right) \right] N_i T^{-3/2} \qquad (3)$$

If we assume that in the ionosphere most of the positively charged particles are singly ionized, then $N_i \approx N_e$.

ν_{ei} is a function of both electron density and temperature. For the same electron density, the collision frequency ν_{ei} decreases with increase of temperature.

There is yet another collision frequency ν_{in} between ions and neutral particles which is given by

$$\nu_{in} = 3.6 \times 10^{-9} (N_0 + N_n) M^{-1/2} \qquad (3)$$

where M is the molecular weight of the ions and neutral particles (assumed equal). However, ν_{in} is very small in the upper parts of the ionosphere and therefore can be neglected. Thus the effective collision frequency of electrons ν would be the sum of ν_{en} and ν_{ei} .

5. CALCULATION OF ABSORPTION AT DIFFERENT LEVELS

5.1 Values of electron collision frequencies

The values of ν_{en} as given by Nicolet (1959) between 63-110 Km were used to calculate the absorption in that region.

To obtain ν_{ei} for different values of N_e and T from equation 8, we have to assume a certain model of temperature distribution in the ionosphere. We calculated ν_{ei} for some fixed values of N_e and temperature ranging from 10^4 to 10^5 el/cc and 200° to 1500° K respectively. We plotted on double log scale ν_{ei} against N_e at fixed T and obtained series of graphs of straight lines for each fixed temperature. Then we adopted a model of temperature distribution by Yonezawa (1960) between 120 and 480 Km at each 20 Km interval. We read off the values of ν_{ei} from the graph corresponding to the temperature at that level and prepared a table showing ν_{ei} at each 20 Km from 120 to 400 Km and for various values of N_e. A condensed table of this type is given in the Appendix at the end of the chapter. Above 500 Km, a constant temperature of 1580° K was assumed according to Nicolet (1960).

There are various upper atmospheric models based on the results from rockets and satellites available at present. The one proposed by Mathur and Mitra (1960) shows higher values of temperature throughout the ionosphere than that given by Yonezawa. Recently, Kallmann (1961) studied the daytime and

nighttime atmospheric properties as revealed by the satellite drag observations and came to the conclusion that the temperature remains constant at about 1230° K above 350 Km during daytime and at 1050° K above 250 Km during nighttime. Mathur and Mitra proposed an isothermal temperature of 2070° K above 700 Km both by day and night. There are considerable differences in the various models and we thought it safe enough to assume an average value of 1500° K above 500 Km as given by Nicolet.

5.2 Values of electron density at different levels

The values of N_0 for zenith sun at levels below 90 Km were taken from Nicolet and Aikin's paper (1960) corresponding to disturbed solar conditions. Between 90-130 Km they were interpolated from the values at 90 and 130 Km. Above 130 Km to the level of maximum electron density in $F2$, the N(h) profile data were calculated from the ionospheric sounding records. For the region above $h_{max}F2$, the values of electron density were estimated for two extreme models, one given by Al'pert et al (1953) and the other by Kasantsev (1959). Al'pert's model was derived from the observations of the time of "radio rise and set" of Sputnik I and that of Kasantsev on the received field strengths of the first two Soviet satellites. Later, a model proposed by Garriott (1960) which is also based on the satellite observations was used. We have reproduced in Fig.5.2 the three models used for the estimation of electron density distribution above h_{max} at Ahmedabad. The dashed lines in the figure are our

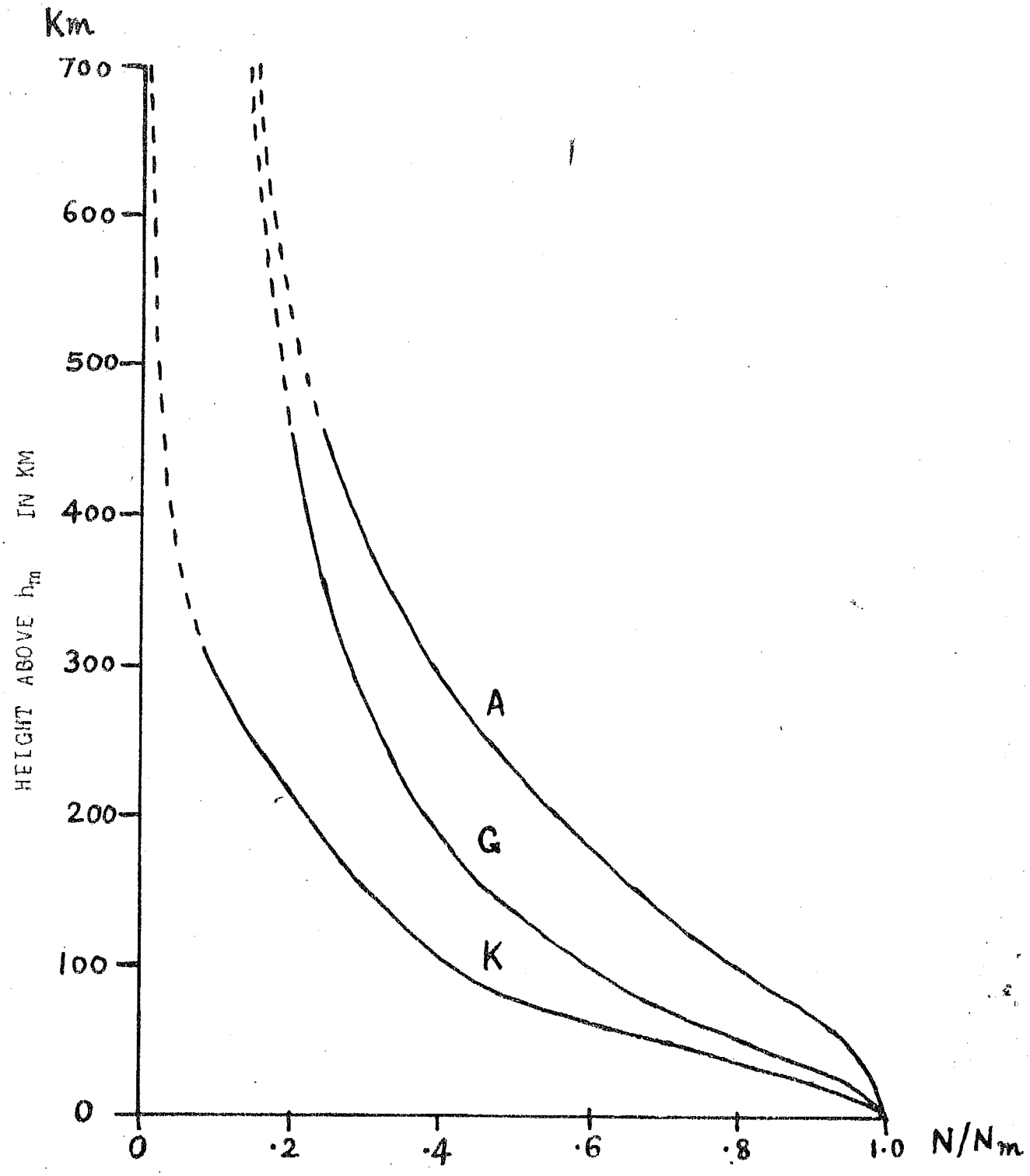

FIG. 5·2 ELECTRON DENSITY DISTRIBUTION ABOVE hm ACCORDING TO AL'PERT ET AL (A), GARRIOTT (G), AND KAZANTSEV (K)

extrapolations. Table 1 shows the values of N_0, N_n, ν_{en}, ν_{ei} and the product $N_0\nu$ from 70 Km to 900 Km at 15 hrs on 1-8-57. Here, Al'pert's model was used for N_0 above h_{max}.

Table 1.

Ht.	T°K	N_n	N_0	ν_{en}	ν_{ei}	$N_0\nu$
70	210		4.2^8	1.1^7		4.2^9
80	197		4.2^8	2.5^6		2.3^9
90	197		1.1^4	4.9^5	1.0^2	5.0^9
100	210	1.5^{13}	3.0^4	1.1^6	4.4^2	3.0^9
120	330	9.6^{11}	1.0^5	1.0^4	1.1^3	2.1^9
140	613	2.2^{11}	2.2^5	3.7^3	6.3^2	7.9^3
160	616	7.9^{10}	2.7^5	1.1^3	3.1^2	3.2^3
180	702	3.5^{10}	3.6^5	5.1^2	3.4^2	4.7^3
200	775	1.8^{10}	4.5^5	3.7^2	9.1^2	5.3^3
250	909	4.9^9	7.9^5	8.0^1	1.3^3	1.5^9
300	1033	1.1^9	1.4^6	2.7^1	2.0^3	3.8^9
350	1140	6.5^8	2.0^6	1.2^1	3.7^3	1.1^{10}
400	1220	3.0^8	3.3^6	5.4^0	3.4^3	1.1^{10}
450	1400	1.1^8	3.1^6		2.5^3	7.8^9
500	1500	6.1^7	2.6^6		1.6^3	4.2^9
600	1530	1.9^7	1.9^6		1.1^3	2.0^9
700	1530	6.6^6	1.3^6		8.0^2	1.0^9
800	1530		9.3^5		6.0^2	5.6^8
900	1530		7.0^5		4.6^2	3.2^8

Here the notation 2.2^6 is used to denote 2.2×10^6.

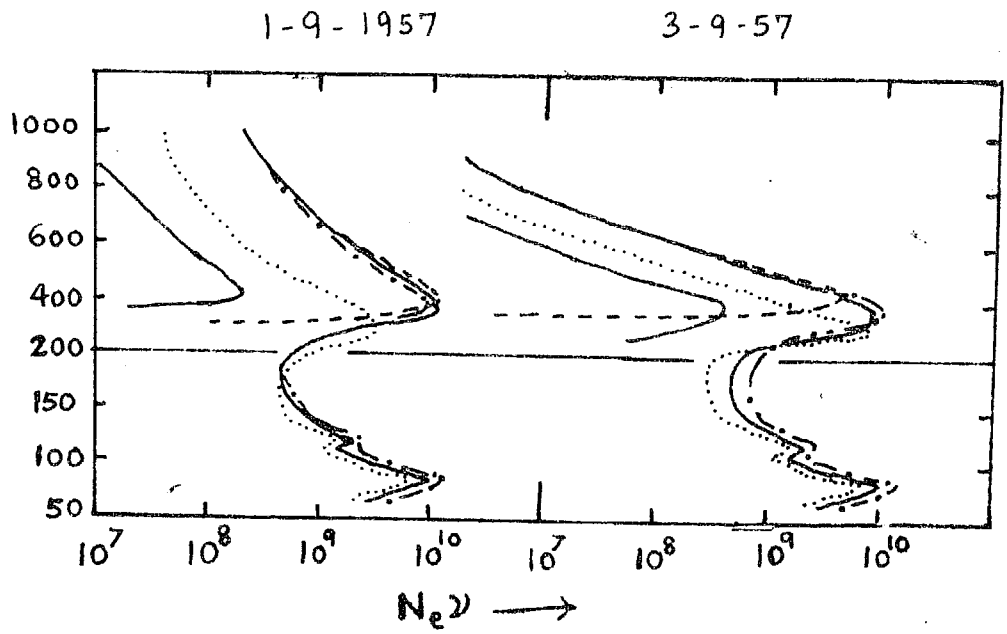

$N_e\nu$ VS. HEIGHT OVER AHMEDABAD ON A DAY WITH HIGH CNA WITH AL'PERT MODEL ABOVE h_{max} (1-9-57) AND ON A DAY OF LOW CNA WITH KAZANTSEV MODEL ABOVE h_{max} (3-9-57) AT —— 03, ···· 08, ·—· 12, — 15 & – – – 20 HRS

FIG. 5·3

Having thus obtained N_0 values from 120 to 1000 Km for each hour during day and from h_0F to 1000 Km during night on each day and knowing ν_{en} and ν_{ei} from the tables, we obtained the product $N_0\nu$. The manner in which the product $N_0\nu$ varies with height is shown in Fig.5.3. The different curves relate to 3, 9, 12, 15 and 20 hrs on 1-9-57 and 3-3-57 over Ahmedabad. The absorption due to electron-neutral particle collisions and electron-positive ion collisions were separately calculated. The product $N_0\nu$ attains a maximum near about 85 Km and falls off with increasing height with a small secondary maximum at 120 Km. Above 240 Km, only electron-ion collisions are important. The absorption is maximum near the level of maximum electron density.

5.3 Numerical integration of $\int N\nu\, dh$

Numerical integration of $\overline{N_0\nu\, dh}$ was carried out by dividing the ionosphere into 5 Km interval between 65 and 120 Km, 20 Km interval between 120 Km and h_mF and 50 Km interval between h_mF and 1000 Km. The calculated absorption in the region 65-120 Km was about 0.3 db for zenith sun in September. The absorption in this region for other values of solar zenith angles was calculated on the assumption that it obeyed a $\cos^n\chi$ law where $n = 0.75$ (Raver 1957). Also for this region, the same average electron density distribution depending on local time was assumed for all the days under investigation.

6. RESULTS OF CALCULATION OF IONOSPHERIC ATTENUATION

We have calculated the ionospheric attenuation of the cosmic radio noise at 25 Mc/s upto 1000 Km by the method outlined above in the case of two series of events, one from August 30 to September 6, 1957 and the other from November 10 to 17, 1960. The reasons for choosing these two periods are the following :

(1) Complete ionospheric data and the cosmic noise data were available without any serious gap.

(2) The first group represented the conditions in the high sunspot period which the second substantially tended towards the waning sunspot cycle.

(3) Geomagnetically both were highly disturbed periods and as such large changes in foF2 and the total attenuation of cosmic radio noise were observed.

We shall first describe the results obtained in the September 1959 period and then those in the November 1960 events.

6.1 August 30 - September 6, 1957

6.1.1 Comparison of observed values of total attenuation and calculated values of absorption below hmF

The total ionospheric attenuations measured with the cosmic radio noise at 25 Mc/s at Ahmedabad for the period August 30-September 6, 1957 are shown in Fig.5.4. The calculated

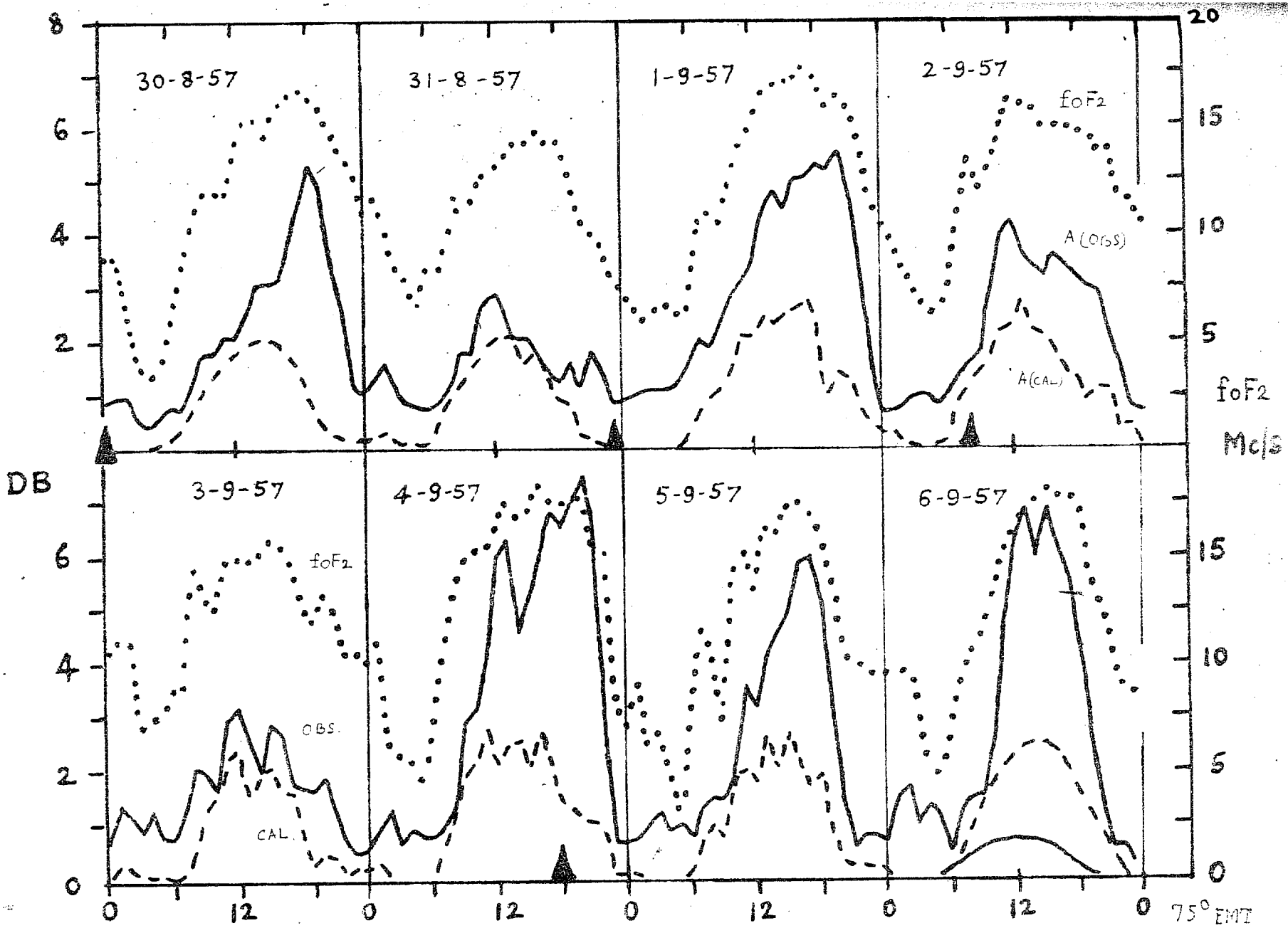

FIG. 5·4 COSMIC RADIO NOISE ABSORPTION ON 25 Mc/s OBSERVED AND CALCULATED AT AHMEDABAD TO-GETHER WITH foF2 AT AHMEDABAD

values of ionospheric absorption below h_{gF} and the values of foF2 are also plotted in the figure. There occurred three SC magnetic storms in this period and are shown by an arrowheads in the same figure. The measurpd total attenuation exhibited a diurnal variation with large day to day changes. The calculated absorptions for the region below h_{max} show maxima of 2 to 3 db between 13 and 16 hr local time on all these days and smaller value of absorption in the morning and evening hours. The measured total attenuations are always higher than the corresponding calculated values of absorption for the region below h_{gF}. This is no doubt largely due to the contribution to absorption from regions above Fg peak.

6.1.2 Calculated absorption upto 1000 Km.

In Fig.6.4 are plotted for 1-3-1957 besides the measured and calculated absorptions below h_{gF}, also the calculated hourly absorptions upto 1000 Km, A(A) and A(K), assuming Al'pert's and Kazantsev's models of electron distribution above h_{max}. On this day, absorption calculated on Al'pert's model, A(A), gave generally good agreement with observation, though there is some disagreement between the observed and calculated curves in the evening hours. Kazantsev's model gave too small values. On 3-3-57, a day on which the measured attenuation was abnormally low, the absorptions calculated on Kazantsev's model gave a reasonable fit except in the evening hours. The results can be interpreted to mean that the total

1-9-57

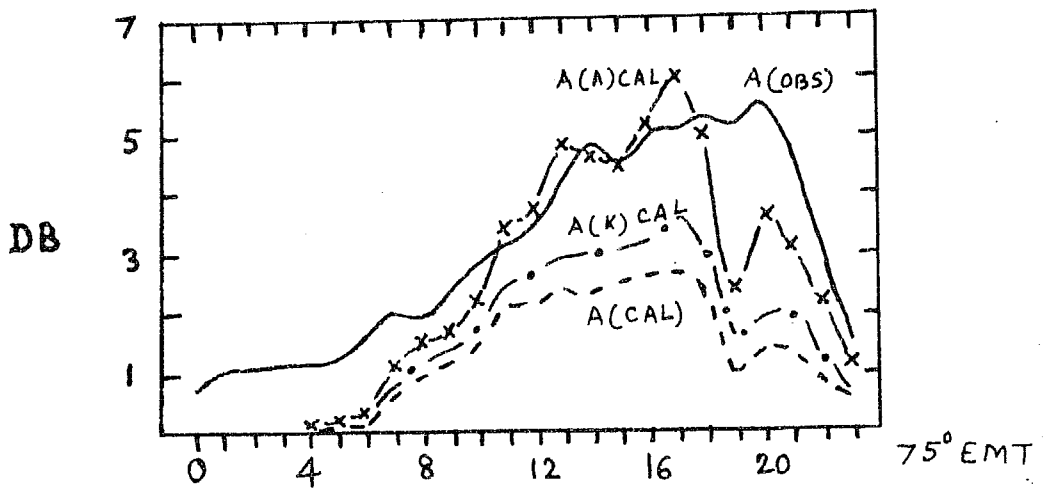

3-9-57

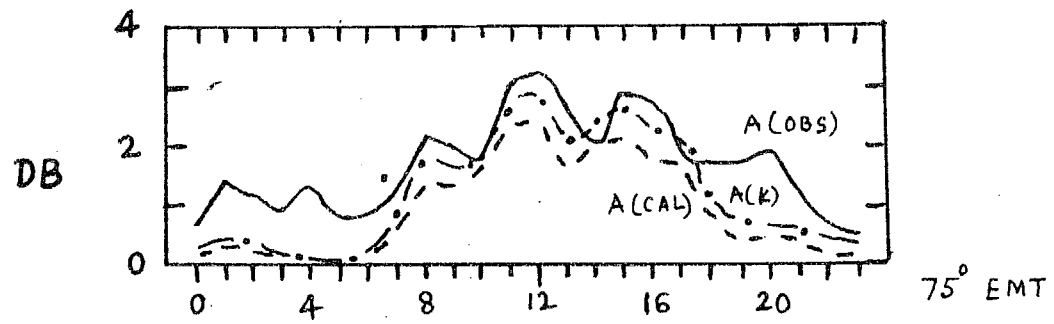

COSMIC RADIO NOISE ABSORPTION ON 25 Mc/s
(OBSERVED AND CALCULATED) AT AHMEDABAD

(×××) – A(A) CAL – ABSORPTION UPTO 100 KM USING ALBERT MODEL

(–·–·–) A(K) CAL – " " " " KAZANTSEV MODEL

(– – –) A(CAL) – " BELOW h_{max}

(——) A(OBS) – OBSERVED ATTENUATION AT 25 Mc/s

number of electrons over unit area above h_{max} was much less on 3-3-57 than on 1-3-57. The evidence is strong that the total number of electrons in the ionosphere above h_{max} is largely depleted on the second day of a magnetic storm and that it is more than restored on the third day after the SC.

6.3 November 10-17, 1960

This period was eventful and has drawn worldwide attention because many interesting phenomena took place within four days between November 11-15, 1960. The cosmic radio noise monitor at Ahmedabad recorded three SCNA's in this period and in one case i.e. on 11-11-60, an SCNA associated with solar radio noise bursts were recorded. Full details of the events and the electron distribution over Ahmedabad have been described earlier in Chapter IV.

We calculated the true height profiles and utilising the data, calculated the ionospheric attenuation upto 1000 Km and compared it with the observed attenuation of cosmic radio noise.

In order to find out a more appropriate model of electron distribution above h_{max} over Ahmedabad, we tried, in addition to the models of Al'pert and Knnantsev, a model due to Garriott. Hourly values of attenuation upto 1000 Km were calculated on each day from 06 to 23 hrs IMT and corresponding hourly values of cosmic radio noise attenuation from cosmic

↓ SOLAR FLARE , ▲ SUDDEN COMMENCEMENT

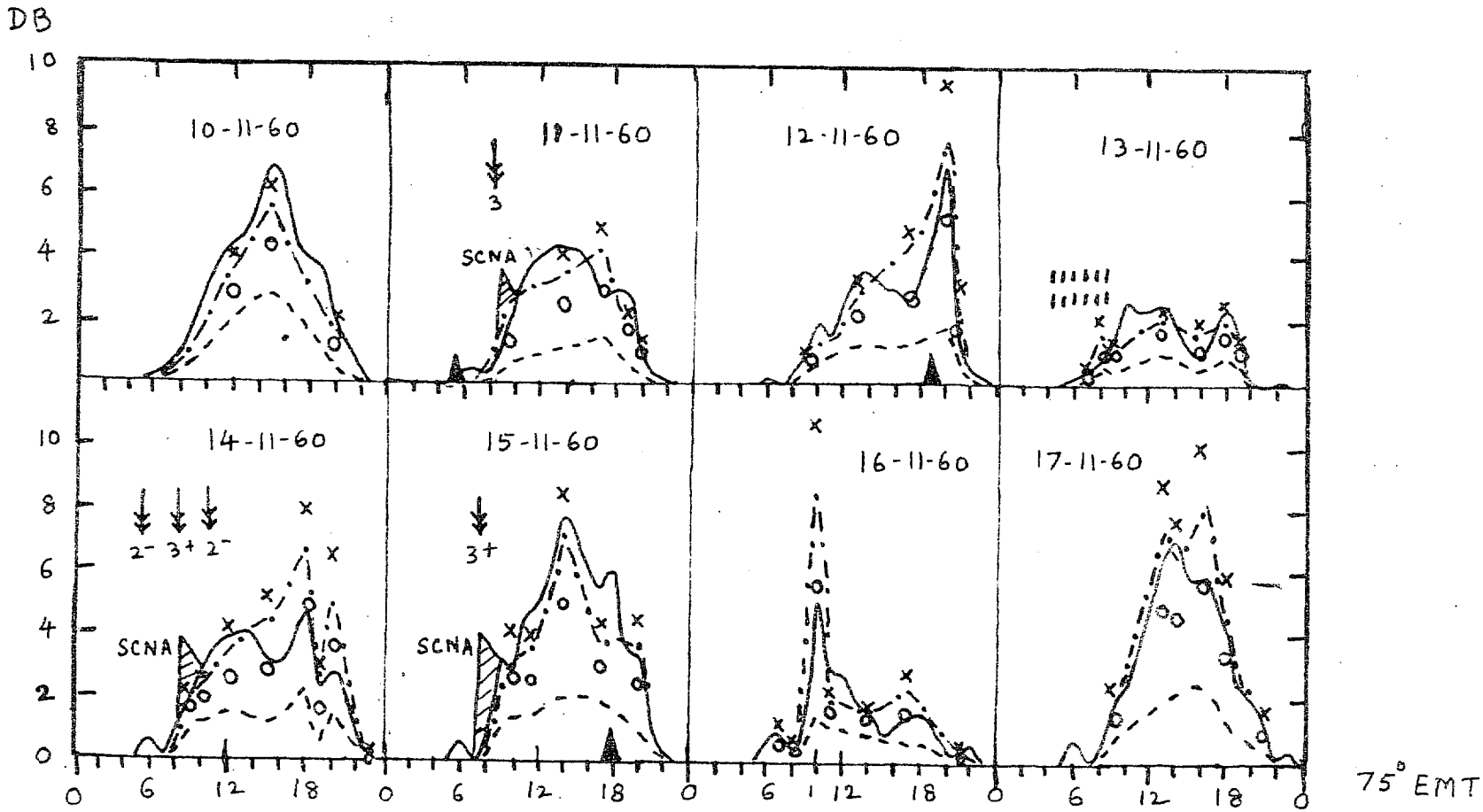

COSMIC RADIO NOISE ABSORPTION ON 25 Mc/s AT AHMEDABAD ·,
OBSERVED ——; CALCULATED ABSORPTION UPTO h_{max} - - -,
CALCULATED TOTAL ABSORPTION UPTO 1000 KM WITH AL'PERT MODEL
ABOVE h_{max} x x x, KAZANTSEV o o o; GARRIOTT —·—·

FIG. 5·6

radio noise records during these hours. As the attenuation was very small (less than 0.1 db) between 00 and 06 hrs, it was not calculated in detail.

6.2.1 Comparison of calculated absorption and observed absorption

In Fig.6.6, we have shown (a) the observed attenuation, (b) the calculated absorption upto h_{max}, and (c) the calculated total absorption upto 1000 Km assuming three models of electron density variation above h_{max}. It can be seen that irrespective of magnetic disturbance, more absorption seems to have occurred above h_{max} than below that level. However, on the second day of the SC, the observed attenuation was abnormally low and so also the calculated absorption.

The hatched portions in Fig.6.6 indicate three SCNA's caused by ionospheric absorption mainly in the D region. These absorptions are but small effects compared to the diurnal F region attenuation.

6.2.2 Absorption above h_{max}

To get an idea of attenuation of cosmic radio noise above the level of h_m in the ionosphere, we subtracted the calculated absorption below h_m from the total observed attenuation of cosmic radio noise. This difference is shown in Fig.6.7 and 6.8. It can be seen that large absorption occurred in the

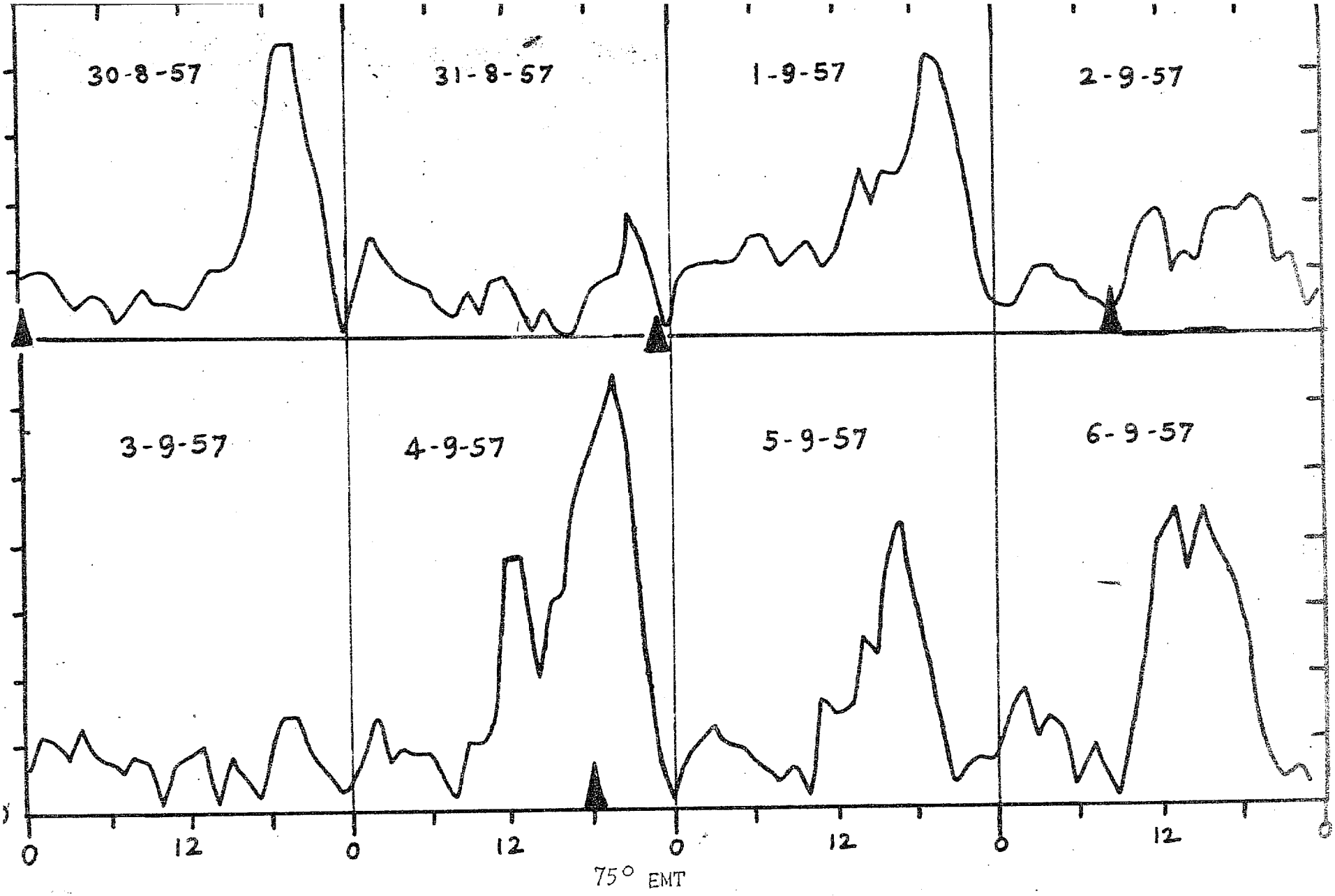

FIG. 5·7 COSMIC RADIO NOISE ABSORPTION ON 25 Mc/s OBSERVED MINUS CALCULATED BELOW hmF AT AHMEDABAD

DURING 30 AUG. – 6 SEP. 1957

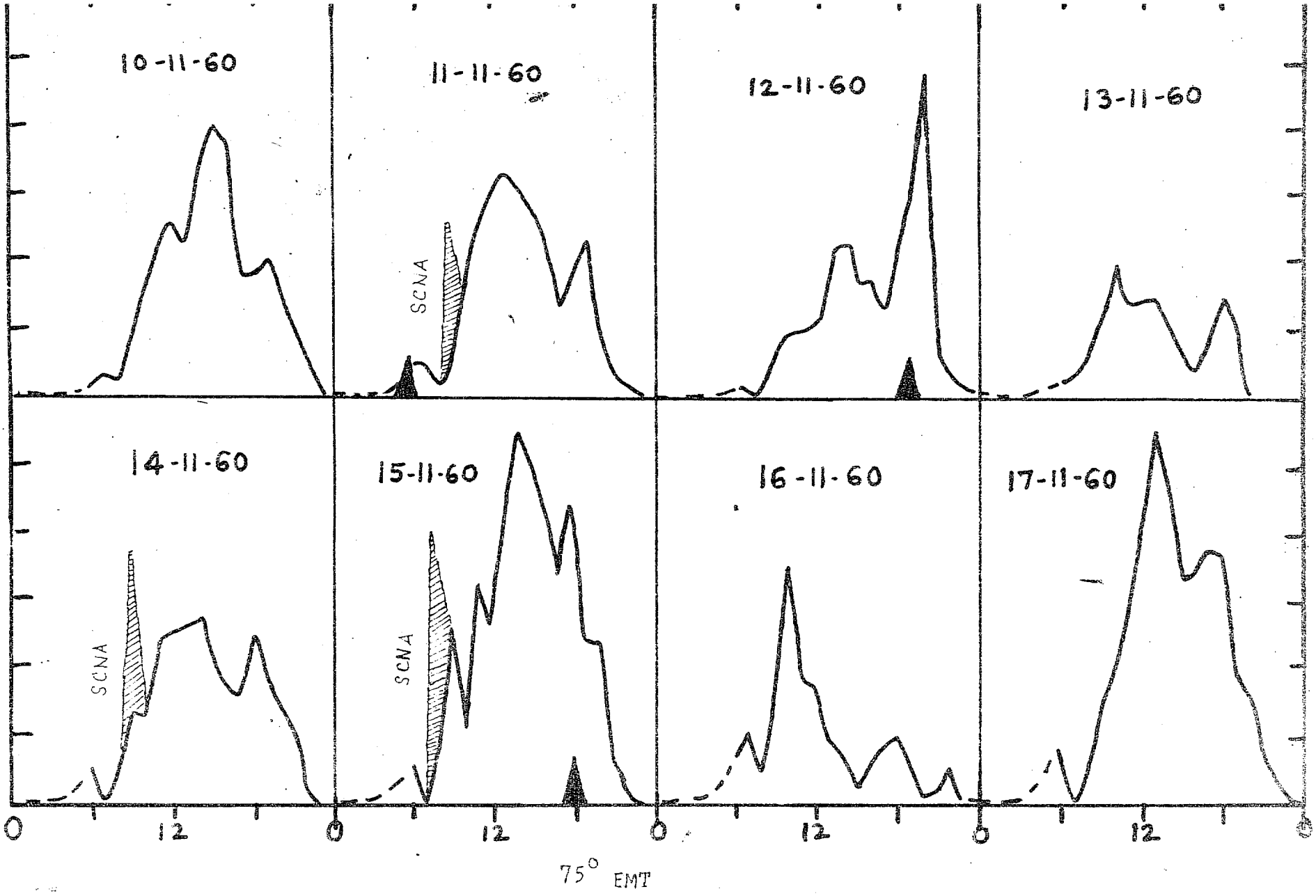

9.58 COSMIC RADIO NOISE ABSORPTION ON 25 Mc/s OBSERVED MINUS CALCULATED BELOW hmF AT AHMEDABAD

DURING 10-17 NOVEMBER 1960

late evening hours (between 20-21 hrs) during September 1957, while it was much less prominent in November 1960.

6.2.3 Electron distribution models above h_m in the two events

In the case of September 1957 events, we had found that the Al'port and Kazantsev models were satisfactory on high and low absorption days respectively. But in the case of November 1960 events, Al'port's and Kazantsev's models served as two extremes, Al'port's showing a slow rate of fall of electron density with height above h_m and Kazantsev's showing much faster rate. Garriott's model strikes a mean between these two models. It was found that on any single day, the calculated attenuations based on these models did not give complete hour to hour agreement with the observed attenuations. The discrepancies were more pronounced when there were sudden increases or decreases of electron concentrations above h_m. To take a few examples, we see from Fig.6.3 that calculated absorptions based on the Al'port model are too high between 16-20 hrs on the 13th, 14-20 hrs on the 14th, 03-10 hrs on the 16th and 12-13 hrs on the 17th; whereas the calculated absorption based on the Kazantsev model are generally lower than the observed ones. This means that at times of rapid change, the rate of fall of electron density with height above h_m is much more rapid than that given by Al'port's model and less rapid than that shown by Kazantsev's. In general it can be said that on quiet or slightly disturbed days, Al'port's or Garriott's

model fits in reasonably well, whereas on days of low h_{mF} (hence low attenuation), Kazantsev's model seems to be better. Deviations from these models are to be expected since there are many variable factors which we cannot yet properly evaluate. One thing is clear that the attenuation above h_{max} is important; and that below 100 Km, it is only a small part of the total attenuation. It seems to us that most of the attenuation of cosmic radio noise can be accounted for by changes in electron content below 1000 Km.

7. DISCUSSION

7.1 Other causes leading to cosmic radio noise attenuations

In the calculation of ionospheric absorption, only the nondeviative part of absorption due to electron collisions has been considered. Deviative absorption and limitation of aerial aperture can also cause attenuation. Both these depend on the nearness of the exploring frequency (which is 25 Mc/s in our case) to the critical frequency of the F2 region. The maximum critical frequency of the F2 region over Ahmedabad rarely exceeds 13-14 Mc/s and since the angular aperture of the aerial was limited to $40^{\circ} \times 30^{\circ}$ in the vertical, we could estimate that the deviative absorption becomes noticeable only after 21-22 Mc/s. There are a few instances when f_0F2 suddenly shot up to 20 Mc/s or more causing corresponding enhanced absorption of cosmic radio noise. Shome and Ramanathan (1959)

pointed out that F scatter might cause an increase in attenuation. This is not a likely cause during magnetically disturbed periods since F scatter is much reduced or even absent at Ahmedabad during such periods.

7.2 Changes in the assumed distribution model above h_m

Fig.5.7 and 5.8 showed an additional diurnal increase in attenuation in the late evening hours. It was much more prominent in September 1957 than in November 1960. This may be due to the fact that the electron distribution above h_{max} may vary with the time of the day. It is probable that at the time when foF2 has begun to decrease in the evening, after reaching its peak, there is a delay in the decrease of electron density at levels above F2 peak. There is an evidence for this from rocket and satellite data. Nisbet (1960) and Nisbet and Bowhill (1960) collected together the available information on electron density distribution in the upper ionosphere from rockets and satellites. They reported that above F2 peak, high electron densities continued to persist in the late evening hours and they decreased with height much more rapidly in the second half of the night and in the morning. Ross (1960) has shown from the Doppler frequency measurements of satellite 1958 δ 2 (Sputnik II) that on the average there was a steady increase in total electron content between the F2 peak and the satellite height (roughly 950 Km) from sunrise to sunset eventhough the electron content below h_mF had begun to show a decrease by sunset.

If we examine the iso-electron density contours on undisturbed days, we find near sunset high gradient of electron density between 250 and 350 Km below h_m. This suggests a change in the model of electron density distribution above h_{max}. Mitra and Gerola (1960), in their determination of the electron content of the outer ionosphere from cosmic radio noise measurements at Delhi, consider the total attenuation to be mainly dependent on foF2 with no dependence on the heights of the layer. This was also the view held earlier by Mitra and Shain. From our study, it is clear that the height of the layer especially the height of maximum electron density in the F region appreciably affects the attenuation. This is understandable since ν_{ei} is a function of both N_e and T which are themselves functions of height.

7.3 Diurnal variation of temperature in the upper atmosphere

We do not yet know clearly the nature and extent of the diurnal variation of temperature in the upper atmosphere although the evidence for such a diurnal variation is steadily increasing. Our present analysis of calculated and observed cosmic noise attenuation suggests that there may be a marked diurnal variation of temperature above 300 Km, the region where electron-ion collisions contribute most towards the attenuation of cosmic radio noise. From the observations of deceleration of satellites as analysed by Jacchia (1959), Martin and Priester (1960), King-Hele and Walker (1960) and others, Nicolet (1960)

concludes that between 300 and 900 Km there is probably a cooling during night of the order 500° K. Since ν_{ei} is proportional to $T^{-3/2}$, a cooling of the upper part of the ionosphere of this order will cause an increase in the collision frequency of electrons in the ratio of 1.3 to 2 if the electron density remains the same. Recently, Kallmann-Bijl (1961) has pointed out the difference between the daytime and nighttime atmospheric properties. Thus it appears that the post-sunset increase in cosmic radio noise attenuation in high sunspot years is due to the combined effect of a decrease in the temperature of the outer ionosphere together with a lag in the rate of attachment of electrons with increasing height.

7.4 Heating of the ionosphere by hydromagnetic waves

Dessler (1959) showed that the power dissipation of the hydromagnetic waves per unit volume in the ionosphere reached a maximum between about 150-200 Km altitude and suggested that the observed lifting of the F region and the reduction of foF2 during a magnetic storm was due to hydromagnetic heating. Francis and Karplus (1960) further examined this problem and came to the conclusion that the hydromagnetic waves can explain, at least in part, the following phenomena : (1) the lifting of the ionospheric F region during magnetic storms, (2) the irregular orbital acceleration of satellites, (3) sudden disappearance of trapped radiation from the Argus nuclear explosion coincident with a geomagnetic storm, (4) the X-ray

flux observed at balloon altitudes, and (5) the decrease in intensity at the lower edge of the Van Allen radiation belt during magnetic storms.

Bauer (1960) inferred the scale heights at the F2 peak from the rocket data and found that the scale height at the F2 peak was higher by 30 per cent on the day following a magnetic storm which showed increased ionospheric heating at such times. The cosmic radio noise attenuation observed at Ahmedabad show a marked reduction in attenuation on the day following a severe magnetic storm which suggests the possibility of such a mechanism taking place even at low latitudes.

8. COMPARISON WITH SATELLITE OBSERVATION

It is interesting to compare these changes in cosmic noise absorption during and after magnetic storms with the changes in particle fluxes that have recently been observed in Van Allen radiation belts during such storms. Table 2 below lists some observations of depletion of radiation belts during magnetic storms.

Table 2.

Satellite	Magnetic Storm	Authors
Explorer IV	September 3-4, 1959	Rothwell and McIlwain, 1960
Explorer VI	August 10-13, 1959	Arnoldy, Hoffman and Winckler, 1960
Explorer VII	March 31-April 3, 1960	Van Allen and Lin, 1960.

EXPLORER VI

SC MAGNETIC STORM AT 0414 UT ON 16-8-59

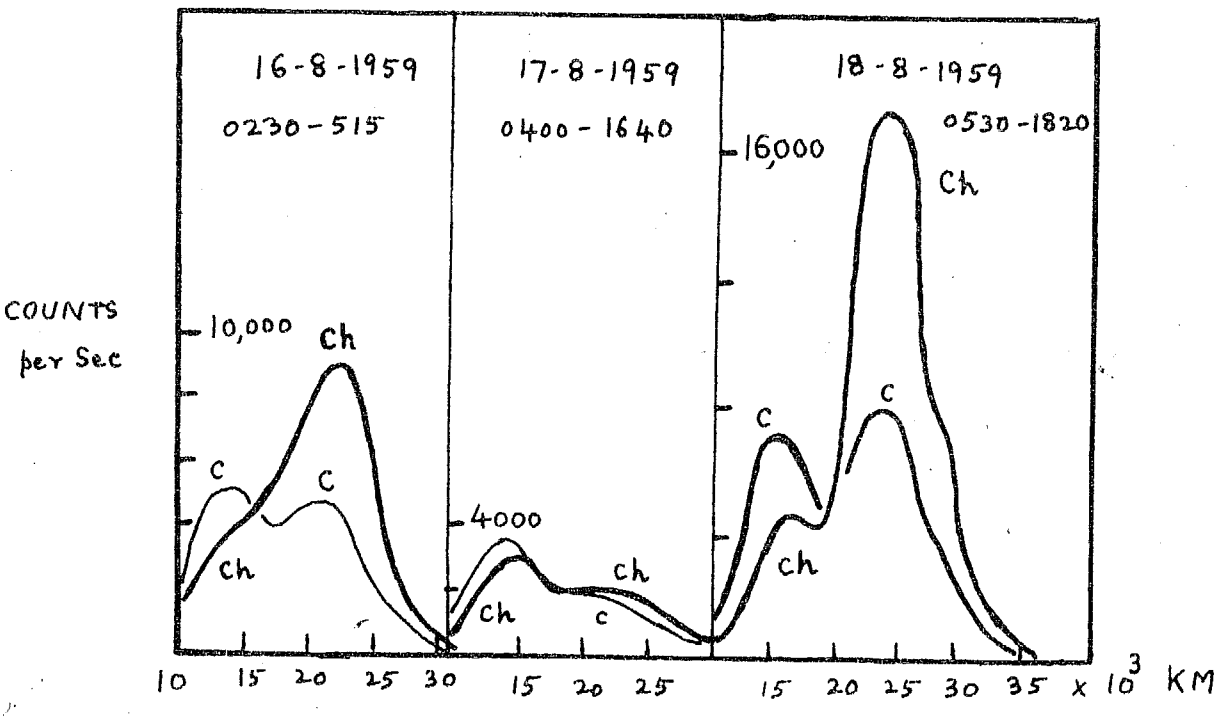

Ch – ION. CHAMBER, C – GEIGER COUNTER

PROTONS ≥ 16 Mev, ELECTRONS ≥ 2 Mev, X-RAYS ≥ 30 kev

(AFTER ARNOLDY, HOFFMAN AND WINCKLER)

FIG. 5·9

We have shown in Fig.3.9 the observations made by Arnoldy et al (1960) during a magnetic storm which commenced at 0414 UT on 16-3-59 with instruments carried in Explorer VI. The observations cover a period of three days and the figure shows the variation in the number of counts per second recorded by an integrating ion chamber and a Geiger counter carried in the satellite. The counts of the ion chamber are shown by thick lines and those of Geiger counter by thin lines. It recorded the number of counts of protons of energy $\geqslant$ 16 Mev and of electrons of energy $\geqslant$ 30 Kev between 10,000 and 30,000 Km from the centre of the earth. The remarkable feature brought out by the observations is that on the second day of the storm, there was a large reduction in radiation in the outer Van Allen belt and this recovered to more than its pre-storm value on the third day. The changes in the harder radiation recorded by the Geiger counter are comparatively smaller, though they are in the same direction. Considering the similarity between the changes in cosmic radio noise absorption and the flux of energetic particles in the Van Allen belts, it appears that during magnetic storms, there is a large decrease in the number of electrons even in the outer ionosphere in low and middle latitudes during the main phase of a magnetic storm and at the end of the storm, the outer region gets refilled with electrons. There are now quite a few examples of satellite observations which bear out this general conclusion. There is a great similarity in the changes of flux of energetic electrons and ions in the Van Allen belts and low energy electrons in the ionosphere below 1000 Km.

9. CONCLUSION

We can draw the following general conclusions from this study of ionospheric attenuation of cosmic radio noise. They are :

(1) The major contribution to absorption arises due to electron-ion collisions in the F region rather than due to electron-neutral particle collisions in the lower ionosphere.

(2) The attenuation below $h_{max}F$ is not appreciably reduced during magnetic storms because the fall in electron density and the rise in height of the F layer tend to balance.

(3) The difference between the observed total attenuation and the calculated attenuation upto $h_{max}F$ is usually large; but on the day following the commencement of a storm, this difference is narrowed down considerably suggesting depletion of electrons above h_mF at such times and rise of temperature near F2 peak.

(4) The observed evening rise in attenuation in equinoxes and some winters can be explained on a model assuming much slower rates of fall of electron density with height above h_mF and a cooling of the ionosphere after sunset.

APPENDIX I

Table giving ν_{ei} for different values of N_0 and T

Height / N_0 \ T°K	120 330	160 613	200 775	240 900	280 993	320 1080	360 1155	400 1213	450 1400	500 1530
1.0^{4}	7.8^{1}	3.8^{1}	2.8^{1}	2.1^{1}	1.8^{1}	1.5^{1}	1.3^{1}	1.4^{1}	1.0^{1}	9.0^{0}
2.0	1.4^{2}	6.3	4.3	4.0	3.4	3.0	2.7	2.5	2.0	1.6^{1}
3.0	2.0	1.0^{2}	7.1	5.8	5.0	4.3	4.1	3.8	2.9	2.3
4.0	2.6	1.3	9.5	7.7	6.6	5.7	5.4	5.0	4.0	3.0
5.0	3.2	1.6	1.2^{2}	9.3	8.3	7.0	6.7	6.3	5.0	3.8
6.0	3.8	1.9	1.4	1.1^{2}	1.0^{2}	8.5	8.0	7.4	5.9	4.4
7.0	4.4	2.2	1.6	1.3	1.1	9.8	9.3	8.6	6.8	5.1
8.0	5.0	2.5	1.8	1.5	1.3	1.1^{2}	1.1^{2}	1.0^{2}	7.0	5.3
9.0	5.6	2.8	2.0	1.7	1.4	1.2	1.2	1.1	8.0	6.5
1.0^{5}	6.2	3.2	2.3	1.8	1.6	1.4	1.3	1.2	9.0	7.2
2.0	1.2^{3}	6.2	4.4	3.6	3.1	2.7	2.5	2.4	1.3^{2}	1.4^{2}
3.0	1.7	9.0	6.6	5.3	4.6	4.0	3.8	3.6	2.7	2.0
4.0	2.3	1.2^{3}	8.5	7.0	6.1	5.3	5.0	4.6	3.5	2.7
5.0	2.9	1.5	1.1^{3}	8.5	7.3	6.6	6.2	5.7	4.5	3.3
6.0	3.4	1.8	1.3	1.0^{3}	9.0	7.8	7.4	6.8	5.1	3.9
7.0	4.0	2.0	1.5	1.2	1.0^{3}	9.0	8.5	7.9	6.1	4.6
8.0	4.5	2.3	1.7	1.4	1.2	1.0^{3}	9.8	8.9	7.0	5.2
9.0	5.0	2.6	1.9	1.5	1.3	1.2	1.1^{3}	9.9	7.5	5.8
1.0^{6}	5.5	2.9	2.1	1.7	1.5	1.3	1.3	1.2^{3}	8.5	6.4
2.0	1.0^{4}	5.5	4.1	3.3	2.9	2.6	2.4	2.2	1.7^{3}	1.3^{3}
3.0	1.6	8.3	6.1	4.9	4.4	3.8	3.6	3.3	2.5	1.9
4.0	2.0	1.1^{4}	8.0	6.3	5.8	5.1	4.7	4.3	3.3	2.4
5.0	2.6	1.3	1.0^{4}	8.0	7.0	6.1	5.8	5.2	4.2	3.3

CHAPTER VI

SUMMARY AND CONCLUSIONS

The present study of the F region of the ionosphere over Ahmedabad has proved interesting as regards its variations with solar activity and in particular with geomagnetic storms. As Ahmedabad is situated near the belt of peak F2 ionization, the seasonal and diurnal changes as well as changes in magnetically disturbed periods are significantly enhanced. Though the noon critical frequency of the E layer showed maxima in summer and minima in winter as expected, its sub-solar frequency K showed an opposite variation. K in winter was higher by about 11 % than in summer both in low and high sunspot years. The change in intensity of the solar radiation due to varying sun-earth distance during a course of a year would account only for half of the change found in K.

The effect of a severe magnetic storm is to reduce foF2 and raise the height within 6-8 hours on the average after the SC in the case of the storms which commence early in the morning before ground sunrise and in the afternoon hours. The severe storms which commence in the forenoon hours affect the foF2 mostly on the second day after the SC. The depression in foF2 is found to occur mostly during night hours.

Among the different methods available for the reduction

of h'-f records to true height profiles, the one due to Schmerling was found convenient. The method automatically corrects for group retardation in the lower layers and also takes into account the effect of the earth's magnetic field if the 10 or 5 point coefficients appropriate to the dip angle of the station are used. The procedure for the complete reduction of h'-f records carried out at Ahmedabad is given in Chapter II together with 10 point and 5 point sampling frequencies from 1 to 25 Mc/s.

The results of true height calculations are discussed in Chapter III. Some N(h) curves at fixed heights are shown for some typical days, including very quiet to very disturbed days. In general the N(h) curves vary smoothly on quiet and slightly disturbed days. The height of maximum density level h_m does not differ much during day from that during night. It is, however, a minimum near about sunrise.

The effect of some selected magnetic storms on the electron density distribution in the ionosphere over Ahmedabad has also been studied. It was found that the electron densities remained low on the day following the SC and were more than restored at the end of the storm. The total electron content in a colum of unit cross-section upto h_{max} was less than the pre-storm value during the main phase of the storm. The storm induced large perturbations in h_m of the order of 300 Km during night hours following the SC.

It is interesting to find large localised concentrations of electron density at about 250 Km in the morning hours between

02-00 LMT. during disturbed periods. It appears that during large disturbances the peak F2 ionization belt gets dilated.

Using the N(h) data, we have calculated the ionospheric absorption on cosmic radio noise at 25 Mc/s at Ahmedabad and compared it with that observed by the cosmic radio noise monitor at Ahmedabad. The calculation is based on the numerical integration of $\int N\nu\, dh$, where ν is the effective collision frequency of electrons with positive ions and neutral particles. It is shown that the electron-positive ion collision is important in the F region of the ionosphere. The electron distribution above h_{max} was assumed according to the models proposed by Al'pert, Kazantsev and Garriott. We found that most of the attenuation of cosmic radio noise can be accounted for by the changes in the electron density below 1000 Km, (1) by choosing an appropriate model of electron distribution above h_{max} and (2) by allowing for the diurnal variation of temperature in the upper atmosphere.

The observed total attenuation of cosmic radio noise on the day following the sudden commencement is probably due to a hydromagnetic heating of the ionosphere. A comparison is made with the recorded flux of energetic particles in the Van Allen radiation belts during magnetic storms with the observed total attenuation of cosmic radio noise. It is found that there is considerable similarity in changes of flux of energetic protons and electrons in the radiation belts and of low energy electrons in the ionosphere below 1000 Km.

-:oooooooo:-

REFERENCES

Allen C.W., J.Atmos.Terres.Phys., 4, 53 (1954).

Al'pert Y.L., Dobriakova, B.C.Chudesenko and B.C.Shapiro, Doklady, AN USSR, 130, 743 (1959).

Appleton E.V., Proc.Phys.Soc., 42, 321 (1930).

Appleton E.V., Proc.Roy.Soc., A, 162, 451 (1937).

Appleton E.V., Nature, 157, 691 (1946).

Appleton E.V. and L.J.Ingram, Nature, 136, 548 (1935).

Appleton E.V. and W.J.G.Beynon, Proc.Phys.Soc., 52, 513 (1940).

Appleton E.V. and W.M.Piggott, Nature, 165, 130 (1950).

Appleton E.V. and W.R.Piggott, J.Atmos.Terres.Phys., 8, 236 (1956).

Arnoldy R., R.Hoffman and J.R.Winckler, "Space Research", North-Holland Publishing Co., Amsterdam, p.577.

Baur S.J., J.Geophys.Res., 68, 1695 (1960).

Berkner L.V. and S.L.Seaton, Terrest.Magnet.Atmos.Elect., 45, 393 (1940a).

Berkner L.V. and S.L.Seaton, Terrest.Magnet.Atmos.Elect., 45, 419 (1940b).

Berkner L.V., S.L.Seaton and H.W.Wells, Terrest.Magnet.Atmos. Elect., 44, 223 (1939).

Beynon W.J.G., Proc.Phys.Soc., 59, 97 (1947).

Beynon W.J.G. and J.O.Thomas, J.Atmos.Terres.Phys., 9, 131 (1956).

Bhargava B.N., Indian J.Met.Geophys., 9, 25 (1958).

Bhonsle R.V., Ph.D. Thesis, Gujarat University (1960).

Bhonsle R.V. and K.R.Ramanathan, J.Sci.Industr.Res.(India), 17A, 40 (1958).

Bhonsle R.V. and K.R.Ramanathan, Planet.Space Sci., 2, 99 (1960).

Booker H.G. and S.L.Seaton, Phys.Rev., 57, 98 (1940).

Budden K.G., Cambridge Conf. on Ionospheric Physics (Phys.Soc.), p.338 (1955).

Campbell W.S. and P.L.Hubert, Can.J.Phys., 39, 630 (1961).

Chapman S., Proc.Phys.Soc., 43, 26; 483 (1931).

Chapman S. and C.G.Little, J.Atmos.Terres.Phys., 10, 20 (1957).

Cowling T.G., Proc.Roy.Soc., A, 183, 453 (1945).

Croom S., A.Robbins and J.O.Thomas, Nature, 184, 2003 (1959).

Croom S., A.Robbins and J.O.Thomas, Nature, 185, 902 (1960).

Deganokar S.S., Proc.Ind.Acad.Sci., A, 34, 24 (1951).

Deganokar S.S. and R.V.Bhonsle, Paper submitted to Kyoto Conference on Earth Storm (1961).

Dessler A.J., J.Geophys.Res., 64, 397 (1959).

Francis W.E. and R.Karplus, J.Geophys.Res., 65, 3593 (1960).

Friedman H., Proc.IRE, 47A, 272 (1959).

Garriott O.K., "Space Research", North-Holland Publishing Co., Amsterdam, p.371 (1960).

Havens R.J., H.Friedman and E.O.Hulbert, Cambridge Conference on Ionospheric Physics (Phys.Soc.), p.237 (1956).

Jacchia L.G., Nature, 183, 526 (1959).

Jackson J.E., J.Geophys.Res., 61, 107 (1956).

Kallmann-Bijl H.K., J.Geophys.Res., 66, 737 (1961).

Kazantsev A.N., Planet.Space Sci., 1, 130 (1959).

Kelso J.M., J.Geophys.Res., 57, 337 (1952).

Kelso J.M., J.Atmos.Terres.Phys., 5, 11 (1954).

Kelso J.M., J.Atmos.Terres.Phys., 10, 103 (1957).

King-Hele D.G. and D.M.C.Walker, Nature, 186, 923 (1960).

Kotadia K.M., Proc.Ind.Acad.Sci.,A, 46, 349 (1957).

Kotadia K.M., Ph.D.Thesis, Gujarat University (1958).

Kotadia K.M., Proc.Ind.Acad.Sci.,A, 50, 259 (1959).

Kotadia K.M. and K.R.Ramanathan, Annals of IGY, XI (in press)(1960).

Krassovsky V.I., Annals of IGY, XII, p.589 (1961).

Lejay P., A.Haubert and J.Durand, C.R.Acad.Sci., 223, 1768 (1946).

Maeda K.I. and T.Sato, Proc.IRE, 47A, 232 (1959).

Manring L.M., J.Geophys.Res., 52, 117 (1947).

Martin H.A. and W.Priester, Nature, 185, 600 (1960).

Martyn D.F., Proc.Roy.Soc., A, 189, 241 (1947).

Martyn D.F., Nature, 171, 14 (1953).

Martyn D.F., Proc.Roy.Soc., A, 218, 1 (1953).

Mathur S.B. and A.P.Mitra, J.Sci.Industr.Res.(India), 19A, 311 (1960).

Matsushita S., J.Geophys.Res., 64, 305 (1959).

Mitra A.P. and K.A.Sarada, Radio Research Committee, CSIR, Scientific Report No.10 (1960).

Mitra A.P. and C.A.Shain, J.Atmos.Terres.Phys., 4, 204 (1953).

Mitra S.K., "Upper Atmosphere", The Asiatic Society, Calcutta, (1952).

Nicolet M., Phys.Fluids, 2, 95 (1959).

Nicolet M., "Space Research", North-Holland Publishing Co., Amsterdam, p.46 (1960).

Hoclet M. and A.C.Aikin, J.Geophys.Res., 65, 1469 (1960).

Hsbot J.S., J.Geophys.Res., 65, 2507 (1960).

Hsbot J.S. and S.A.Bowhill, J.Geophys.Res., 65, 3600 (1960).

Pokorla C.L., Terr.Magnet.Atmos.Elect., 45, 805 (1940).

Pierce J.A., Phys.Rev., 71, 633 (1947).

Ramanathan K.R., R.V.Ghorale and S.S.Degaonkar, J.Geophys.Res., 66, No.9 (1961) (In press).

Ratcliffe J.A., J.Geophys.Res., 56, 463; 467 (1951).

Ratcliffe J.A., "The Magneto-Ionic Theory", Cambridge Univ. Press, Cambridge (1959).

Rastogi R.G., Ph.D.Thesis, Gujarat University (1956).

Rastogi R.G., Can.J.Phys., 34, 674 (1959).

Rastogi R.G., Zeit.fur Geophysik, 26, 317 (1960).

Rawer K., "The Ionosphere", Frederick Ungar Publishing Co., New York, p.182 (1957).

Rees M.H. and Wm.A.Reese, J.Geophys.Res., 64, 1351 (1959).

Ross W.J., J.Geophys.Res., 65, 2307 (1960).

Rothwell P. and C.S.McIlwain, J.Geophys.Res., 65, 799 (1960).

Rydbeck O.E.H., Phil.Mag., 30, 233 (1940).

Schmerling E.R., Scientific Report No.24, Ionosphere Research Lab., The Pennsylvania State Univ. (1957).

Schmerling E.R., J.Atmos.Terres.Phys., 12, 8 (1958).

Schmerling E.R. and J.O.Thomas, Phil.Trans.Roy.Soc., 249, 75 (1956).

Schmerling E.R. and C.A.Vantrieo, J.Atmos.Terres.Phys., 14, 249 (1959).

Seddon J.C. and J.E.Jackson, Ann.de Geophys., 14, 456 (1958).

Seddon J.C. and J.E.Jackson, Annals of IGY, XII, p.573, 580 (1961).

Sheriff R.M., J.Atmos.Terres.Phys., 3, 81 (1953).

Shimazaki T., J.Radio Res.Lab., Japan, 6, 107 (1959).

Shinn D.H., J.Geophys.Res., 58, 415 (1953).

Shinn D.H. and H.A.Whale, J.Atmos.Terres.Phys., 3, 85 (1952).

Singleton D.G., J.Geophys.Res., 65, 3615 (1960).

Sreenivasan S.R., Ph.D.Thesis, Gujarat University (1953).

Steiger W.R. and J.W.Warwick, J.Geophys.Res., 66, 67 (1961).

Stelljes J.F., H.Carmichael and K.G.McCracken, J.Geophys.Res., 66, 1383 (1961).

Thomas J.O., Proc.IRE, 47A, 162 (1959).

Thomas J.O., J.Hasselgrove and A.R.Robbins, J.Atmos.Terres.Phys., 12, 43 (1958).

Thomas J.O. and M.D.Vickers, D.S.I.R.Radio Research Special Report No.33 (1958).

Titheridge J.E., J.Atmos.Terres.Phys., 17, 98 (1959).

Titheridge J.E., J.Atmos.Terres.Phys., 21, 1 (1961).

Van Allen J.A. and W.C.Lin, J.Geophys.Res., 65, 2993 (1960).

Vogan E.L. and T.R.Hartz, Can.J.Phys., 39, 630 (1961).

Wright H.W., J.R.Koster and N.J.Skinner, J.Atmos.Terres.Phys., 3, 240 (1956).

Yonezawa T., J.Radio Res.Lab., Japan, 7, 60 (1960).

-:oooOOOooo:-